

DTIC FILE COPY

contraves
Contraves USA

AD-A226 508

INTERIM REPORT ON
THE IMPROVED THREE AXIS
TEST TABLE (ITATT):
PROGRAM STATUS AND
RECOMMENDATION FOR COMPLETION

1
DTIC
REF ID: A67252
S ECTE SEP 05 1990
CD

TR-27824

K-97012

F08635-89-C-0297

DISTRIBUTION STATEMENT A

Approved for public release
Distribution Unlimited

A004

August, 1990

Prepared for:

EGLIN/HOLLOMAN AFB

We reserve all rights in connection with this document and in the subject matter represented therein. The recipient hereby acknowledges these rights and shall not, without our permission in writing, disclose or divulge this document in whole or in part to third parties or use it for any purpose other than that for which it was delivered to recipient.

A Member of the Oerlikon-Bührle Group

90 0831 037



INTERIM REPORT ON
THE IMPROVED THREE AXIS
TEST TABLE (ITATT):
PROGRAM STATUS AND
RECOMMENDATION FOR COMPLETION

TR-27824

We reserve all rights in connection with this document and in the subject matter represented therein. The recipient hereby acknowledges these rights and shall not, without our permission in writing, disclose or divulge this document in whole or in part to third parties or use it for any purpose other than that for which it was delivered to recipient.

INTERIM REPORT ON
THE IMPROVED THREE AXIS
TEST TABLE (ITATT):
PROGRAM STATUS AND
RECOMMENDATION FOR COMPLETION

TR-27824

STATEMENT "A" per Dick Alexander
6585th Test Group/GDL
Holloman AFB, NM 88330-5000
TELECON 9/4/90

K-97012

VG

F08635-89-C-0297

A004

August, 1990

Accession For	
3 NTIS /RA&I	
DHC TAB	
Unannounced	
Justification	
By <i>per call</i>	
Distribution /	
Availability Codes	
Dist	Avail or d/ or Special
A-1	

Prepared for:

EGLIN/HOLLOMAN AFB

We reserve all rights in connection with this document and in the subject matter represented therein. The recipient hereby acknowledges these rights and shall not, without our permission in writing, disclose or divulge this document in whole or in part to third parties or use it for any purpose other than that for which it was delivered to recipient.

TABLE OF CONTENTS

	Page
1 INTRODUCTION – EXECUTIVE SUMMARY	1
2 PURPOSE OF THIS REPORT	5
3 REVIEW OF THE ITATT PROGRAM AND PERFORMANCE GOALS	6
4 PROGRESS IN DEVELOPING THE CRITICAL ITATT TECHNOLOGIES	7
4.1 Magnetic Bearing	7
4.1.1 Progress and Status	7
4.1.2 Data	7
4.1.3 What Has Contraves Learned?	8
4.1.4 Remaining Issues and Possible Solutions	8
4.2 CFRP Inner Gimbal	8
4.2.1 Progress and Status	8
4.2.2 Data	8
4.2.3 What Has Contraves Learned?	11
4.2.4 Remaining Issues And Possible Solutions	11
4.3 Encoding System	11
4.3.1 Progress and Status	11
4.3.2 Data	12
4.3.3 What Has Contraves Learned?	12
4.3.4 Remaining Issues And Possible Solutions	12
4.4 Roll Rings	12
4.4.1 Progress And Status	12
4.4.2 Data	13
4.4.3 What Has Been Learned?	13
4.4.4 Remaining Issues And Possible Solutions	14
4.5 Drive System	14
4.5.1 Progress And Status	14
4.5.2 Data	14
4.5.3 What Has Been Learned?	14
4.5.4 Remaining Issues And Possible Solutions	16

We reserve all rights in connection with this document and in the subject matter represented therein. The recipient hereby acknowledges these rights and shall not, without our permission in writing, disclose or divulge this document in whole or in part to third parties or use it for any purpose other than that for which it was delivered to recipient.

TABLE OF CONTENTS

	Page
4.6 Control System	16
4.6.1 Progress and Status	16
4.6.2 Data	16
4.6.3 What Has Contraves Learned?	20
4.6.4 Remaining Issues And Possible Solutions	20
4.7 Test And Validation Methods	20
4.7.1 Progress And Status	20
4.7.2 Data	20
4.7.3 What Has Contraves Learned?	22
4.7.4 Remaining Issues And Possible Solutions	22
5 NEW HIGH RISK AREAS IDENTIFIED IN PHASE I	23
5.1 Trunnion Shaft Thermal Distortion	23
5.2 Gimbal Configuration	23
5.3 Trunnion Shaft Wobble Affecting The Inductosyns	23
5.4 Limitations Of Current Test Equipment	23
5.5 Multi-Axis Control System Interactions	24
6 CONTRAVES' PROPOSAL FOR COMPLETING PHASE I AND PHASE II	25
6.1 First Priority: Identify and Solve Inner Axis Deficiencies	25
6.2 Second Priority: Reduce Phase II Risk By Building The Middle Axis	25
6.3 Completing Phase II	25
APPENDIX A - TR-27630	
APPENDIX B - TR-27764	
APPENDIX C - ITATT BEARING AND AXIS CONTROLS SYSTEMS ANALYSIS A MULTI-AXIS PERSPECTIVE	
APPENDIX D - HONEYWELL REPORT 5000-112892 ON THE INNER AXIS ROLL RING ASSEMBLY	

We reserve all rights in connection with this document and in the subject matter represented therein. The recipient hereby acknowledges these rights and shall not, without our permission in writing, disclose or divulge this document in whole or in part to third parties or use it for any purpose other than that for which it was delivered to recipient.

1 INTRODUCTION - EXECUTIVE SUMMARY

In May 1989 Contraves was awarded Phase I of the Improved Three-Axis Test Table (ITATT) program to develop the inner axis of what will eventually be the complete three axis ITATT. Phase I is a "proof of principle" research and development effort and is a cost plus incentive fee contract. Phase II is a firm fixed price "not to exceed" option that will incorporate the Phase I inner axis into new middle and outer axes.

Several critical ITATT technologies are being demonstrated in Phase I including: CFRP gimbals, roll rings, magnetic bearings, induction or A.C. motors, and back-to-back Inductosyn encoding. Based on a 1984 government funded design study, these technologies can be used to produce a test table with 0.1 arc second pointing accuracy, which is a factor of ten improvement over current test tables.

Contraves has worked diligently over the past 14 months to achieve the Phase I proof of principle objectives and has made significant progress. As of August 10, 1990, the baseline hardware is assembled, wired, integrated, and partially tested. This hardware is shown in Figures 1-1, 1-2, and 1-4. Specifically, the magnetic bearing and AMCS are operational and preliminary test data is available. This data shows that the ITATT performance requirements can be achieved if several repeatable errors can be eliminated through design modifications and/or calibration.

During the past 14 months, Contraves has also learned much about the ITATT "design challenge" and has identified several new high risk areas that must be addressed which include: trunnion shaft thermal distortion, gimbal configuration, trunnion shaft wobble, test equipment limitations, and active control system interactions. Several of these items can only be tested in a multi-axis configuration and, therefore, are now part of the Phase II scope. Based on the significant risk these items add to the currently defined Phase II, Contraves believes that it is not reasonable for Phase II to be completed on a fixed price basis.

To mitigate the Phase II risk, Contraves recommends that the high risk portions of Phase II be moved to Phase I. Phase I will be extended to include several system analysis tasks and the middle axis design, fabrication, and testing. Completing the middle axis early allows the ITATT technologies to be demonstrated on a two-axis machine, thus validating the multi-axis capabilities in Phase I. As a result, Phase II risk is reduced and can be reasonably completed as a fixed price effort. Contraves firmly believes that if this new program plan is implemented, the ITATT performance requirements can be achieved at a lower cost and risk to the government.

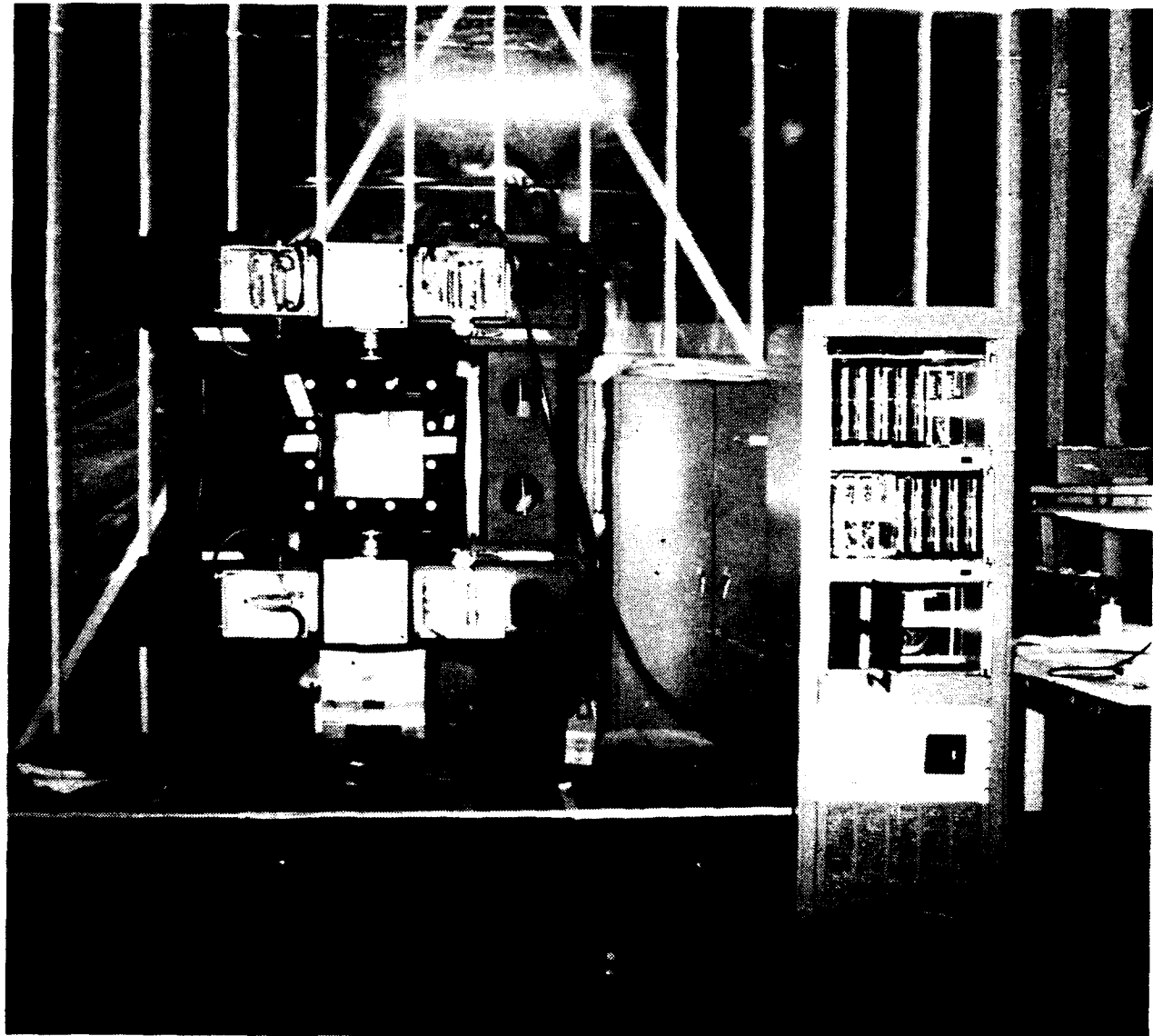


Figure 1-1. ITATT Inner Axis and Magnetic Bearing Console

We reserve all rights in connection with this document and in the subject matter represented therein. The recipient hereby acknowledges these rights and shall not, without our permission in writing, disclose or divulge this document in whole or in part to third parties or use it for any purpose other than that for which it was delivered to recipient.

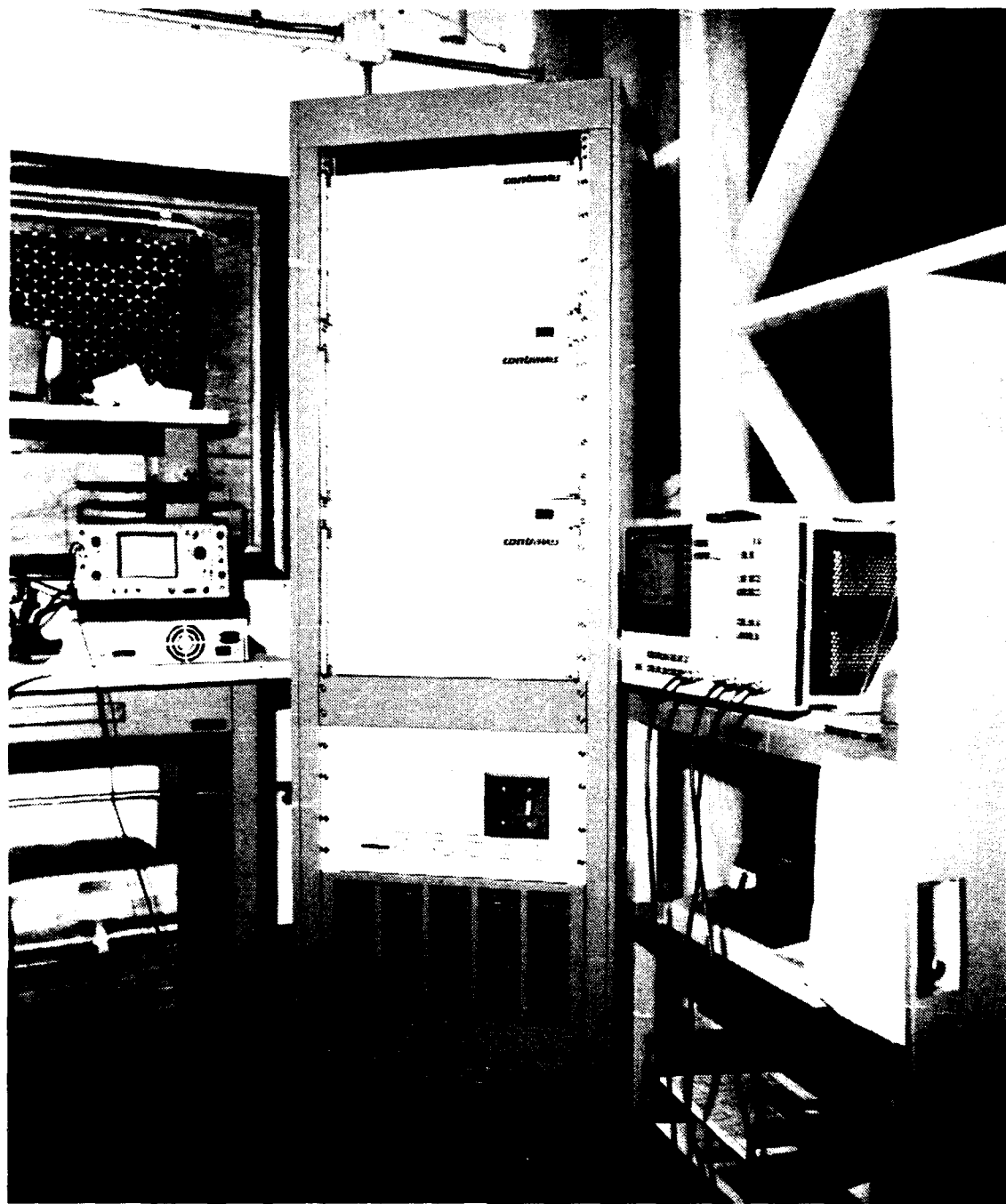


Figure 1-2. Magnetic Bearing Console

We reserve all rights in connection with this document and in the subject matter represented therein. The recipient hereby acknowledges these rights and shall not, without our permission in writing, disclose or divulge this document in whole or in part to third parties or use it for any purpose other than that for which it was delivered to recipient.



Figure 1-3. AMCS Console and P. C. Interface

We reserve all rights in connection with this document and in the subject matter represented therein. The recipient hereby acknowledges these rights and shall not, without our permission in writing, disclose or divulge this document in whole or in part to third parties or use it for any purpose other than that for which it was delivered to recipient.

2 PURPOSE OF THIS REPORT

This report provides the Air Force with the current project status and recommendations for completion of the ITATT program. Its purpose is to inform the Air Force of the successes and setbacks occurring during Phase I and to apply these lessons learned to modifying the current ITATT program plan. The lessons learned are discussed in Sections 4.0 and 5.0 and show that several high risk portions of this program must be completed in Phase II. To reduce Phase II risk, Contraves recommends that Phase I be extended and Phase II reduced as described in Section 6. Contraves strongly believes that, if this modified program plan is implemented, the ITATT performance goals can be achieved at lower cost and risk to the government.

3 REVIEW OF THE ITATT PROGRAM AND PERFORMANCE GOALS

In May 1989 Contraves was awarded the Phase I of the ITATT program to design, fabricate, and test the inner axis of what will ultimately be a three-axis test table. The inner axis is a "proof of principle" test bed of the critical ITATT technologies which include:

- Carbon Fiber Reinforced Plastic (CFRP) Gimbals
- Roll Rings
- Magnetic Bearings
- Low Torque Disturbance Induction or A.C. Motors
- Back-to-Back Inductosyr Encoding

These critical technologies were selected during a government funded design study in 1984 and are expected to give the ITATT a pointing accuracy of less than 0.1 arc seconds which is a factor of ten improvement over current inertial navigation test tables. Phase I is a high risk development effort and is a cost plus incentive fee type contract.

ITATT Phase II is an option, included in the Phase I contract, and requires that Contraves design, fabricate, and test the middle and outer axes of the ITATT for a "not to exceed" firm fixed price. The government can exercise this option after Contraves demonstrates the following fundamental performance requirements:

- Axis wobble of less than 0.02 arc seconds
- Axis position accuracy of less than 0.02 arc seconds
- Axis rate stability of less than 1 ppm
- Axis position servo bandwidth greater than 200 Hz

4 PROGRESS IN DEVELOPING THE CRITICAL ITATT TECHNOLOGIES

The primary goal of Phase I is the "proof of principle" of the critical ITATT technologies. This section review Contraves' progress in applying these technologies by reviewing the available test data, describing the lessons learned, and identifying the remaining problems that must be solved.

4.1 Magnetic Bearing

4.1.1 Progress and Status

The ITATT inner axis magnetic bearing sensors and electromagnets have been successfully integrated with the bearing control electronics. The result is a stable, magnetically levitated gimbal with low friction and noise. The magnetic bearing control electronics have been compensated to provide zero error and are stable independent of radial or axial position.

Contraves has measured 0.5 arc seconds of axis wobble, which is 25 times the 0.02 arc seconds specification. However, we have found that the wobble is dependent on shaft angular position. The excessive wobble appears to be caused by the radial shaft position sensors. The sensor feedback appears to be "telling" the shaft to change positions as a function of angular position. The exact cause of the problem cannot be confirmed until the bearings are disassembled, inspected, and the sensors tested on an air bearing.

4.1.2 Data

The following performance data has been collected:

	<u>Actual</u>	<u>Spec.</u>
Bandwidth (See Figure 4.2)	213 Hz	200 Hz
Wobble (See Figure 4.1)	0.53 arc sec	0.02 arc sec
Drift and Repeatability (1)	Approx. 0.1 arc-sec	<0.02 arc-sec
Radial Runout, Drive Side	100x10 ⁻⁶ inches	4x10 ⁻⁶ inches
Radial Runout, Readout Side	200x10 ⁻⁶ inches	4x10 ⁻⁶ inches
Axial Runout	50x10 ⁻⁶ inches	N/A

(1) The measurements of drift and repeatability are limited by the background noise of the wobble measurement setup. See Section 4.7 for more information.

4.1.3 What Has Contraves Learned?

Contraves has learned much from the ITATT magnetic bearing development and is confident that this technology can achieve this program's performance goals. While the absolute accuracy has not yet been achieved, the high repeatability and low drift¹ indicate that it is feasible. We have learned that tight mechanical tolerances don't necessarily ensure tight run-out tolerances in a magnetic bearing. This, in the long run, may be favorable since mechanical tolerances in the future may not need to be so tight for improved bearing performance.

4.1.4 Remaining Issues and Possible Solutions

Clearly, the major outstanding issue is the wobble performance. To correct this deficiency, Contraves must isolate the error sources by completing subsystem tests on the sensors, electromagnets, and control electronics. Another major issue, which is discussed in more detail in Section 5, is the control system dynamic performance and its effect on the angular (i.e., axis position and rate) control system. A system analysis of the control loops must be completed to optimize and characterize the bandwidth, disturbance rejection, and other dynamic performance parameters.

4.2 CFRP Inner Gimbal

4.2.1 Progress and Status

The ITATT Inner Gimbal was received from Composite Optics Inc. (COI) in San Diego, California in March of 1990 and machined and assembled into the inner axis by Contraves. This critical structural component was engineered by Contraves and COI and manufactured by COI.

During the conceptual engineering phase Contraves completed an FEM trade study which indicated a rectangular shape is preferable to a spherical shape and received the government's approval to build a rectangular gimbal. An important result of Contraves' FEM analysis is a set of quantified manufacturing tolerances which are needed to achieve the pointing accuracy error budget allocated to the gimbal. COI successfully achieved all the manufacturing tolerances required by Contraves. A more detailed discussion of the inner gimbal design is presented in Appendix A.

The inner gimbal is currently assembled into the inner axis and is performing as expected.

4.2.2 Data

COI completed several in-process manufacturing tests that produced the following results:

- The in-plane stiffness modulus of the CFRP laminate was measured from test coupons and found to be within the 10 percent variation requirement with an average value of 9 million psi.

¹ The measurements of drift and repeatability are limited by the background noise of the wobble measurement setup. See Section 4.7 for more information.

ITATT (K97012) Wobble Test - X/Y Plot

Axis: 3 07-20-1990 10:20
Scaling: 15 mm / arc second
Wobble: 0.5401 arc sec (O-Pk)
Avg Radius: 3.359 arc sec
Max Radius: 3.864 arc sec
Min Radius: 2.819 arc sec

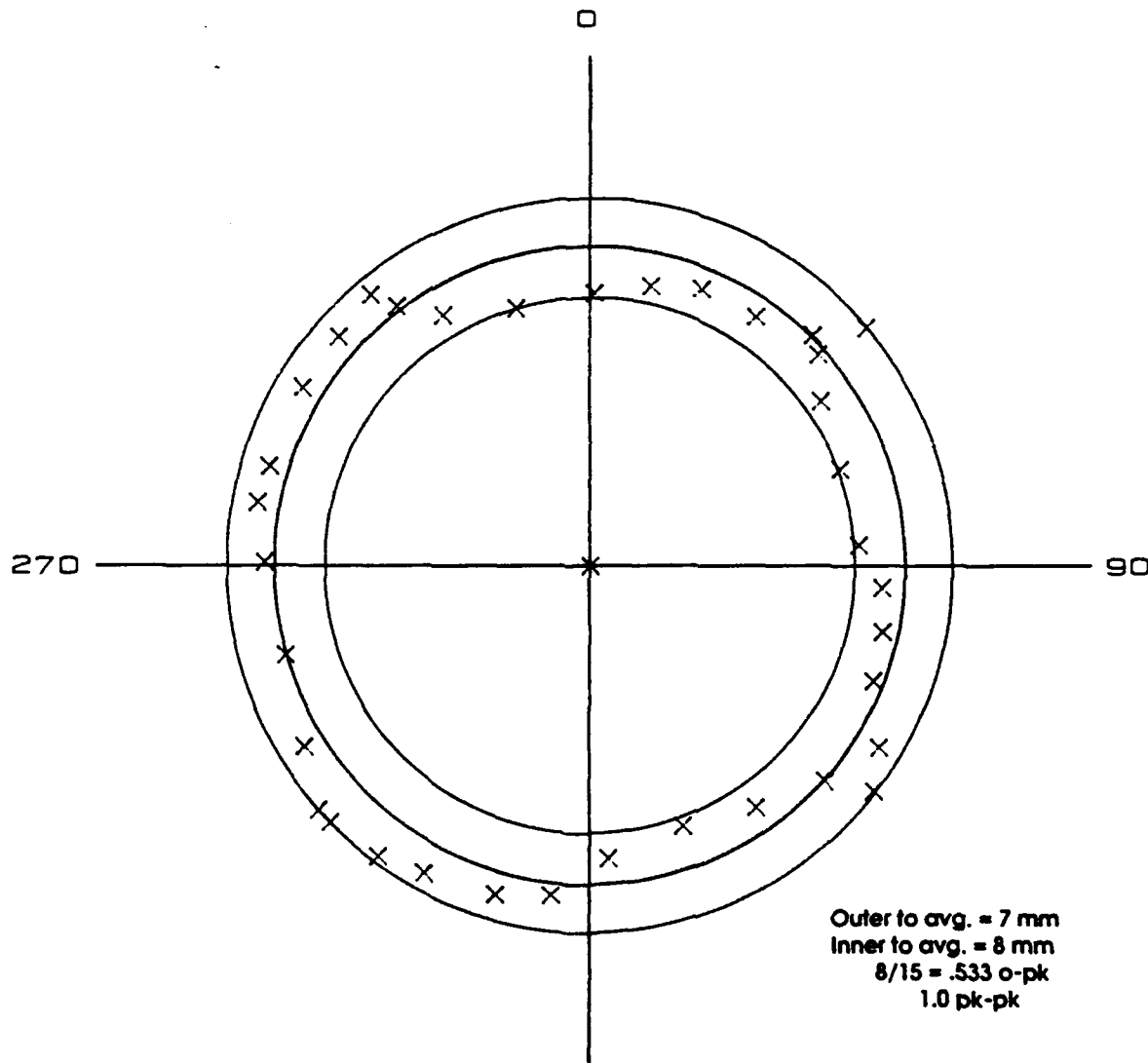


Figure 4-1. ITATT Wobble Data Mollen Wedel Collimator Mirror on Shaft.

We reserve all rights in connection with this document and in the subject matter represented therein. The recipient hereby acknowledges these rights and shall not, without our permission in writing, disclose or divulge this document in whole or in part to third parties or use it for any purpose other than that for which it was delivered to recipient.

X=213.18 Hz
Y_a=-3.0108 dB

FREQ RESP
20.0

dB

-20.0

Fxd Y 999.9m Log Hz

ITATT MAG BEAR M3-MR (Radial)

999.99

FREQ RESP
180

Phase

Deg

-180

Fxd Y 999.9m Log Hz

ITATT MAG BEAR M3-MR (Radial)

999.99

Figure 4-2. ITATT Radial Magnetic Bearing

We reserve all rights in connection with this document and in the subject matter represented therein. The recipient hereby acknowledges these rights and shall not, without our permission in writing, disclose or divulge this document in whole or in part to third parties or use it for any purpose other than that for which it was delivered to recipient.

- The in-plane coefficient of thermal expansion (CTE) was measured from test coupons and found to be within the 25 percent variation requirement with an average value of 0.6 ppm/deg F.
- All geometric tolerance requirements were met or exceeded. Contraves required that the gimbal surfaces be flat, square, and/or parallel to within 0.010 inches. In most instances 0.005 inches was achieved.

4.2.3 What Has Contraves Learned?

This is Contraves' first use of composite structures on an inertial navigation test table and several important lessons have been learned. One lesson is that precision composite applications are a very specialized niche of the general composites industry. The technologies used to make this gimbal are very different from the technologies used to make an airplane wing. The ITATT inner gimbal was manufactured using the same techniques used to manufacture space telescopes and optical benches. Another lesson is that the specific stiffness of the inner gimbal is much lower than predicted by preliminary studies and is about the same as aluminum. This is due to the need for the laminate to have in-plane isotropic properties. Thus, thermal dimensional stability is the primary advantage of the CFRP gimbal when compared to aluminum. This is due to the low in-plane CTE of the laminate and the special fabrication techniques used by COI to achieve the same CTE for the assembled gimbal.

4.2.4 Remaining Issues And Possible Solutions

A key issue that must be addressed is: should the middle and outer gimbals be rectangular or spherical? The essential trade off is between absolute stiffness and stiffness symmetry. A spherical gimbal is the stiffest configuration possible, but is difficult to manufacture to a high degree of precision. As the spherical gimbal rotates in the Earth's gravity, the absolute deflections are small, but the variations, due to manufacturing tolerances, may significantly degrade pointing accuracy. On the other hand, the rectangular gimbal can be manufactured with high precision, as achieved with the inner gimbal, but will have lower absolute stiffness. Thus, as a rectangular gimbal rotates the deflections variations will be small, but the larger absolute deflections may degrade pointing accuracy. A system FEM analysis and trade study must be completed to resolve this issue.

4.3 Encoding System

4.3.1 Progress and Status

The encoding system consists of the two 720-pole Inductosyns, mounted in a back-to-back arrangement, and two Encoder Input/Output Processor (EIOP) boards which are part of the Advanced Motion Control System (AMCS). This system is operating with one EIOP while the second EIOP is being calibrated off-line to provide improvements in encoding drift. A back-to-back calibration procedure has been generated that uses the ITATT hardware to determine the error curve of each inductosyn. This calibration procedure is automated to collect 16,384 data points over one 8-hour work shift.

4.3.2 Data

No data has been taken yet on the encoding system accuracy. However, Contraves has demonstrated drift and repeatability to less than 0.02 arc seconds for the EIOP and is confident that the ITATT requirement can be achieved.

4.3.3 What Has Contraves Learned?

Contraves has applied generic "back-to-back" calibration methods to an inductosyn-based encoding system. From this process we have learned that the back-to-back procedure is very sensitive to random encoder wobble and decentering errors. These errors can be introduced by the mechanical phasing mechanism and by the magnetic bearing and structure. One area of specific concern, addressed in Section 5, is the trunnion shaft wobble.

Contraves has also learned that some of the errors, inherent to inductosyns, occur at high frequencies and, therefore, require high frequency data sampling to be measured. To make this calibration feasible, Contraves has automated the data collection process and uses special data reduction methods to allow the high frequency inductosyn errors to be characterized with lower frequency sampling. This approach is presented in more detail in Appendix B.

4.3.4 Remaining Issues And Possible Solutions

Several issues remain for the encoding system. The back-to-back encoder calibration has not yet been performed because other subsystem efforts have delayed the installation of the calibration inductosyn. While the back-to-back calibration algorithms have been simulated successfully, the procedure must still be demonstrated.

4.4 Roll Rings

4.4.1 Progress And Status

The roll ring unit was received at Contraves in July, 1990. All mechanical dimensions were per the vendor control drawing. One hundred of the 120 circuits meet the 100 milliohm noise spec. Pairing by numerical order results in 53 out of 60 pairs being within specification. Selected pairing (high and lows together) will result in all 60 pairs being within the 100 milliohm noise specification. Contraves has not yet installed or tested this roll ring in the inner axis. The complete test report from Honeywell is provided in Appendix D.

4.4.2 Data

<u>Specification</u>	<u>Actual</u>
• 120 parallel circuits	Same
• 3 amp continuous rating	Same (Except circuits 97 and 101 which have flexures that are too small and therefore, will not handle the current.)
• 0.16-0.2 ounce inch starting torque	0.18-0.38
• 200 RPM maximum speed	Same
• 100 milliohm per pair maximum dynamic resistance variation	Same if using selected pairing (highs and lows together)
• Insulation resistance:	
1000 M ohms Lead to Lead	10 ⁴ -10 ⁶ Mega ohm
1000 M ohms Lead to Ground	20K-200K Mega ohm (1)
1000 M ohms Lead to Shield	20K-2x10 ⁶ Mega ohm (2)
• -70dB minimum (circuit to circuit) isolation at 1KHz into 0 50 Ω load.	(1) Except circuit 1 had 1.4K Mega ohm and circuit 120 had 13 Mega ohm. (2) Except circuit 13 had 2K Mega ohm resistance 90 min. - 100 max.

4.4.3 What Has Been Learned?

Many improvements in roll ring technology have resulted from manufacture of this roll ring:

- Processes for machining and plating of the flexures are well defined and are producing excellent quality flexures.
- Improved tooling for inspection and assembly of the flexures have decreased assembly times and the noise variation in each circuit. The next roll ring built should have all circuits with less than 10 milliohm (maximum) noise.
- Because of the above improvements, commercial slipring manufacturers (i.e., Electro-Tec and Litton) are capable of and very interested in building roll rings in a competitive environment.

4.4.4 Remaining Issues And Possible Solutions

Roll ring improvements in the future could include the following:

- Improved tooling for packaging of the rotor lead wires. This would decrease assembly times and lessen the chance of rotor lead wire damage.
- Fatigue perturbation studies that would result in reduced manufacturing tolerances and thereby lower manufacturing costs of the roll ring.

4.5 Drive System

4.5.1 Progress And Status

The drive system consists of the slotless, brushless DC permanent magnet motor manufactured by Inland Motors and the Three Phase Linear Power Amplifier manufactured by Contraves. The motor has been installed in the simulator and the drive system is presently fully operational and meeting the specifications.

4.5.2 Data

This test data has been collected:

	<u>Specification</u>	<u>Actual</u>
Peak Torque	5 ft.lb.	5.2 ft.lb.
Max Rate	1000 deg/sec	Same
Friction	0.09 ft.lb.	0.02 ft.lb.
Cogging Torque	0.004 ft.lb.	0.003 ft.lb.

Based upon the cogging torque data of 0.003 ft.lb. as measured by the motor vendor, the rate stability error due to cogging can be predicted. Figure 4-3 shows that for a 100Hz bandwidth system, cogging will contribute to 0.13 ppm of the 1 ppm error budget at 1000 deg/sec.

4.5.3 What Has Been Learned?

The slotless, brushless DC permanent magnet motor is the first of its kind and results in extremely low cogging torques. Typically, a brushless DC permanent magnet motor has a cogging torque of 1 percent while this slotless motor has a cogging torque of only 0.06 percent.

The motor has been wound to generate trapezoidal back EMF voltages while the power amplifier and motor commutation have been designed to generate sinusoidal drives. This will result in a slightly increased torque ripple. The effect on rate stability, however, will be minimal due to the very low system friction. In the future, the ITATT motors will be sinusoidally wound for optimum torque ripple.

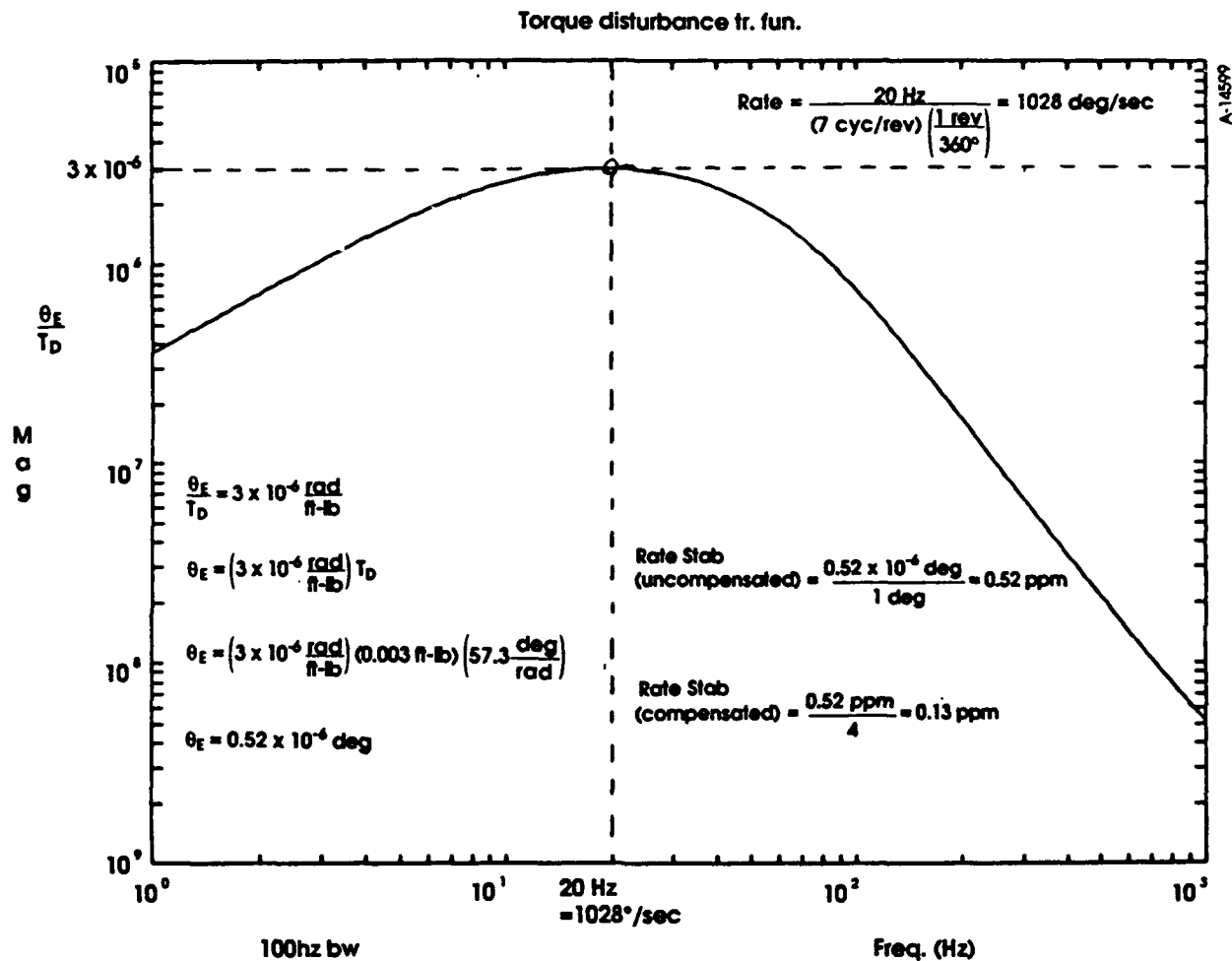


Figure 4-3. ITATT Phase I Rate Stability due to Cogging Torque

We reserve all rights in connection with this document and in the subject matter represented therein. The recipient hereby acknowledges these rights and shall not, without our permission in writing, disclose or divulge this document in whole or in part to third parties or use it for any purpose other than that for which it was delivered to recipient.

4.5.4 Remaining Issues And Possible Solutions

Rate stability tests still need to be performed to verify the predicted effect of the cogging torque.

4.6 Control System

4.6.1 Progress and Status

The ITATT Phase 1 AMCS rotational control system has been implemented using one Intel SBC386 MultiBus I computer board, one primary EIOP for control feedback and digital I/O, one calibration EIOP for encoding positions from the calibration inductosyn during the back-to-back procedure, and one Zeos 386SX PC which is connected to the SBC386 board via two communications links: RS-232C and GPIB (via a National Instruments GPIB-AT adapter in the PC).

The communications protocol, which is exactly the same for both channels, is ASCII character based and is IEEE-488.2 compliant. While most of our work thus far has employed the serial channel, both channels have been tested and are fully operational. PC-based software has been written for exercising both communications channels in order to provide the following system capabilities:

Serial: - Load and start up the ITATT AMCS control software.
- Simple command line entry of any ITATT command or query.
- Download of command/query sequences from a disk file for automating system operation.
- Capture realtime position or rate data to a disk file.

GPIB: - Perform rate stability data collection and processing.
- Perform back-to-back calibration data collection and processing.

The analog I/O capabilities of the ITATT AMCS have been successfully employed to measure the plant response and the control system response in the two control modes (see Figures 4-4 through 4-6):

1. Type III position loop using the encoder position as the feedback signal.
2. Type II rate loop using the observer rate state as the feedback signal.

Bandwidths achieved for these loops thus far are approximately 53 Hz and 40 Hz for the Type III and the Type II loops respectively.

4.6.2 Data

See Figures 4-4, 4-5 and 4-6 for frequency response data.

Figure 4-4: Plant Response Curve
Figure 4-5: Type III Position Loop Response Curve
Figure 4-6: Type II Rate Loop Response Curve

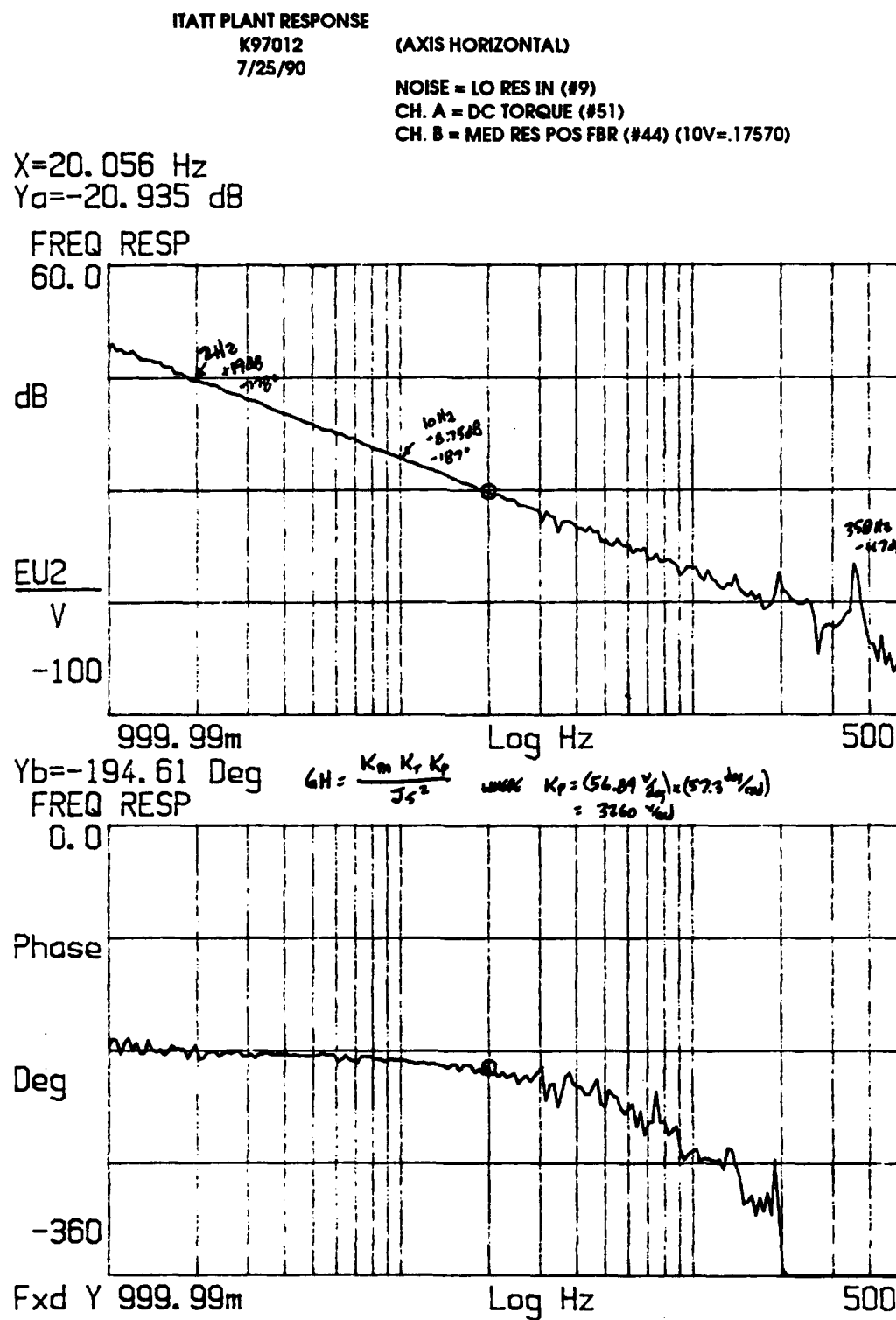


Figure 4-4: Plant Response Curve

We reserve all rights in connection with this document and in the subject matter represented therein. The recipient hereby acknowledges these rights and shall not, without our permission in writing, disclose or divulge this document in whole or in part to third parties or use it for any purpose other than that for which it was delivered to recipient.

ITATT TYPE III POS LOOP
K97012 7/26/90 11:30 (AXIS HORIZONTAL)

NOISE &	- TORQUE CMP (#1)	COMP. CONSTANTS
CH. A		4379.0823
CH. B	- RATE COMP OUT (#50)	-43528078
		SOURCE = 2V

X=13.591 Hz
Y_a=-17.049dB

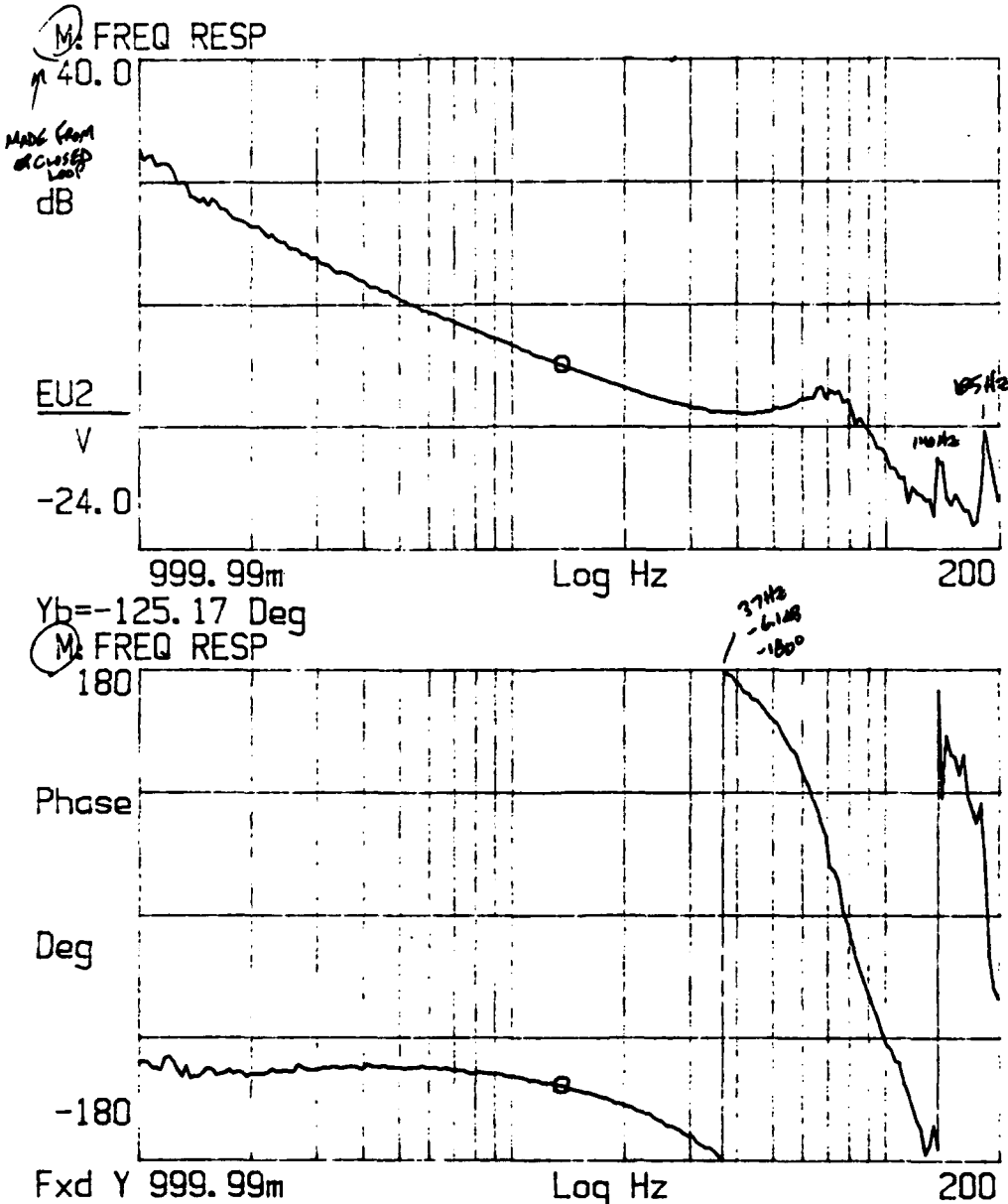


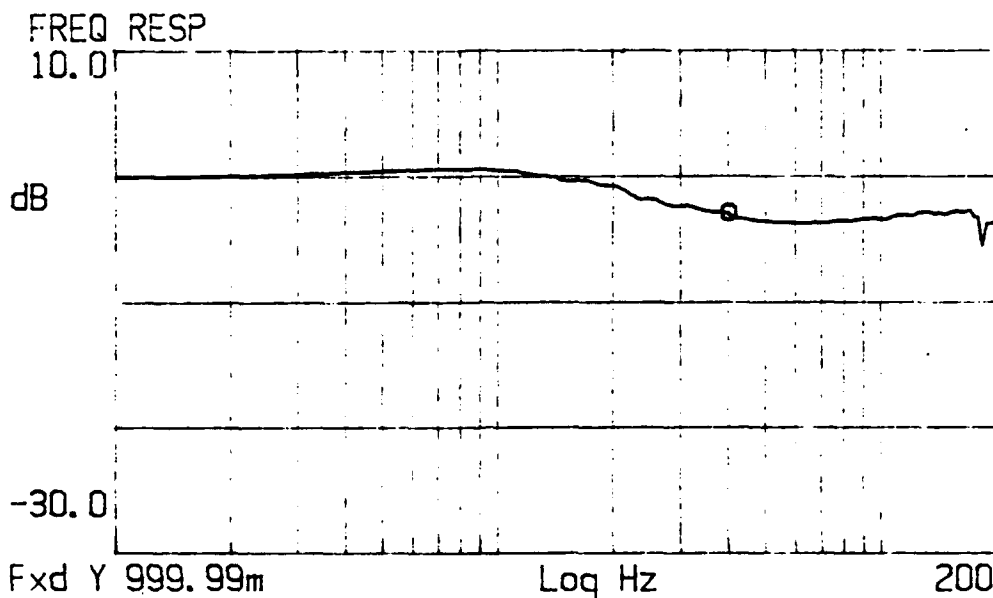
Figure 4-5: Type III Position Loop Response Curve

We reserve all rights in connection with this document and in the subject matter represented therein. The recipient hereby acknowledges these rights and shall not, without our permission in writing, disclose or divulge this document in whole or in part to third parties or use it for any purpose other than that for which it was delivered to recipient.

TYPE II RATE LOOP WITH STATE ESTIMATOR (AXIS HORIZONTAL)
K97012 7/27/90 9:30

NOISE &		COMP. CONSTANTS	ELGIN & 2
CH. A	- TORQUE CMP (#1)	+31086.83	.83923
CH. B	- RATE COMP OUT (#50)	-29935.82	254.1606

X=40.003 Hz
Y_a=-3.0141 dB



Y_b=-111.41 Deg

FREQ RESP

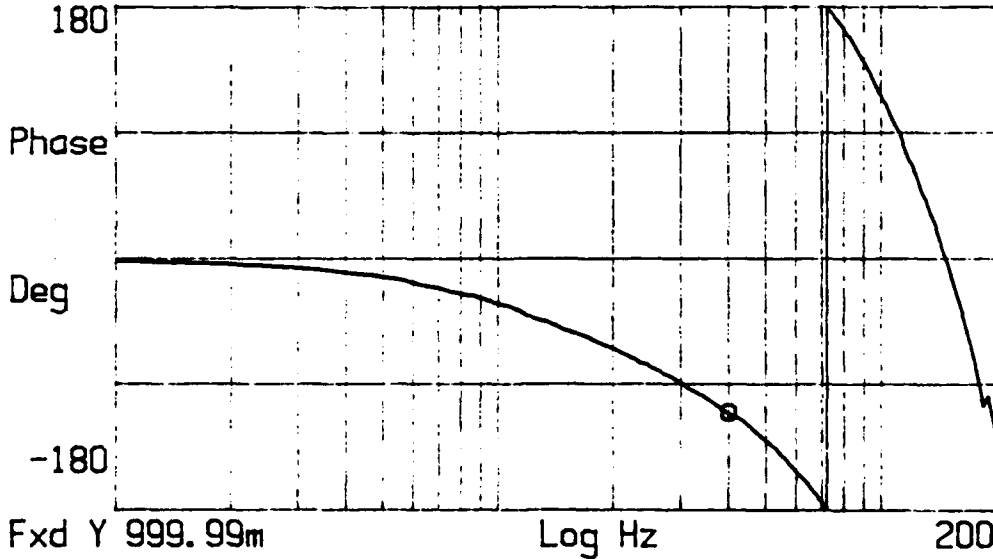


Figure 4-6: Type II Rate Loop Response Curve

We reserve all rights in connection with this document and in the subject matter represented therein. The recipient hereby acknowledges these rights and shall not, without our permission in writing, disclose or divulge this document in whole or in part to third parties or use it for any purpose other than that for which it was delivered to recipient.

4.6.3 What Has Contraves Learned?

1. We have confirmed the efficacy of our rotational control hardware and software architectures.
2. We have confirmed the suitability of our digital control algorithms and have verified their implementation in software. The digital controllers react in a predictable way to changes in the compensation constants.

4.6.4 Remaining Issues And Possible Solutions

Two disturbances are present in the angular encoding system which significantly hinder our rate stability. A twice per degree disturbance is present and is most probably due to errors in the EIOP's non-volatile Inductosyn constants. A once per degree disturbance is also present and is most likely due to Inductosyn drive signal coupling into the Inductosyn feedback. To solve this problem the EIOPs are being modified to calibrate against a reference during system operation continually, rather than depend upon the stored results of a one-time calibration as they currently do. The power supply and signal grounding scheme needs to be verified in order to eliminate any encoder signal coupling.

Another open issue is a mechanical resonance at 400 Hz which may make a 200 Hz bandwidth unfeasible. The short term solution is to insert an analog notch filter to eliminate the resonance's effect. However, the long term solution is to complete a control systems analysis to evaluate the feasibility of a 200 Hz bandwidth given the mechanical resonances and interaction with the magnetic bearings (see Section 5).

4.7 Test And Validation Methods

4.7.1 Progress And Status

The ITATT test and validation plans and procedures were submitted to the government in November 1989. (See Contraves acceptance test plans ATP-27498 and ATP-27501.) These plans have been updated in 1990 and are currently being resubmitted for government approval. A key element of this acceptance test plan is the Moller Wedel Elcomat 2HR collimator with 0.001 arc second resolution. This collimator was received by Contraves in July 1990 and has been used to collect wobble data on the magnetic bearing.

4.7.2 Data

The Moller Wedel collimator worked well in measuring the 0.5 arc second wobble of the magnetic bearing. However, a background noise measurements (i.e., measurements with the magnetic bearing and AMCS turned off) show that the test setup and environment produce approximately 0.1 arc seconds of noise. A plot of this background noise is shown in Figure 4-7.

Autocollimator Readings - mirror and autocol on granite
10 minute sample period

$\approx 2 \text{ sec}/\text{rdg} - 10 \text{ rdg avg}$ ($\approx .3 \text{ sec of data per read}$)

295 data points

(Elcomat had 24 hr. warmup-test run 17:30, 14 Avg)

X avg = 17.201 sec

X max = 17.260

X min = 17.085

Y avg = 18.961 sec

Y max = 19.025

Y min = 18.863

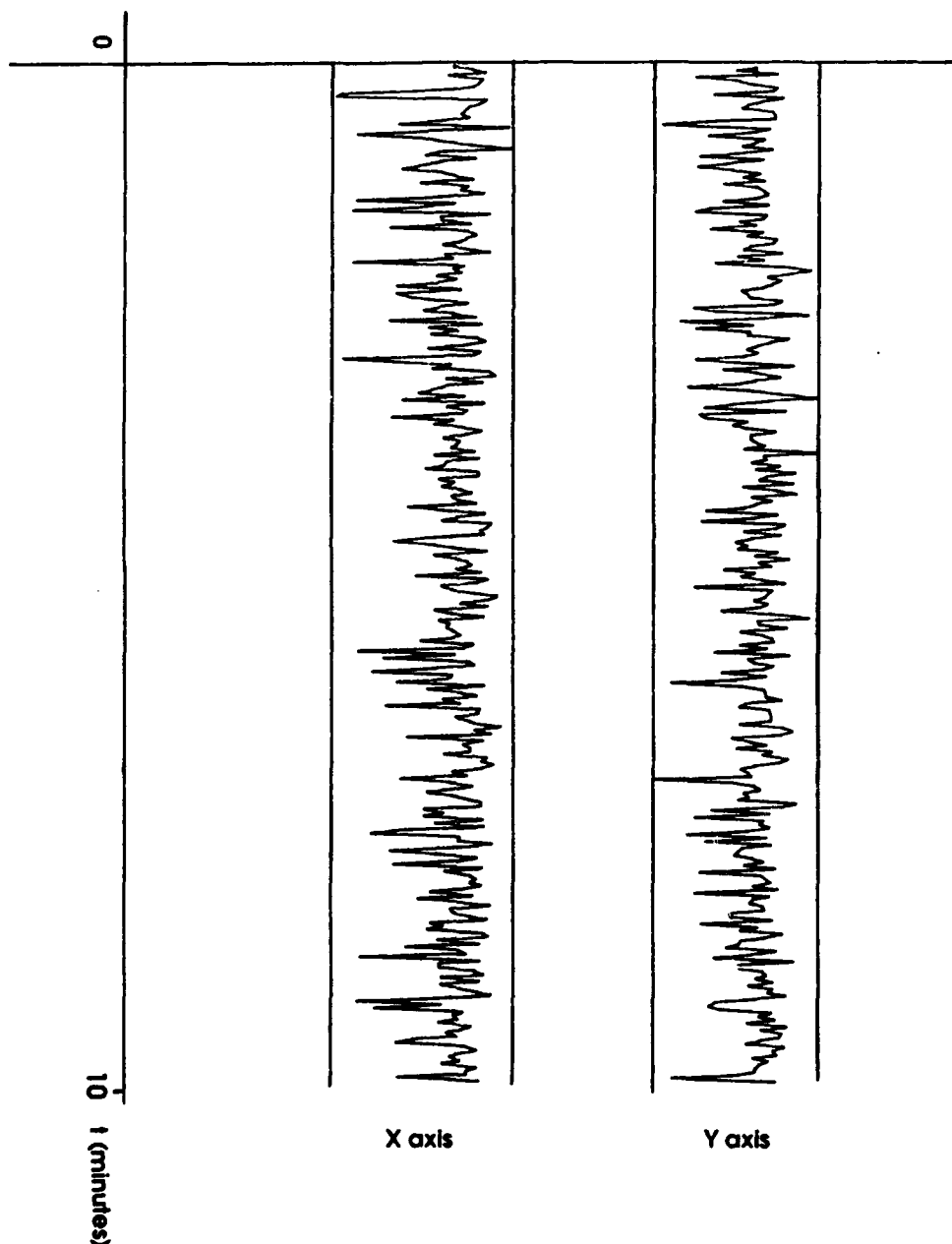


Figure 4-7.

We reserve all rights in connection with this document and in the subject matter represented therein. The recipient hereby acknowledges these rights and shall not, without our permission in writing, disclose or divulge this document in whole or in part to third parties or use it for any purpose other than that for which it was delivered to recipient.

4.7.3 What Has Contraves Learned?

Contraves has learned that test and validation of the ITATT is essentially noise limited. The ITATT specification is 0.02 arc seconds and the current background noise is 0.1 arc seconds. Thus, while the theoretical accuracy and resolution of the Moller Wedel collimator is sufficient to test the ITATT, the current test environment noise is five times the ITATT specification.

4.7.4 Remaining Issues And Possible Solutions

Background noise is the major issue affecting test and validation and is most likely caused by seismic floor vibrations, and air temperature, pressure, and humidity variations. Contraves recommends that the current test setup be tested and analyzed for these effects and appropriate design changes implemented.

5 NEW HIGH RISK AREAS IDENTIFIED IN PHASE I

Several new high risk areas have been identified during the first 14 months of Phase I that make it unreasonable for Contraves to accept a firm fixed price Phase II as currently defined. This section identifies these new issues and makes recommendations on how to reduce their risk.

5.1 Trunnion Shaft Thermal Distortion

During the 95 percent design review, Contraves identified shaft thermal distortion as a potential source of large wobble errors. (See Contraves report TR-27518, ITATT Thermal Analysis, previously submitted to the government.) The permanent solution proposed by Contraves, in December 1989, was CFRP shafts. This is an expensive option which the government chose not to implement. Thus, the problem remains. Contraves recommends that additional FEM structural and thermal analysis trade studies be completed with the goal of finding an acceptable and cost-effective solution.

5.2 Gimbal Configuration

The current requirement is for spherical middle and outer axis gimbals. Manufacturing tolerance and cost considerations, however, may require rectangular gimbals. This issue is discussed in more detail and recommendations made in Section 4.2.4.

5.3 Trunnion Shaft Wobble Affecting The Inductosyns

FEM analysis of the inner axis (see Contraves report TR-27463, Finite Element Analysis And Software Specification For ITATT Phase I, previously submitted to the government) indicates that the inner axis trunnions will have angular deflections significantly greater than the ITATT wobble specification. This is true for any gimbal configuration and is due to the fact that the magnetic bearings have essentially zero moment stiffness. Thus, as the inner gimbal is "tumbled" by the middle and outer axes the trunnion shafts will wobble and degrade the accuracy of the Inductosyns. This phenomenon is discussed in further detail in Appendix A.

Contraves recommends that the inductosyn sensitivity to wobble be measured using the existing hardware. The magnitude of this sensitivity will determine if corrective action must be taken. In addition, Contraves proposes to build the middle axis under Phase I, to allow direct measurement of the inductosyn errors as the middle axis tumbles.

5.4 Limitations Of Current Test Equipment

Preliminary tests using the Moller Wedel collimator, with 0.001 arc second resolution, indicate that the background noise in Contraves' facility is approximately 0.1 arc seconds. (See Section 4.7.) This is five times the ITATT requirement of 0.02 arc seconds and is most likely caused by room vibrations and air temperature, pressure, and humidity variations.

Contraves recommends that testing continue, using the current test setup, until the wobble performance is demonstrated to be less than the background noise. At the same time Contraves will investigate alternative environmental controls for the ITATT test area and propose a solution to the government.

5.5 Multi-Axis Control System Interactions

The ITATT is unique in that the rotating components of each axis are completely suspended by actively controlled magnetic fields. The magnetic bearing on each axis "fixes" five degrees of freedom (DOF) while the sixth and final DOF is controlled by the AMCS. Thus, the magnetic bearing holds the axis in the same manner as a mechanical or air bearing and the AMCS accurately positions the rotational axis.

A critical assumption of the 1984 ITATT design study is that active control of the magnetic bearings and AMCS can be separated into independent problems. This approach ignores the torque/force coupling from axis to axis and can only work if the coupling is weak or the bearing servo bandwidth is sufficient to reject the coupling torque/force disturbances. In addition, a multi-axis system will tumble the inner axes and subject the inner axis magnetic bearings to sinusoidally varying gravitational loads. Thus, the magnetic bearing must be insensitive to load orientation.

Unfortunately, Phase I is a single axis prototype that cannot test these control system assumptions. In addition, the preliminary test data shows that the magnetic bearing and AMCS bandwidths are of similar magnitude and are likely to interact. Therefore, the Phase II multi-axis control system design is a high risk task.

To reduce the risk of Phase II, Contraves proposes to complete a detailed analysis of the multi-axis coupling between the magnetic bearing and AMCS as described in Appendix C. In addition, to confirm the results of this analysis, Contraves will design and manufacture the middle axis as part of Phase I. By building the middle axis under the Phase I, a major risk source for Phase II is eliminated.

6 CONTRAVES' PROPOSAL FOR COMPLETING PHASE I AND PHASE II

This section describes Contraves' recommendation for completing the ITATT program. Described is the general technical approach and rational for completing an extended Phase I and reduced Phase II with the end result being unchanged from the original plan. A separate proposal provides the detailed scope of work and corresponding price and schedule.

6.1 First Priority: Identify and Solve Inner Axis Deficiencies

Contraves proposes to continue testing the inner axis hardware, within the current support frame and on a separate air bearing, to fully characterize its performance. The air bearing test hardware is shown in Figures 6-1 and 6-2. In parallel with these test efforts, Contraves will complete mechanical and electrical system level analysis to evaluate the current design approach as a multi-axis machine. Contraves will then use the lessons learned from this testing and analysis to modify the current inner axis design and complete the middle axis design.

6.2 Second Priority: Reduce Phase II Risk By Building The Middle Axis

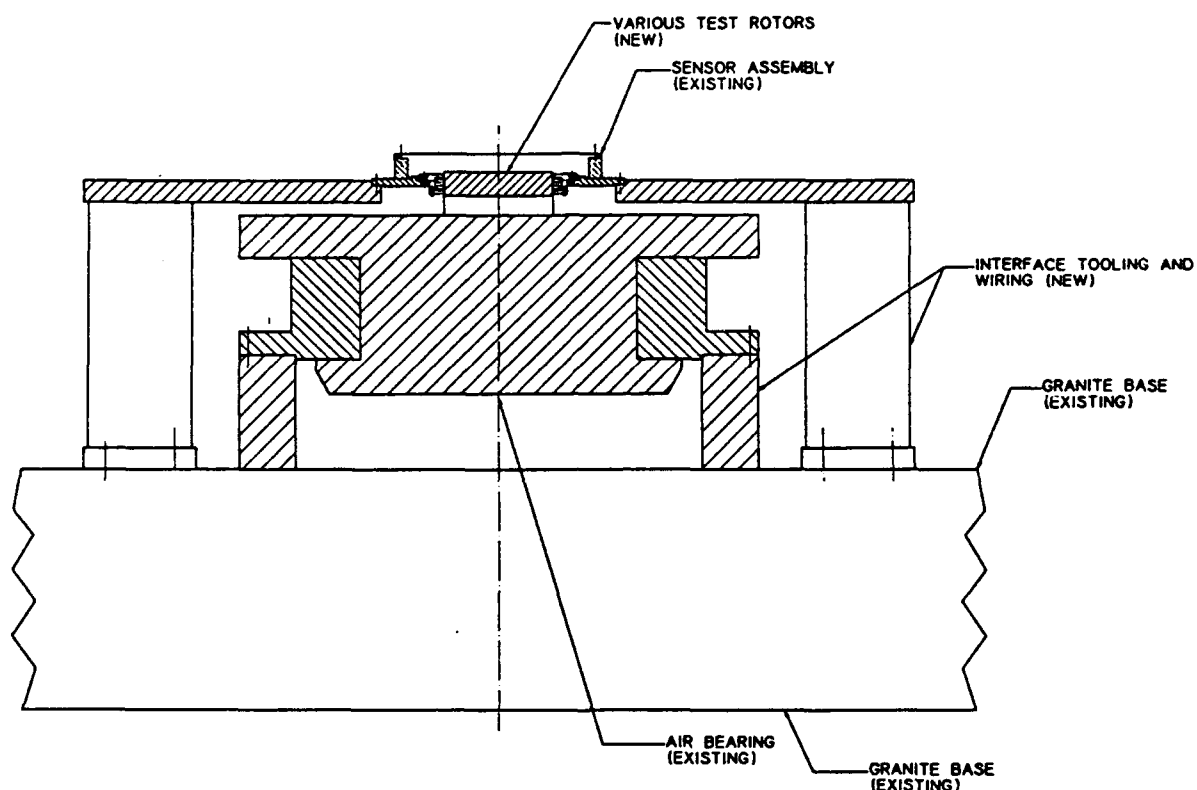
After the inner axis deficiencies have been corrected, Contraves proposes to complete an extended Phase I effort which will include some work that was previously part of Phase II. This recommendation is based on the discovery, during the last 14 months, of several new high risk areas that will not be addressed within the current Phase I scope. This risk is sufficiently large that it should not be included as part of a firm fixed price Phase II. Thus Contraves proposes to address these problems under an extended Phase I effort so that the risks can be mitigated before Phase II.

- Unknown Multi-Axis Effects

The most serious of these problems are the unknown effects of placing the inner axis inside the middle and outer axes. At least two multi-axis effects are of concern. The first concern is that the interactions between the magnetic bearing control system and the AMCS control system may produce unexpected pointing errors and also may fundamentally limit bandwidth. These control system interactions are only present with a multi-axis system. The second concern is that the inner axis "tumbling", due to the middle and outer axis rotations, may significantly degrade the position accuracy. Therefore, Contraves proposes to build the middle axis of the ITATT in Phase I to allow these problems to be evaluated. A drawing of the Inner and Middle Axes is shown in Figure 6-3.

6.3 Completing Phase II

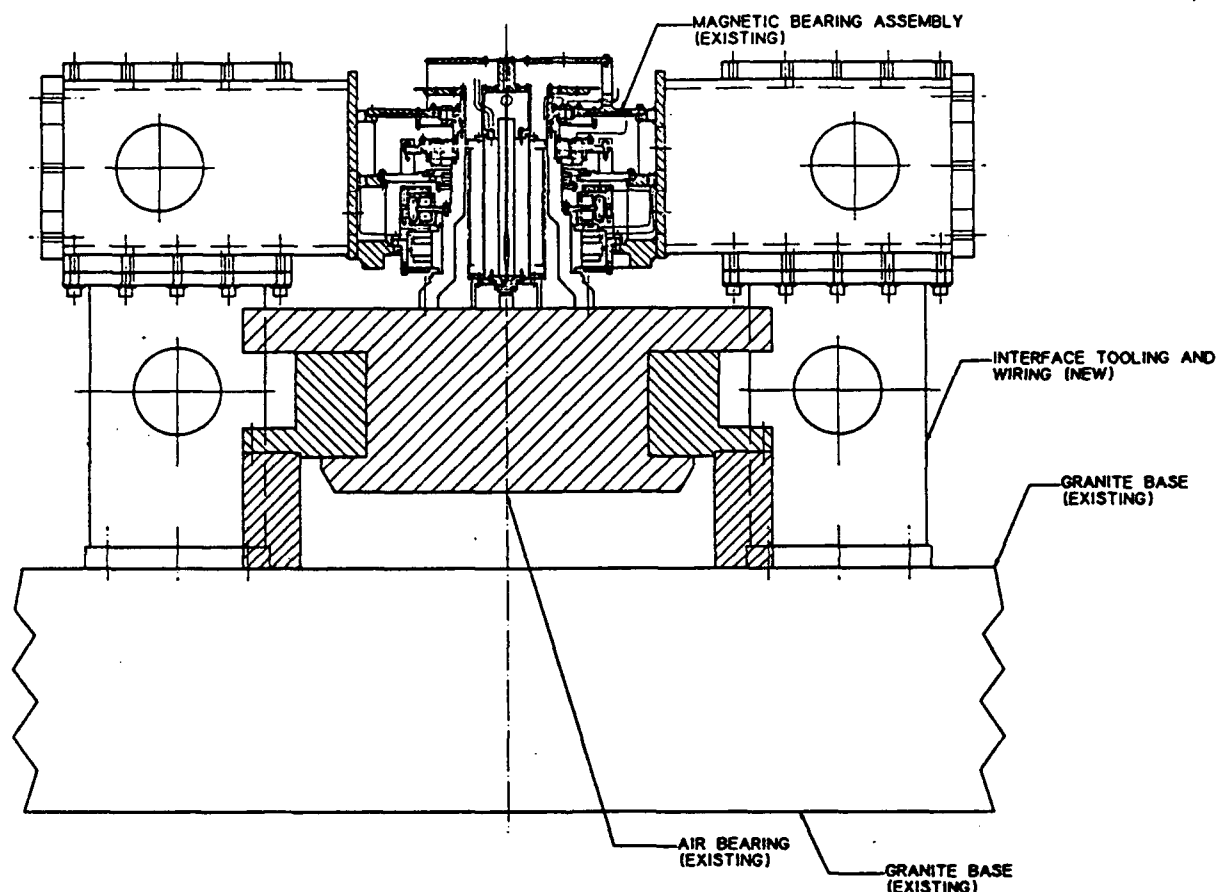
After successively testing the inner and middle axes in Phase I, the Phase II risk will be significantly reduced. Thus, Phase II can be realistically completed on a fixed price basis. The scope of Phase II will include the design and fabrication of the outer axis and the assembly, wiring, integration, and testing of the complete three-axis system and this configuration is shown in Figure 6-4.



RADIAL SENSOR TEST USING AIR BEARING

Figure 6-1. Radial Sensor Test Using Air Bearing

We reserve all rights in connection with this document and in the subject matter represented therein. The recipient hereby acknowledges these rights and shall not, without our permission in writing, disclose or divulge this document in whole or in part to third parties or use it for any purpose other than that for which it was delivered to recipient.



MAGNETIC BEARING SYSTEM TEST USING AIR BEARING

Figure 6-2. Magnetic Bearing System Test Using Air Bearing

We reserve all rights in connection with this document and in the subject matter represented therein. The recipient hereby acknowledges these rights and shall not, without our permission in writing, disclose or divulge this document in whole or in part to third parties or use it for any purpose other than that for which it was delivered to recipient.

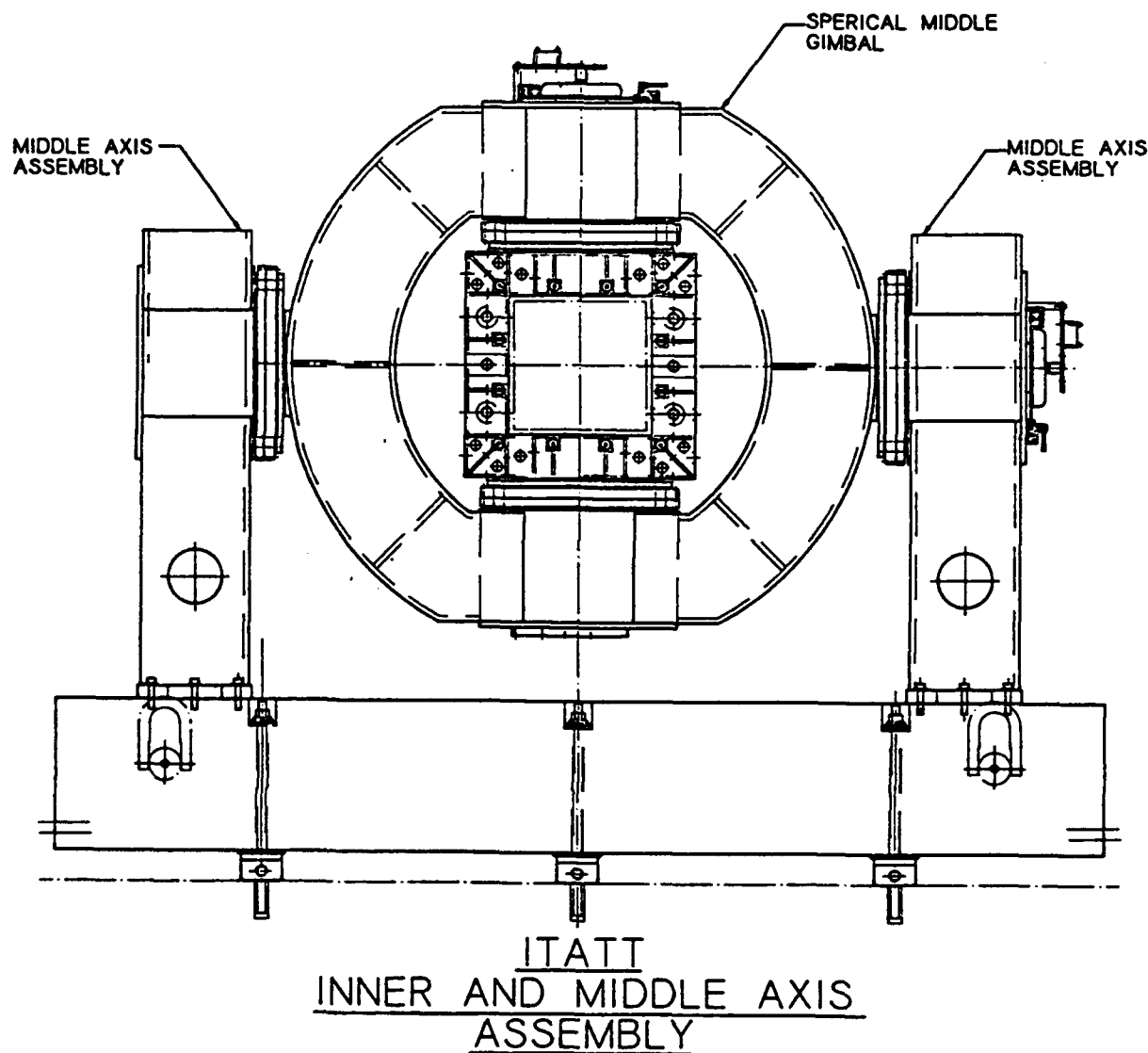


Figure 6-3. ITATT Inner and Middle Axis Assembly

We reserve all rights in connection with this document and in the subject matter represented therein. The recipient hereby acknowledges these rights and shall not, without our permission in writing, disclose or divulge this document in whole or in part to third parties or use it for any purpose other than that for which it was delivered to recipient.

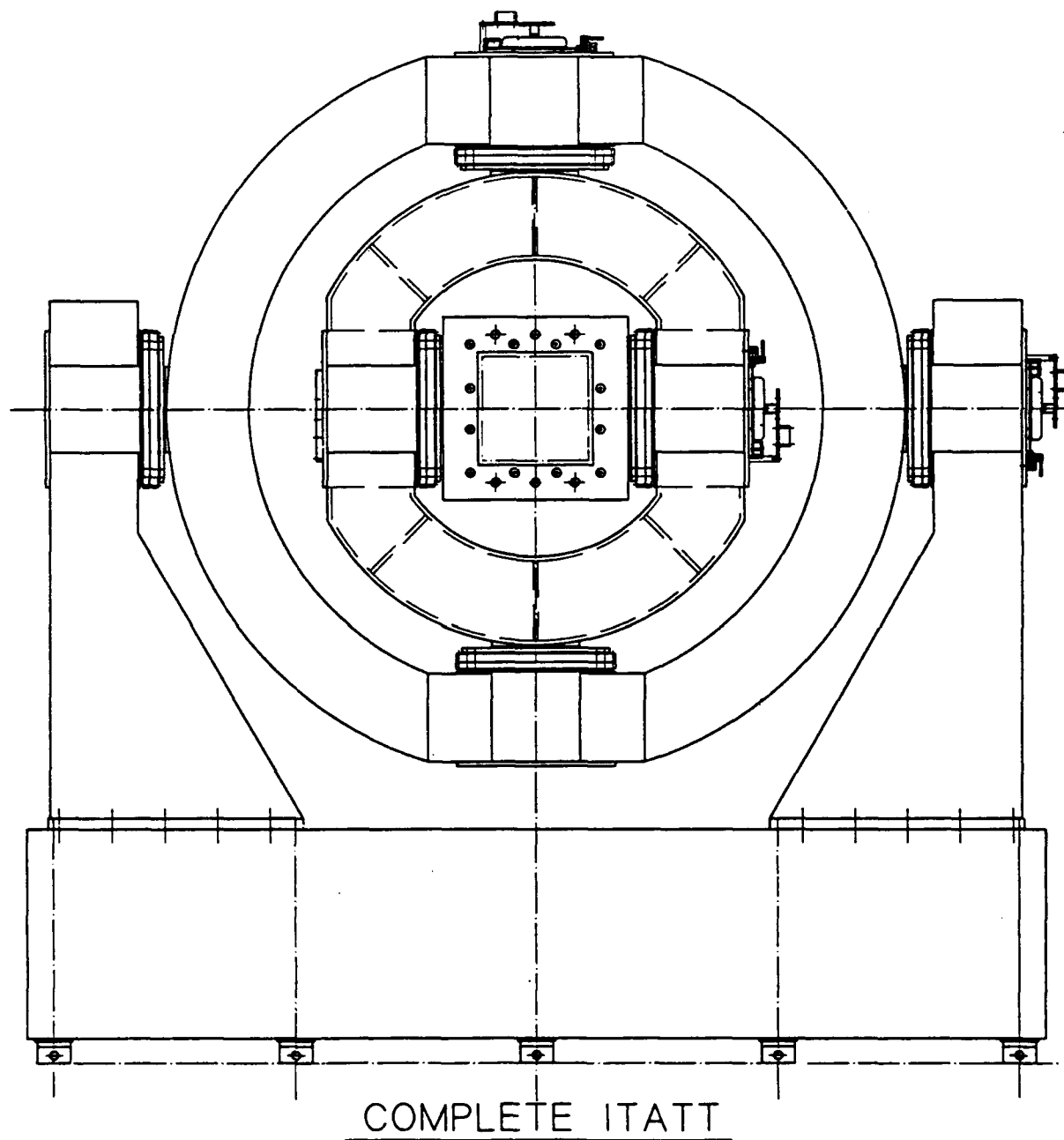


Figure 6-4. Complete ITATT Assembly

We reserve all rights in connection with this document and in the subject matter represented thereon. The recipient hereby acknowledges these rights and shall not, without our permission in writing, disclose or divulge this document in whole or in part to third parties or use it for any purpose other than that for which it was delivered to recipient.

APPENDIX A

TR-27630

We reserve all rights in connection with this document and in the subject matter represented therein. The recipient hereby acknowledges these rights and shall not, without our permission in writing, disclose or divulge this document in whole or in part to third parties or use it for any purpose other than that for which it was delivered to recipient.

Development of a composite gimbal for a high precision inertial guidance test table

Brian Cuerden and David Henderson

Contraves USA
610 Epsilon Drive, Pittsburgh, PA 15238

ABSTRACT

This document discusses material selection, design, and analysis of a composite gimbal for use on a high precision inertial guidance test table with active magnetic bearing suspension. The test table's system performance goals of 0.1 arc second angular pointing accuracy and one part per million angular rate stability, can only be achieved by using a gimbal with high specific stiffness, highly symmetric elastic properties, and high dimensional stability. These characteristics are achieved by proper selection of the gimbal's construction material, configuration, and fabrication processes.

Both traditional and advanced composite materials are considered and evaluated for specific stiffness, coefficient of thermal expansion, thermal conductivity, dimensional stability, fabrication problems, and cost. Using the candidate materials, several gimbal configurations are evaluated with respect to the test table's system performance goals for angular pointing accuracy and angular rate stability. Specific gimbal design parameters affecting the system performance goals for angular pointing accuracy and angular rate stability include: the angular payload deflections due to torsional wind-up and asymmetrical stiffness; the linear payload deflections that cause torque disturbances and shaft wobble; and the natural frequencies affecting the control system bandwidths. Detailed finite element models of each configuration are used to predict the performance characteristics and demonstrate the advantages of the graphite/epoxy composite design.

INTRODUCTION: WHAT IS THE APPLICATION OF THIS GIMBAL?

The composite gimbal is a key component of the Improved Three-Axis Test Table (ITATT) program for the USAF Central Inertial Guidance Test Facility at Holloman AFB. The goal of this program is to improve the state-of-the-art in inertial guidance testing by two orders of magnitude. The specific ITATT system performance requirements are a pointing accuracy of 0.1 arc second, a rate stability of one part per million, and a servo bandwidth of 200 Hz.

Phase I of the ITATT program is currently underway and is the development of a single axis "proof of principle" prototype that is shown in Figure 1. This single axis prototype will be the inner axis of the complete three-axis machine and includes the rotating gimbal, trunnion shafts, active magnetic bearing suspension, a low cogging torque motor, and dual Inductosyn encoders.

What are the performance requirements of the Inner Axis Gimbal?

The overall ITATT system performance requirements place a stringent set of requirements on the gimbal structure. The flow down of these ITATT system requirements to the gimbal is shown in Table 1. The essential gimbal requirements are high specific stiffness, high absolute stiffness, high stiffness symmetry, and high dimensional stability for both the construction material and the configuration. These attributes are needed to make the gimbal act as close to a rigid body as possible. For example, the gimbal stiffness must be sufficient to make all elastic payload angular deflections negligible under any gimbal load orientation. In addition, the dimensional stability must be sufficient to make long and short term gimbal angular distortions negligible.

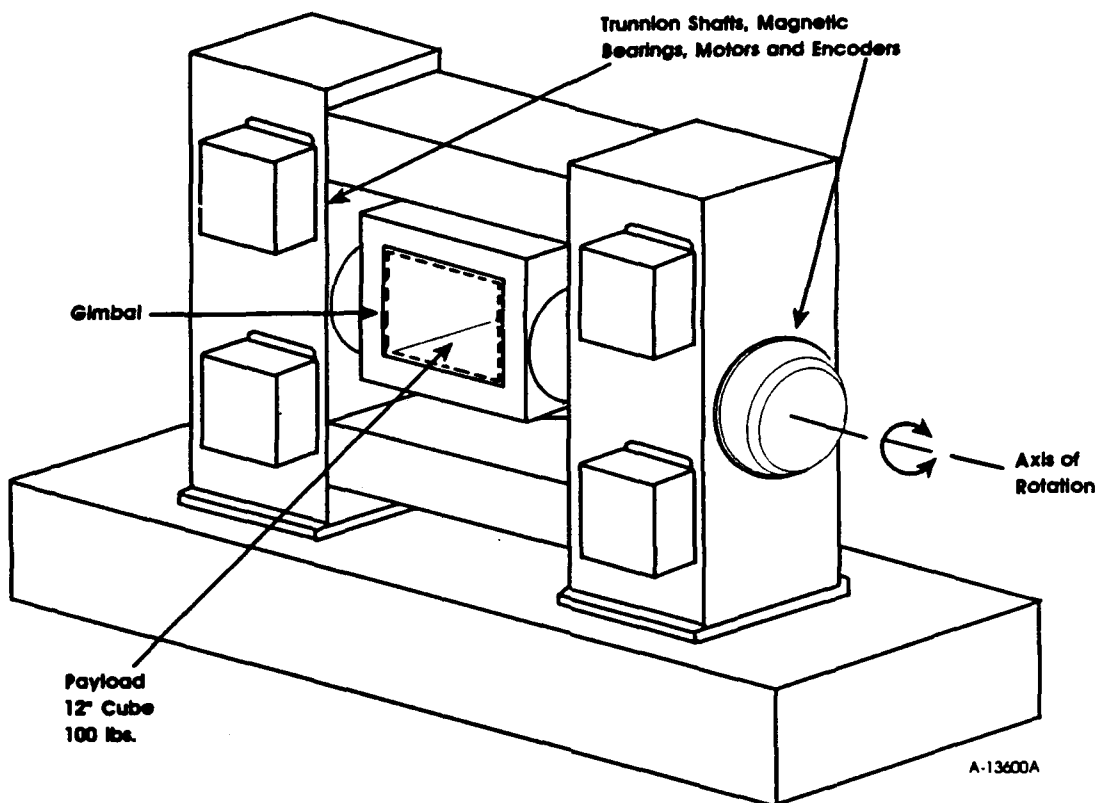


Table 1.
Flow Down of ITATT System Performance Requirements to the Gimbal

<u>System Requirements</u>	<u>Gimbal Requirements</u>	<u>Specific Performance Requirements</u>
0.1 arc second Pointing Accuracy	Support payload with: (100 lb, 12-inch cube) - Stiffness Symmetry - High Stiffness - Dimensional Stability	Negligible angular distortion achieved by: - Low Modulus Variations - High Specific Modulus - High Absolute Modulus - High Transient Thermal Distortion Index - Negligible Hydroscopic and Microcreep Effects - Tight Manufacturing Tolerances
1 ppm Rate Stability	Support payload with: - High Torsional Stiffness - Stiffness Symmetry	Negligible rate errors achieved by: - Low Modulus Variations - High Specific Modulus - High Absolute Modulus - Close Manufacturing Tolerances
200 Hz Bandwidth	Support payload with: - High Torsional Resonances	Resonances greater than 600 Hz achieved by: - High Specific Modulus - High Absolute Modulus

THE KEY DEVELOPMENT ISSUES: MATERIAL AND CONFIGURATION

The gimbal development effort can be divided into two key issues: the selection of the material and the selection of the configuration. To a large extent these decisions can be made independently; the one exception being the manufacturing issues. For example, the material selected may require certain fabrication processes that limit the possible shapes of the final gimbal. Within these manufacturing limitations, the gimbal development is presented as two tasks: material analysis and configuration analysis.

MATERIAL SELECTION ANALYSIS

Several construction materials were considered for the ITATT inner gimbal and their performance characteristics evaluated against the gimbal's requirements for stiffness and stability. The conventional materials considered are aluminum, titanium, magnesium, Invar, and beryllium which are homogeneous metal alloys. The non-standard materials considered are SiC aluminum and graphite epoxy. SiC aluminum is a metal matrix composite that mixes 20 percent silicon carbide particles into an aluminum matrix to produce a homogeneous material. Graphite/epoxy is an advanced composite material that bonds continuous graphite fibers together in an epoxy matrix to produce an in-plane isotropic material.

The important material performance factors considered are the microcreep strength (σ_{my}) (Ref. 1), specific stiffness (E/ρ), the transient thermal distortion index ($K/\alpha \rho Cp$) (Ref. 1), cost, and producibility. Microcreep strength is the amount of stress needed to produce microinch strains in the material, and specific stiffness is the stiffness to weight ratio. The transient thermal distortion index is the diffusivity ($K/\rho Cp$) divided by the CTE (α) and is a figure of merit that is useful in describing the thermal dimensional stability of the material. The results of this analysis are summarized in Table 2.

Table 2.
Performance Comparison of Candidate Materials for the ITATT Gimbal (1)

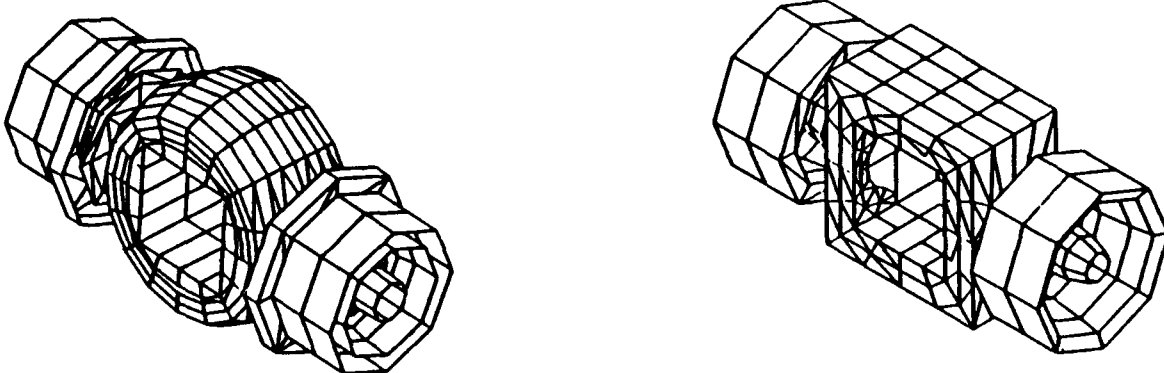
Material	σ_{my} (Kpsi)	E (Mpsi)	ρ (lb/in ³)	E/ρ (specific stiffness)	CTE (α) (ppm/ $^{\circ}$ F)	Cp (Btu/lb. $^{\circ}$ F)	K (Btu/hr-ft. $^{\circ}$ F)	$K/\alpha \rho Cp$ (Transient Thermal Distortion Index)	Cost (1 to 100 Scale)	Producibility
Aluminum	25	10	0.1	100	12	0.22	92	348	1	Excellent
Titanium	80	16.5	0.16	103	5.3	0.12	5	49	10	Fair
Magnesium	-	6.5	0.065	100	14	0.25	31	136	2	Excellent
Invar	10	21	0.29	72	0.8	0.12	8	287	10	Fair
Beryllium	8	42	0.067	627	6.4	0.45	87	451	<25	Poor
SiC Aluminum (20% SiC)	<25	13	0.1	130	8	0.24	70	364	10	Good
Graphite/Epoxy (In-Plane Isotropic) (PSSS Tape)	<20	10	0.065	154	0.3	0.22	14	3263	<25	Fair

Material analysis conclusions and comments

1. The microcreep strength of all materials is adequate for the ITATT gimbal, based on the expected low operational stresses.
2. The specific stiffness of beryllium is approximately four times higher than graphite/epoxy and SiC aluminum, the next highest materials. Thus, beryllium will provide the highest bandwidth.
3. The transient thermal distortion index of graphite/epoxy is seven to eight times higher than beryllium and SiC aluminum, the next highest materials. Thus, graphite/epoxy will provide the best thermal dimensional stability.
4. Beryllium and graphite/epoxy are at least 25 times more expensive than the least expensive material (aluminum), and 2.5 times more expensive than SiC aluminum.
5. A beryllium gimbal is somewhat more difficult to produce than a graphite/epoxy gimbal. The conclusion is based on the toxicity and size limitations of beryllium stock. However, the producibility of graphite/epoxy is limited by its non-homogeneous properties (out of plane) and the need for elaborate layup and or assembly tooling.
6. One unique limitation of graphite/epoxy is its sensitivity to changes in humidity. This characteristic is well known and the effects can be made negligible using proper design techniques and environmental controls.

INNER GIMBAL STRUCTURAL ANALYSISModel and analysis overview

Two groups of finite element models were developed, using ANSYS, to evaluate the achievable performance levels on the ITATT inner axis. Representative models from each group are shown in Figure 2. The first group of models all had spherical outer shells and cylindrical inner shells, with the spherical radius being either 13.0 or 14.75 inches, and the length of the gimbal along the cylindrical bore being from 13 to 19 inches. The second group of models consisted of rectangular gimbals 12 inches or 20 inches in depth and having various wall thicknesses. All models included detailed representations of the shafts and the magnetic bearings.



A-13437A

Fig. 2. Representative spherical and rectangular gimbals

Since the inner axis can be oriented in any direction relative to the earth's gravitational field, each model was subjected to gravitational accelerations along the three principal axes. In addition, load cases representing payload and axis imbalance and load cases designed to investigate the effect of mass and structural asymmetries were run so that balance requirements and fabrication tolerances for each candidate configuration could be established and compared. The critical displacement results were the net rotations and translation of the payload, and the shaft rotation at the bearings and at the encoder. Finally, a harmonic analysis of the gimbal and the inner axis assembly was completed to predict the open loop transfer function that the servo system will control.

Structural asymmetry effects

Due to symmetry, the angular deflection at the payload is nominally zero for the gravitational cases. Position errors of the payload, relative to the encoder, can still arise because the required drive torque will vary at a 2 per revolution frequency if the gimbal's linear deflection (sag) is not uniform for any gravitational load orientation. The drive torque variation can be related to the work required to change the height and hence the potential energy of the payload and deflected structure between the most compliant and the least compliant orientations. This situation is shown schematically in Figure 3 where it is apparent that a potential energy differential exists between the vertical and horizontal load cases. Torque variations and the resulting payload angular errors were computed for all gimbal configurations. It has been determined that these non-constant linear gimbal deflections are not a significant error source as the position and rate errors do not exceed 0.00021 arc second and 0.002 ppm.

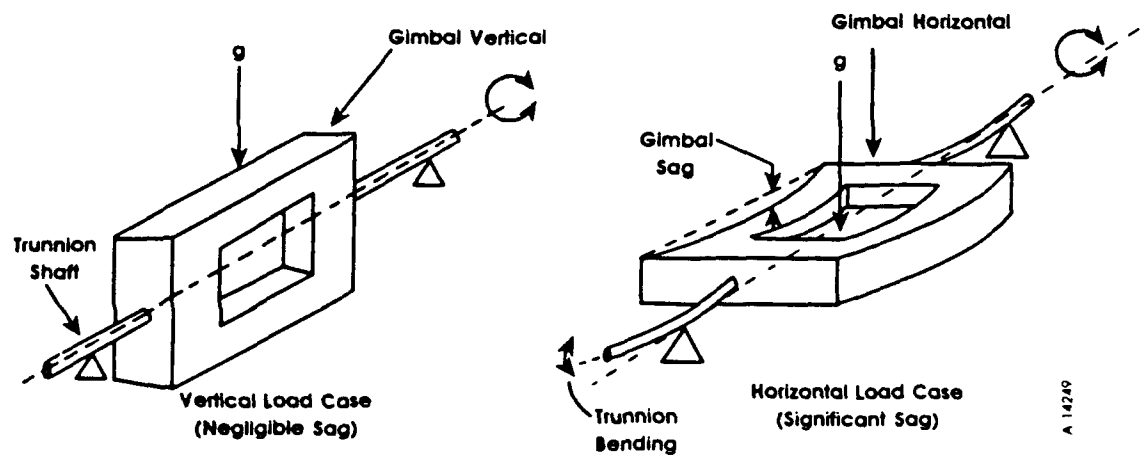


Fig. 3. The an-isoelastic gimbal effect (non constant deflections)

Three distinct areas were addressed in the final design manufacturing tolerance evaluation:

1. Flatness requirements for a single unsupported plate section.
2. General dimensional tolerances.
3. Material uniformity requirements.

The effect of unsupported panel flatness deviations of 0.010" is a payload rotation of 0.000006 arc second. The effect of gross dimensional deviations of 0.020" is a payload rotation of 0.0015 arc second. The effect of a 5% modulus change in one panel is a rotation of 0.0003 arc second.

The results described above apply to both the spherical and rectangular gimbal configurations. The spherical configuration was initially expected to provide better performance because it approximates an axisymmetric configuration. With the axisymmetric gimbal, the bearings on opposite sides were spaced farther apart than for the rectangular gimbals, a significant disadvantage when considering that two additional gimbal axes will eventually be wrapped around the axis currently being evaluated. In the end, the fabrication tolerance requirements drove the design conclusively to the rectangular configuration. Since it is assembled from flat plate segments, flatness and lay-up elastic properties can be controlled more precisely with the rectangular configuration resulting in a significantly more accurate axis.

Harmonic analysis

Having a stiff and highly symmetric inner axis is not sufficient to ensure that the required accuracies are achieved since the control system must have sufficient bandwidth to maintain the axis in precisely the desired position at any given instant. The design goal for this system was a 200 Hz bandwidth which ordinarily means that the first torsional resonance must be above 600 Hz. The open loop response of the axis was simulated using the harmonic response analysis option of the ANSYS finite element code. The input load is motor torque applied to the shaft with the reaction torque applied to the stator at the motor location. The angle encoder response is derived from the complex difference of resulting axis and stator rotations at the encoder location.

Harmonic analyses were performed for several arrangements of axis components including: motors on each side, inboard and outboard of the encoder, and a single motor on one side with the encoder mounted on the opposite side. The results of two of these cases are presented in Figure 6. Both of these configurations provide adequate bandwidth, although the resonances between 1350 and 2150 Hz will probably have to be notched out for the motor opposite encoder case. The motor opposite encoder case was selected for implementation for several reasons: the frequency performance is adequate, it gives a better match between available and required torque within the motor size envelope possible (given the shaft diameter), and it results in reduced imbalance sensitivity since it eliminates shaft drive torque between the encoder and the package.

THE FINAL GIMBAL DESIGN

The final gimbal design is constructed of graphite/epoxy with Invar fittings in a rectangular configuration. This design is shown in Figures 7 and 8 and is summarized in Table 3.

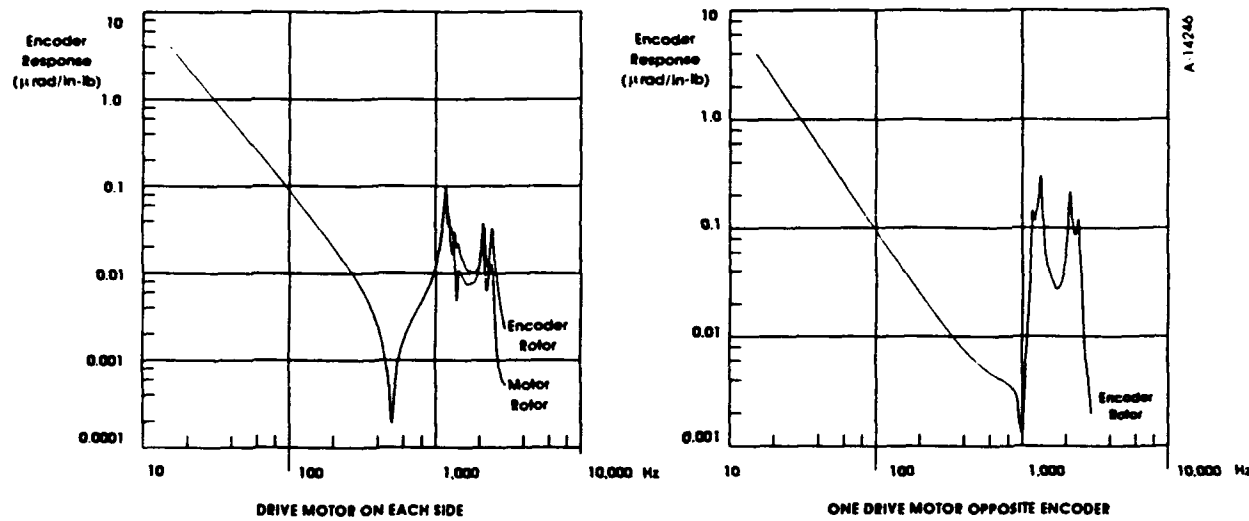


Fig. 6. Open loop responses for two possible axis configurations

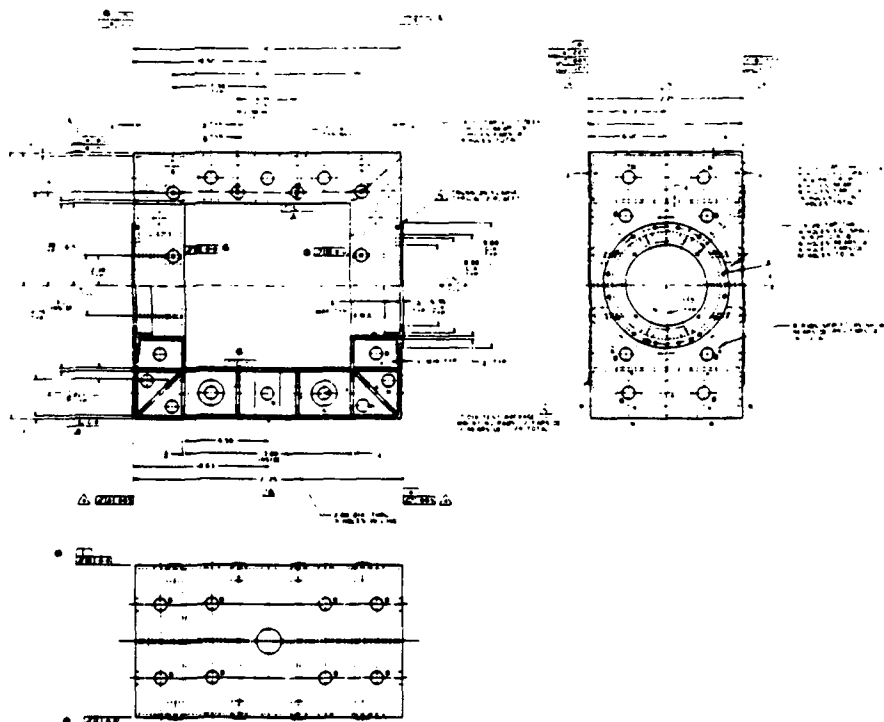


Fig. 7. Inner gimbal configuration

Other errors may be introduced by excessive trunnion shaft rotation (i.e., trunnion bending that is inherent with gimbal sag) since the encoder accuracy is affected by trunnion shaft deflections. The magnitude of shaft angular deflections at the encoders is reduced by using large diameter shafts and by minimizing the space between the radial bearings. In conjunction with the high stiffness of the composite gimbal, these design features make it possible to hold shaft rotation at the encoders to 3.7 microradians.

Mass asymmetry effects

Imbalance and other asymmetries result in angular deflections of the payload (i.e., windup of the gimbal) that vary with a once per revolution frequency. Imbalance about the inner axis results in a sinusoidally varying imbalance torque when the inner gimbal is rotated with the axis horizontal. Since the final inner axis design has the torque motor mounted on the opposite side of the gimbal from the encoder, the effect of torque variations on position and rate accuracy is quite low, 0.0004 microrad/in-lb of imbalance and 0.002 ppm/in-lb of imbalance respectively. A 1 in-lb imbalance due to a mass shift along the inner axis was found to result in a position error of 0.0023 arc second and a rate error of 0.0044 ppm.

Asymmetric mass distributions in a balanced axis can also result in payload position errors. This condition could arise if an unbalanced payload was installed in the gimbal, and then weights were attached to the gimbal to balance the system. This effect was evaluated by running several cases in which an imbalance moment was applied to the payload package and equipollent forces were applied to likely counterweight mounting points on the gimbal as shown in Figure 4. It was determined that the composite gimbal design can tolerate 5 in-lb of payload imbalance with net position and rate errors of 0.0035 arc second and 0.017 ppm, respectively.

Manufacturing tolerance effects

All the gimbal designs considered were nominally symmetrical about a central plan normal to the inner axis but the finite element results demonstrated that stringent dimensional tolerances were required to maintain adequate symmetry in the fabricated part in order to satisfy the design requirements. The dimensional variations expected in the finished part were built into one quadrant of the finite element model, as shown in Figure 5, and the results compared to those for the same configuration but with nominal dimensions throughout.

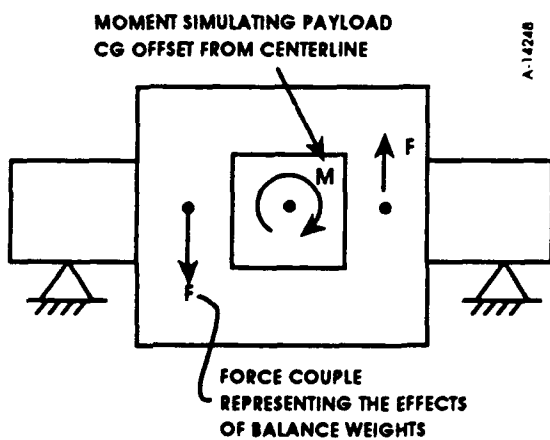


Fig. 4. Simulation of mass asymmetries

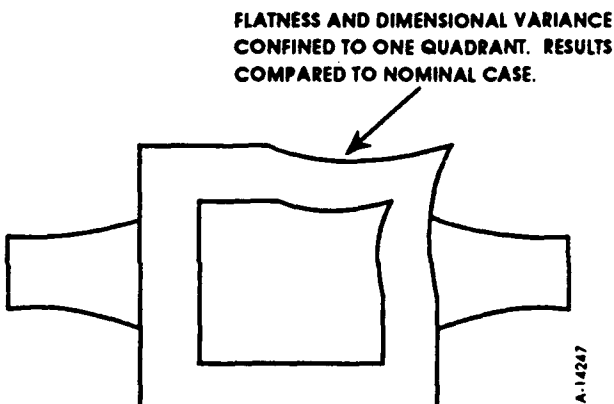


Fig. 5. Simulation of dimensional asymmetry

WHY WAS GRAPHITE/EPOXY MATERIAL SELECTED?

The graphite/epoxy material was selected because of its outstanding thermal distortion index and superior specific stiffness. The thermal properties of graphite/epoxy justify the additional costs and manufacturing complexity. The Invar fittings are used for the machining interfaces because they have a CTE relatively close to the graphite/epoxy. The laminate thickness is a constant 0.25 inch throughout the part to maintain symmetric hydroscopic expansion. By using special design techniques¹, the impact of the poor "out of plane" properties of the graphite/epoxy laminate can be made negligible.

WHY WAS THE RECTANGULAR GIMBAL CONFIGURATION SELECTED?

The rectangular gimbal shape was selected because it provides essentially the same sectional stiffness and symmetry properties as a spherical shape yet it has a superior interface to the cubic test payload. The stiffness and symmetry properties are equivalent because the inner gimbal must provide an opening for installation of the test payload. This opening truncates the spherical gimbal and negates its axisymmetric properties.

The manufacturing tolerance requirements proved to be an important link between the gimbal material and configuration decisions. The rectangular gimbal is constructed from flat stock graphite/epoxy laminate glued together to form the shells and stiffeners. This construction method proved to be the most practical method for achieving 5 percent modulus symmetry and 0.010 inch geometric tolerances. In contrast, the spherical gimbal is made using filament winding or special tape laying techniques and achieving the required manufacturing tolerances (with these techniques) is expensive and risky.

FUTURE ISSUES FOR THE ITATT GIMBALS AND STRUCTURAL COMPONENTS

During the development of the ITATT inner gimbal, several new technical issues have been uncovered that require further review and analysis.

Trunnion shaft material

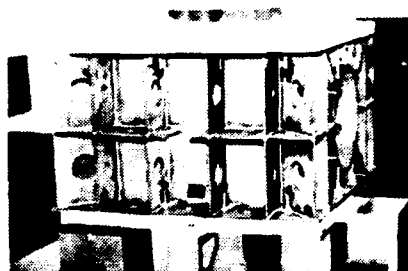
The trunnion shafts, attached to the gimbal, were not part of this initial analysis effort and are currently made of aluminum. Aluminum was selected based on the assumption that all temperature gradients, experienced by the shafts, are axisymmetric. A full review of the magnetic bearings revealed that the radial magnetic bearings produce non-symmetric thermal loads that make the top of the shafts hotter than the bottom. Thus, trunnion shaft thermal distortion is a significant error source that must be considered during the three-axis development effort. Most likely, the shafts will be made from a graphite/epoxy type material.

New and improved materials

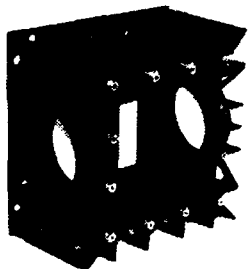
Recent advances in graphite/epoxy and graphite/aluminum composite materials may be applicable to Phase II of the ITATT program. These materials have higher specific stiffness, lower CTE (i.e., near zero), and higher thermal conductivity and are just becoming commercially available. The most important improvement will be in the thermal distortion index which is directly affected by the higher conductivity and lower CTE. These new materials will make the larger Phase II gimbals less sensitive to thermal gradients and offset the increased sensitivity that results from increased size.

Trunnion Shaft Deflections (Wobble)

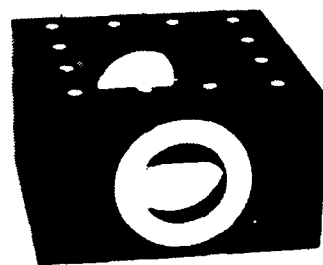
The structural analysis results indicate that the gimbal sag results in average trunnion deflections of approximately 0.6 arc second (see Figure 3) which effects the axis encoders. Deflections of this magnitude are inherent with this type of gimballed system but are magnified by the stiffness characteristics of the magnetic bearings. The magnetic bearings are true pin joints that produce zero moment stiffness and, as a result, maximize the trunnion deflections.



Gimbal in assembly fixture



Gimbal partially assembled



Final assembly

Fig. 8. Picture of gimbal

Table 3.
Inner Gimbal Summary

Shell Material	Pitch carbon fiber/epoxy (Amoco P55S/ERL 1962)
Insert Material	Invar
Configuration	Rectangular
Weight	70 lbs
Modulus Symmetry	Within 5%
Manufacturing Tolerances	Flatness, parallelism, squareness less than 0.010 inch
Encoder Location	Opposite motor
First Major Torsional Resonance	Above 600 Hz
Linear Deflections at Center:	
Gimbal Vertical	50 μ inches
Gimbal Horizontal	204 μ inches
Shaft (Trunnion) Deflection:	
Average Shaft Angular Deflection	3.06 μ rad (0.6 arc sec)
Variation in Shaft Angular Deflection	1.32 μ rad (0.26 arc sec)

The effect of trunnion bending on the encoders is a manageable problem for the single axis prototype but will be a serious problem when the second and third axis gimbals are "wrapped" around the inner axis in Phase II. This three-axis machine will tumble the inner gimbal and trunnions through the full range of their compliance. The effect of this tumbling will be an "apparent wobble" at the encoders of twice the static deflection value or 1.2 arc seconds. This is a significant error source for the encoders and must be considered in Phase II.

REFERENCES

1. Graphite/Epoxy Material Characteristics and Design Techniques for Airborne Instrument Applications, J.E. Stumm, G.E. Pynchon, and G.C. Krumweide, *SPIE Vol. 308 Airborne Reconnaissance V (1981)*.

APPENDIX B

TR-27764

We reserve all rights in connection with this document and in the subject matter represented therein. The recipient hereby acknowledges these rights and shall not, without our permission in writing, disclose or divulge this document in whole or in part to third parties or use it for any purpose other than that for which it was delivered to recipient.



**INDUCTOSYN CALIBRATION
PROCEDURES FOR THE
IMPROVED THREE AXIS
TEST TABLE (ITATT)**

TR-27764

We reserve all rights in connection with this document and in the subject matter represented therein. The recipient hereby acknowledges these rights and shall not, without our permission in writing, disclose or divulge this document in whole or in part to third parties or use it for any purpose other than that for which it was delivered to recipient.

A Member of the Oerlikon-Bühler Group



**INDUCTOSYN CALIBRATION
PROCEDURES FOR THE
IMPROVED THREE AXIS
TEST TABLE (ITATT)**

TR-27764

K97012

July, 1990

Prepared for:

**THE CENTRAL INERTIAL GUIDANCE TEST FACILITY
Holloman AFB**

We reserve all rights in connection with this document and in the subject matter represented therein. The recipient hereby acknowledges these rights and shall not, without our permission in writing, disclose or divulge this document in whole or in part to third parties or use it for any purpose other than that for which it was delivered to recipient.

A Member of the Oerlikon-Bührle Group

TABLE OF CONTENTS

	<u>Page</u>
1 BACKGROUND INFORMATION	1
1.1 Algorithm	1
1.1.1 Data Collection	1
1.1.2 Data Processing	1
1.1.3 Error Correction	1
1.1.4 Verification Of Error Correction	1
1.2 Assumptions	1
1.3 Complications	2
2 CALIBRATION PROCEDURE	4
2.1 Environmental Conditions	4
2.2 Test Equipment	4
2.3 Repeatability Testing	4
2.4 Calibration	5
2.5 Verification	5

APPENDIX A - SAMPLE DATA

APPENDIX B - ALIASING EFFECTS

APPENDIX C - SIMULATION

1 BACKGROUND INFORMATION

1.1 Algorithm

The basic calibration cycle involves the following steps:

1.1.1 Data Collection

Readings from each inductosyn are recorded at N "equally spaced" intervals through a full circle with the two inductosyn rotors locked together. The rotor of the slave inductosyn is then unlocked, turned through $360/N$ degrees, and re-locked; another set of equally spaced readings are recorded with the rotors locked. The process is repeated until N data sets are recorded with each data set consisting of N readings from each inductosyn with a new relative angle between their rotors.

1.1.2 Data Processing

The two data sets obtained are processed using an algorithm based upon the "Rockwell" analysis technique. See "Analysis Technique for Calibrating Angular Measuring Devices" by R. L. Hall presented at the AIAA Guidance and Control Conference of 16-18 August 1976, San Diego, California. The output of this algorithm comprises the error curves of each inductosyn. The error curves are then processed using a fast Fourier transform, FFT, to obtain the Fourier series representation of each curve.

1.1.3 Error Correction

The significant Fourier series coefficients are used to generate an interpolation table within the readout system which is then used to correct readout errors in real time.

1.1.4 Verification Of Error Correction

Error correction is verified by repeating the data collection step of calibration cycle with the readout system interpolation table enabled and then examining the difference between the two readout systems at each sample point. For a perfect calibration, the difference will be a constant value equal to the relative angle between the two inductosyn rotors.

1.2 Assumptions

The following assumptions justify this method:

1. The significant readout system errors are periodic and consist of:
 - a few harmonics based upon a "once per revolution" sinusoid

- a few harmonics based upon a "once per fine cycle" sinusoid
- a few sidebands around each of the fine harmonics caused by modulation of the fine structure error.

Data are presented in Appendix A to justify this assumption.

2. The readout system errors are repeatable.

1.3 Complications

1. Test time

The fourth harmonic of the fine cycle of a 720 pole inductosyn has a frequency of 1440 cycles per revolution. Using minimal sampling techniques for the FFT would require that about 16 million readings be taken (4096 equally spaced readings be recorded for each of 4096 data sets). Using an optimistic data collection rate of one reading per second, the initial calibration would take 16 million seconds or about six months. Some other sample rates:

- 2048 sets of 2048 readings - about 48 days
- 1024 sets of 1024 readings - about 12 days
- 512 sets of 512 readings - about 3 days
- 256 sets of 256 readings - about 18 hours
- 128 sets of 128 readings - about 5 hours

The calibration procedure is designed to use 128 sets of 128 readings so that a complete data set can be taken and analyzed over the course of a single day. Since the fine errors are not being properly sampled at this rate, they will alias into the 0 to 64 cycles per revolution region (see Appendix B). Coarse errors based upon a once per revolution sinusoid will be properly sampled. For the expected frequencies of a 720 pole inductosyn:

- Fine cycle and its sidebands centered about 360 cycles/rev will alias and be centered about 24 cycles/rev and be phase inverted.
- The second harmonic and its sidebands centered about 720 cycles/rev will alias and be centered about 48 cycles/rev and be phase inverted.
- The third harmonic and its sidebands centered about 1080 cycles/rev will alias and be centered about 56 cycles/rev.
- The fourth harmonic and its sidebands centered about 1440 cycles/rev will alias and be centered about 32 cycles/rev.

Appendix C contains the results of performing the 128 point FFT on simulated data containing most expected error harmonics.

An additional problem involved with this method is that the actual data in Appendix A contains a significant sideband of the fine cycle at 352 cycles/rev (8 cycle/rev modulation of the fine error) probably caused by the segmentation of the inductosyn stator. This sideband will alias to 32 cycles/rev and thus be indistinguishable from the fourth harmonic of the fine cycle. This problem will be solved experimentally using a spectrum analyzer to analyze the position error while driving the system at a constant rate as discussed in Appendix A.

2. Noise/Drift

Noise occurring randomly across the frequency spectrum will alias to the observable region of 0-63 cycles per revolution. Averaging of several readings at each position has been incorporated into the calibration procedure in order to minimize the effects of bit flicker and other noise sources in the readout.

Readout drift over time due to temperature sensitivities or other causes has been minimized electronically. Further, the calibration is performed in a temperature/humidity controlled environment. The actual calibration cycle is preceded in the procedure by testing to ensure that readout drift is not a significant contributor to total error.

2 CALIBRATION PROCEDURE

2.1 Environmental Conditions

1. Temperature
2. Humidity

2.2 Test Equipment

HP Spectrum Analyzer, Model _____ or equivalent.

2.3 Repeatability Testing

Calibration repeatability will be verified as follows:

- The correction mechanism of the readout system is disabled.
- The calibration start angle will be zero.
- The total calibration angle will be 2π radians.
- The calibration cycle will be repeated 16 times with a sample rate of 16 samples/revolution for 16 data sets (relative rotor angles). Coefficients will be calculated for each cycle and saved in their raw form:

$$A_n \cos(\theta_n) + B_n i \sin(\theta_n)$$

instead of their processed form:

$$C_n \cos(\theta_n + \phi_n)$$

where

$$C_n = \text{magnitude}(A_n \cos(\theta_n) + B_n i \sin(\theta_n))$$

and

$$\phi_n = \text{phase}(A_n \cos(\theta_n) + B_n i \sin(\theta_n))$$

The C_n 's of each component from each calibration cycle will be averaged. These coefficients will be used to construct a nominal correction vector, CORRnom. Then for each of the 16 sets of coefficients:

- another correction vector will be generated, CORRn
- a correction difference vector will be calculated:

$$\text{CORRdif} = \text{CORRnom} - \text{CORRn}$$

- an rms value will be calculated for the difference vector:

$$\text{rms} = \sqrt{(\text{CORRdif} * \text{CORRdif}) / 16}$$

The calibration will be considered repeatable if the rms value calculated for each case is less than _____ arcsec.

2.4 Calibration

The calibration will be done in one calibration cycle taking 128 data sets each containing 128 data points using a start angle of zero and a total angle of 2π radians. Adjustments to the significant coefficients will be made for aliasing and recorded. These coefficients will be loaded into the readout system and used there to generate an interpolation table.

2.5 Verification

The effectiveness of the readout system corrections will be checked as follows:

- Establish a relative angle between the two inductosyn rotors and lock the rotors as in the calibration cycle.
- Collect a large number of readings from each readout at equally spaced points as in the calibration. A large number of data points ensures that the corrections are effective between the original sample points used in the calibration.
- Form a difference vector from the two vectors of readings.
- Remove the mean of the difference vector. This is the relative angle.
- Compute the minimum, maximum, and rms of the difference vector.
- Repeat for two more relative angles approximately 120 degrees apart.

For example:

<u>Run Number</u>	<u>Number of Samples</u>	<u>Relative Angle</u>	<u>Start Angle (deg)</u>	<u>Total Angle (deg)</u>
1	4096	44.250	0.125	360
2	4096	165.375	0.250	360
3	3333	287.333	0.375	360

The calibration will be considered done if:

- The maximum element of each difference vector is less than _____ arcsec.
- The absolute value of minimum element of each difference vector is less than _____ arcsec.

- The rms of each difference vector is less than _____ arcsec.

If there is effectively no improvement at some frequency, further investigations using a spectrum analyzer or other method will be used to resolve any ambiguities arising due to 8th and 16th sidebands of the fine error harmonics.

**APPENDIX A
SAMPLE DATA**

We reserve all rights in connection with this document and in the subject matter represented therein. The recipient hereby acknowledges these rights and shall not, without our permission in writing, disclose or divulge this document in whole or in part to third parties or use it for any purpose other than that for which it was delivered to recipient.

This appendix presents actual data taken from a completed system that demonstrates the harmonic content of the error in a typical uncalibrated readout. Position error was monitored while the axis rotated in a precision rate mode at 100 degrees/sec. The error signal was processed by an HP Spectrum Analyzer which created the graphs included here. The system used a 720 pole inductosyn (360 speed). At 100 degrees/sec, the axis rotated through one complete revolution in 3.6 seconds so that a 1/rev error component is represented by 0.2777777 Hz; similarly, the first harmonic fine error produces a 100 Hz component (0.2777777×360), etc.

Three data sets were taken in order to see the sidebands of the fine fundamental and its second and fourth harmonics; a fourth reading examined the error at low frequency. No attempt to determine the exact amplitudes of the various harmonics has been made since the purpose of taking the data was only to observe their presence. The amplitudes cannot be determined without taking servo characteristics into account at low frequencies and bandwidth limitations of the monitored signal at high frequencies.

Figure A-1 shows the harmonic content of the error signal centered around the fundamental fine frequency. Sidebands are present at a distance of 1/rev, 2/rev, 4/rev, and a large one at 8/rev.

Figure A-2 shows the harmonic content of the error signal centered around the second harmonic of the fine frequency. Only one sideband is evident at a distance 2/rev.

Figure A-3 shows the harmonic content of the error signal centered around the fourth harmonic of the fine frequency. A relatively large sideband at a distance of 16/rev is present as well as small ones at 4/rev, and 8/rev.

Figure A-4 shows the spectrum at low frequencies; harmonics of the 1/rev are flagged. The graph shows that this particular system has relatively large 8/rev and 16/rev disturbances present with the rest of the harmonics barely out of the background noise. These two components are thought to be due to the segmentation of the inductosyn stator pattern.

This data cannot be used to draw conclusions about inductosyn readout errors in a general sense since it represents only one axis which has its own particular inductosyn pattern and mechanical alignment errors, axis wobble, runout, etc. However, it does show that for this system the significant errors are periodic and therefore representable by a Fourier series as is intended in the proposed calibration procedure.

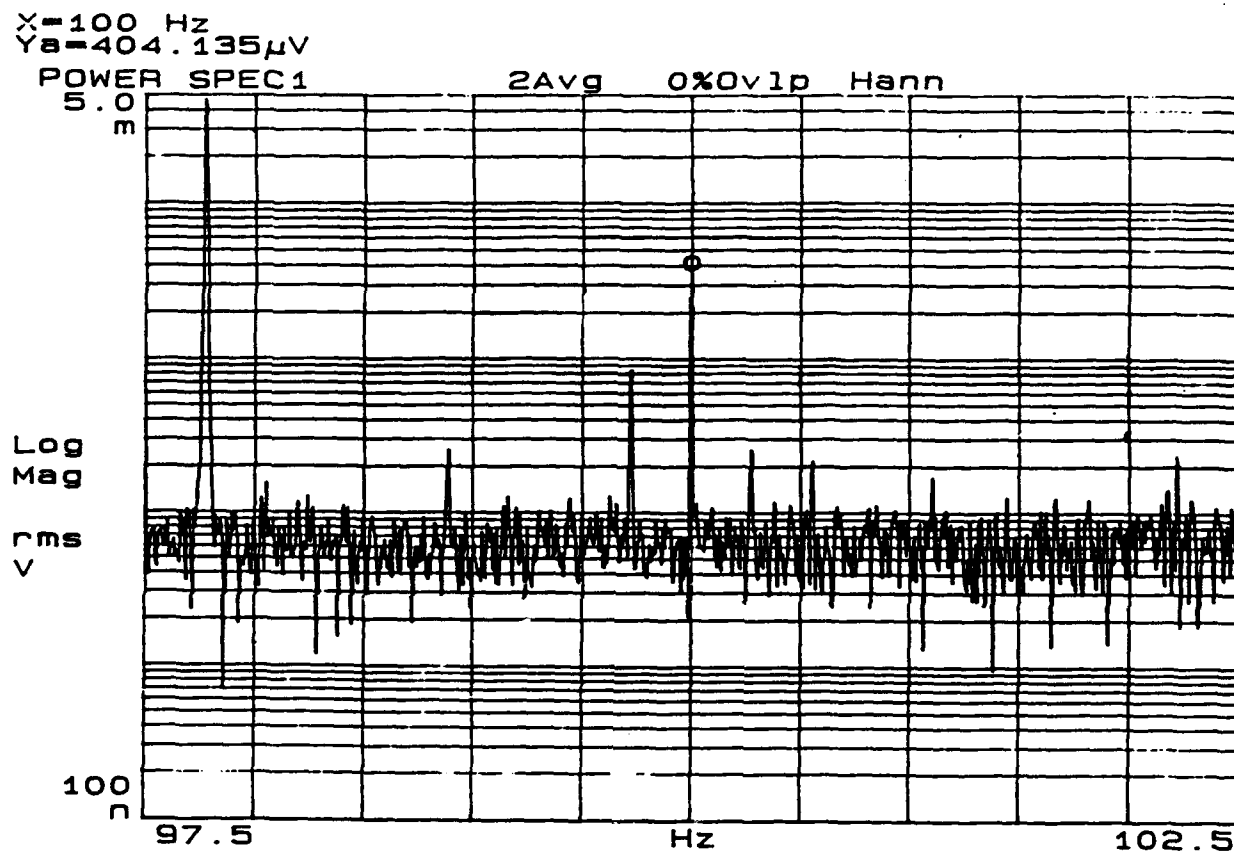


Figure A-1.

We reserve all rights in connection with this document and in the subject matter represented therein. The recipient hereby acknowledges these rights and shall not, without our permission in writing, disclose or divulge this document in whole or in part to third parties or use it for any purpose other than that for which it was delivered to recipient.

X=200 Hz
Y_a=3.72175mV

POWER SPEC1

2Avg

0%Ovlp

Hann

4.0 m

Log Mag

rms V

100 n

197.5

Hz

202.5



Figure A-2.

We reserve all rights in connection with this document and in the subject matter represented therein. The recipient hereby acknowledges these rights and shall not, without our permission in writing, disclose or divulge this document in whole or in part to third parties or use it for any purpose other than that for which it was delivered to recipient.

X=400 Hz
Y_a=96.7902 μ V

POWER SPEC1

1Avg 0%Ovlp Hann

100
 μ Log
Mag
rms
V100
n

395

Hz

405

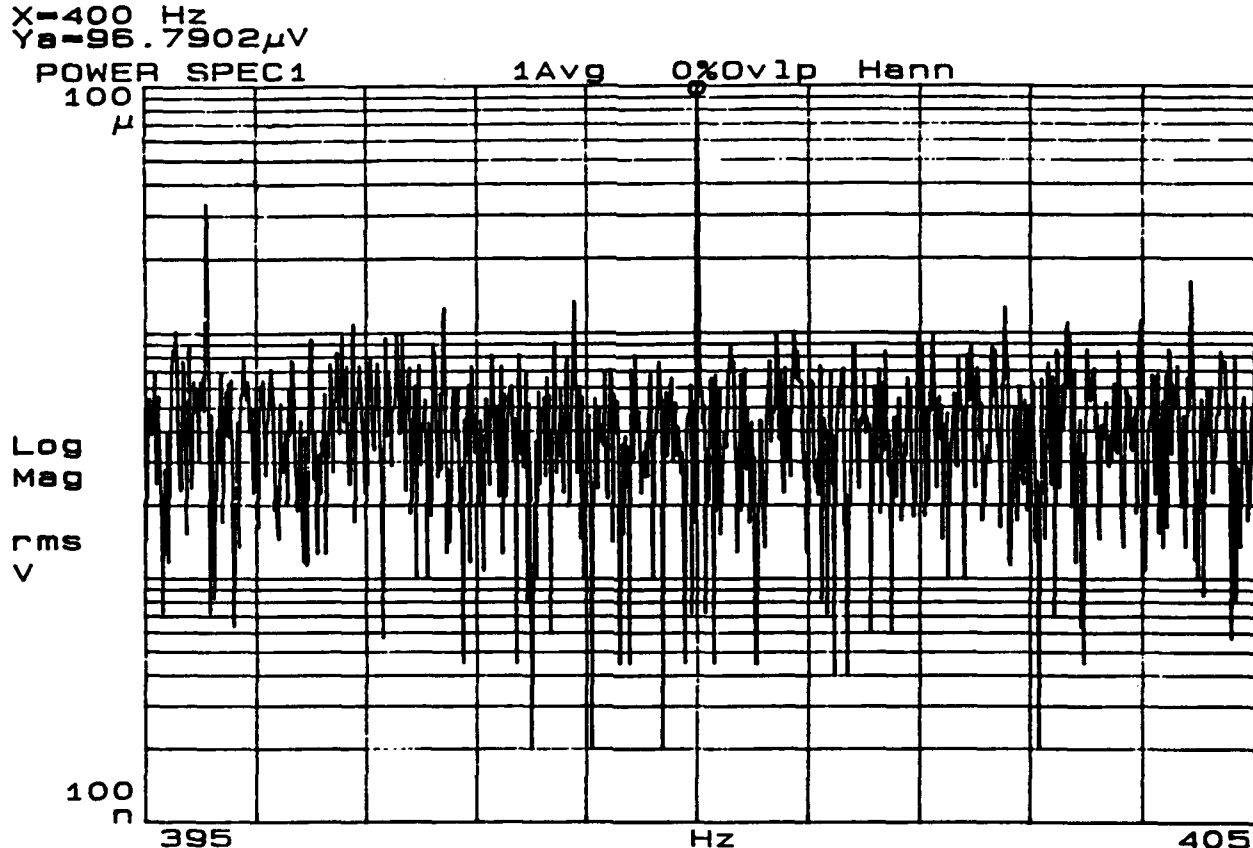


Figure A-3.

We reserve all rights in connection with this document and in the subject matter represented therein. The recipient hereby acknowledges these rights and shall not, without our permission in writing, disclose or divulge this document in whole or in part to third parties or use it for any purpose other than that for which it was delivered to recipient.

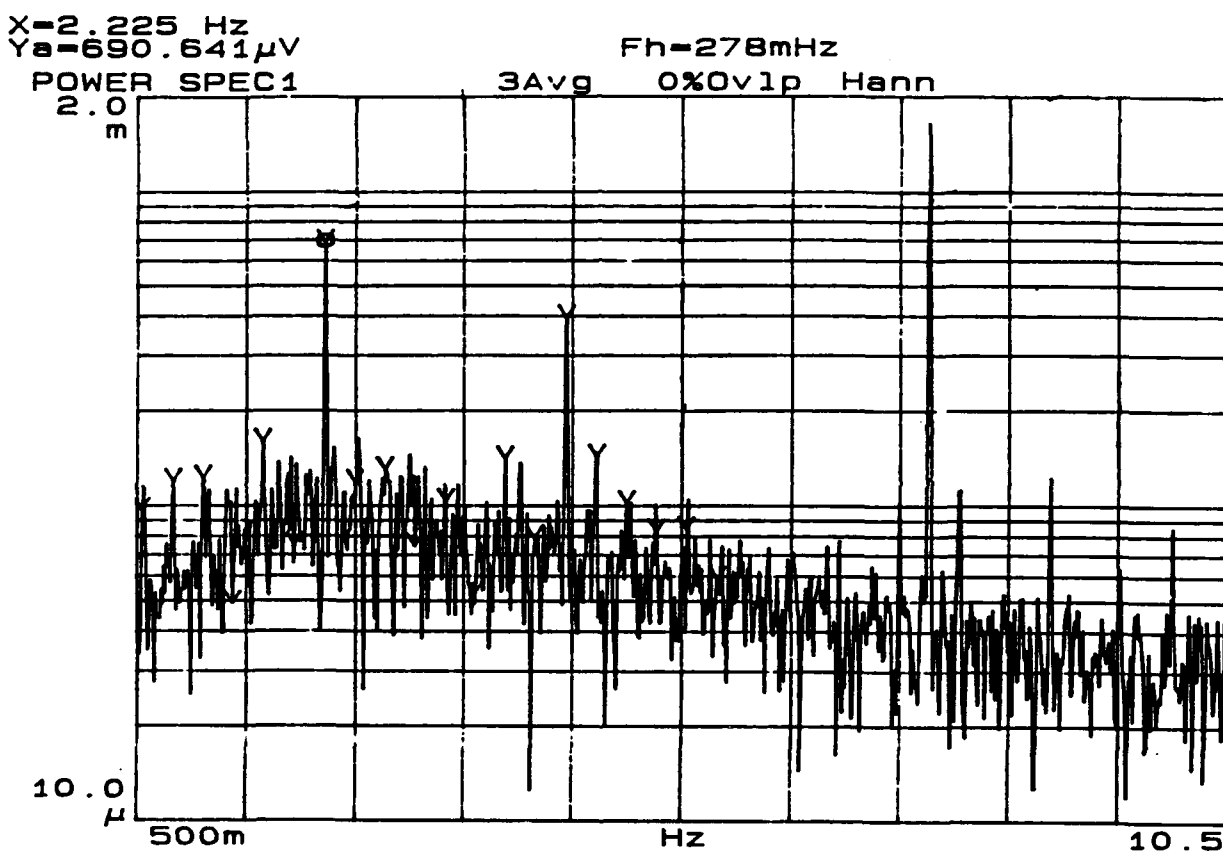


Figure A-4.

We reserve all rights in connection with this document and in the subject matter represented therein. The recipient hereby acknowledges these rights and shall not, without our permission in writing, disclose or divulge this document in whole or in part to third parties or use it for any purpose other than that for which it was delivered to recipient.

**APPENDIX B
ALIASING EFFECTS**

We reserve all rights in connection with this document and in the subject matter represented therein. The recipient hereby acknowledges these rights and shall not, without our permission in writing, disclose or divulge this document in whole or in part to third parties or use it for any purpose other than that for which it was delivered to recipient.

The error curve obtained via the data collection and reduction techniques described elsewhere in this document is in fact an equally-spaced sampled version of the actual readout system error curve. As such, any conclusions drawn regarding the actual curve as a result of processing the sampled version must take into account the effects of aliasing. This appendix is included only to demonstrate how aliasing affects and is taken advantage of by the calibration procedure; see any text on digital filtering or sampled data systems for a more detailed account of the aliasing process and the sampling theorem mentioned below.

The calibration procedure attempts to characterize the readout system error curve by processing the sampled error curve with a Fast Fourier Transform algorithm, FFT, to obtain the coefficients of a Fourier series representation of the curve. (In the following, the frequencies under consideration are expressed as cycles/revolution instead of cycles/second as is normally done.) Without prior knowledge of the frequency content of the actual error curve, the number of points required to characterize a 1440 cycle/rev wave form with a resolution of 1 cycle/rev would require that a minimum of 2880 equally spaced data points be acquired in order to avoid the effects of aliasing (sampling theorem). With prior knowledge of the frequency content of the actual error curve, the effects of aliasing can be used to advantage as the accompanying chart (next page) shows.

This chart assumes a sample rate of 128 samples/revolution which restricts the observable frequency range to the interval from 0-64 cycles/revolution. Frequencies above 64 cycles/rev are aliased into this interval. The horizontal axis of the chart is broken into 128 cycles/rev segments which are drawn below one another for increasing frequency. The dashed lines on the chart show how high frequencies travel to the observable interval. Any frequency above 128 cycles/rev is aliased down directly to a frequency within the 0-128 cycles/rev interval. Furthermore, frequencies in the upper half of the 0-128 interval are reflected about the center line, labelled Nyquist frequency (64 cycles/rev), to appear in the 0-64 interval; i.e. frequencies near the Nyquist frequency remain near and those far away remain far away. For example, the fine cycle error is actually at a frequency of 360 cycles/rev but is aliased to 24 cycles/rev via the right half of the 0-128 interval. Perhaps not clearly shown on the chart, an upper sideband of the fine frequency, such as 361 cycles/rev, will appear as a lower sideband of the aliased fine frequency, or 23 cycles/rev. In addition, the phase of the fourier term calculated for 24 cycles/rev must be inverted when used at 360 cycles/rev. Aliased frequencies which do not pass through the right half of the 0-128 interval have the correct amplitude and phase when computed; in addition, these frequencies appear in the correct order so that lower sidebands of the fourth fine harmonic, 1440 cycles/rev, appear as lower sidebands of 32 cycles/rev.

Since it is not expected that the coarse (1/rev and harmonics) inductosyn error curve will contain any significant frequency content at 24, 32, 48, or 56 cycles/rev, any significant coefficients obtained from the FFT at these frequencies is assumed to have originated at the fine frequencies shown in the chart, 360, 1440, 720, and 1080 cycles/rev respectively, and subsequently used after suitable inversion at the higher frequency to build the interpolation table from which readout corrections will be obtained.

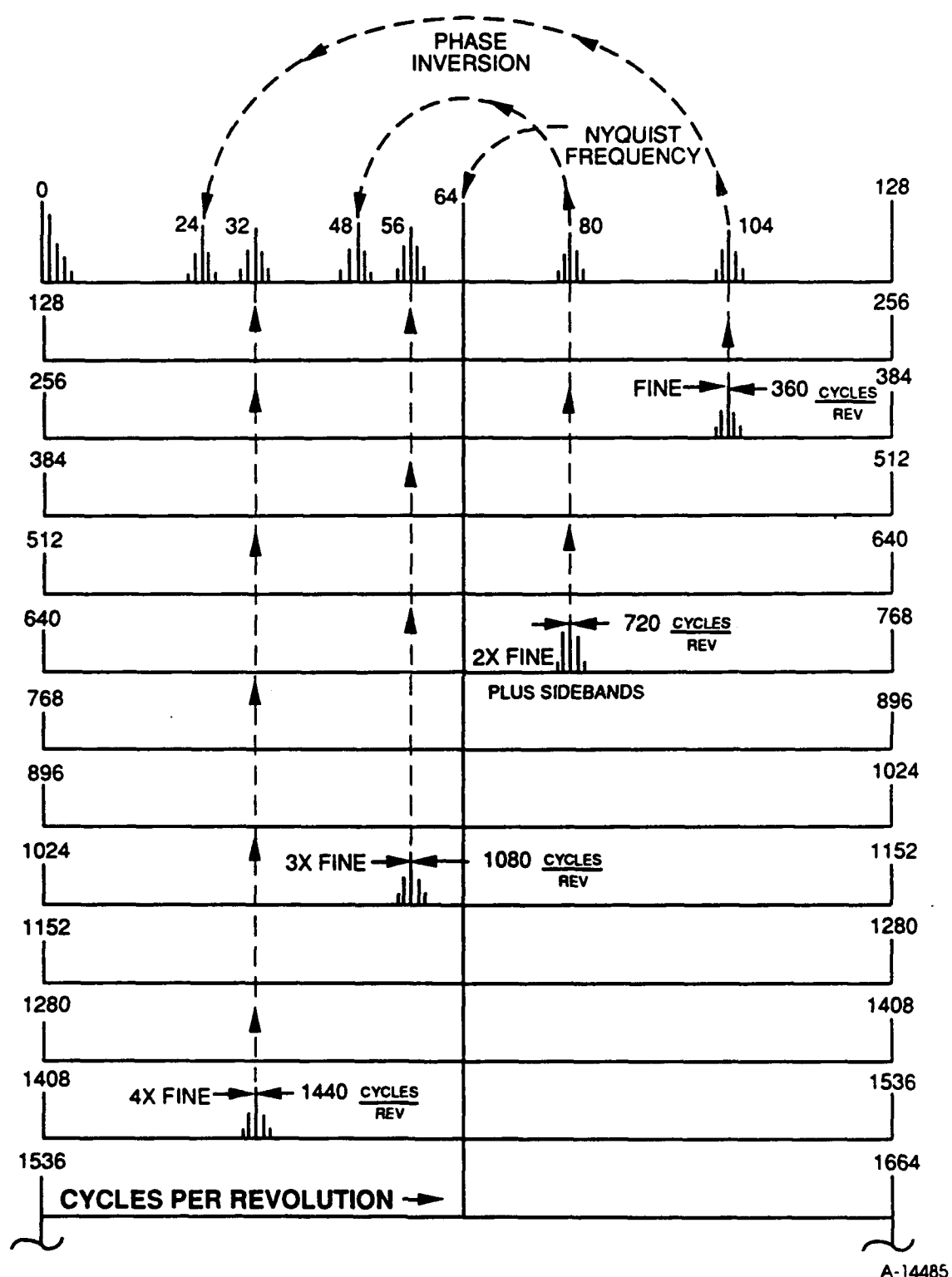


Figure B-1. Aliasing of Fine Harmonics and Sidebands using 128 Samples per Revolution

We reserve all rights in connection with this document and in the subject matter represented therein. The recipient hereby acknowledges these rights and shall not, without our permission in writing, disclose or divulge this document in whole or in part to third parties or use it for any purpose other than that for which it was delivered to recipient.

**APPENDIX C
SIMULATION**

We reserve all rights in connection with this document and in the subject matter represented therein. The recipient hereby acknowledges these rights and shall not, without our permission in writing, disclose or divulge this document in whole or in part to third parties or use it for any purpose other than that for which it was delivered to recipient.

This appendix presents output graphs of simulated inductosyn errors from a MATLAB program. The errors were generated by varying the parameters of the following equations (reduced from a more complicated version).

$$g1=g1amp*(g1_360*sinthm+1+g1mod*sinthm)$$

where g1amp is set to one, g1_360 and g1mod to zero for a perfect readout. (g1_360 and g1mod multiplied different terms originally - here they have the same effect). The sinthm and costhm are vectors representing the sine and cosine of the input angle. Variable g1 is used as the gain of the inductosyn sine winding below.

$$g2=g2amp*(g2_360*costhm+1+g2mod*costhm)$$

where the parameters modify the cosine winding gain, g2.

The inductosyn sine winding signal is computed from:

$$sinsig=g1.*sin(thmf+p1+p1_360*sinthm)$$

where thmf is the input fine angle ($thm*360$). Parameter p1 is used to introduce a constant phase error into the sine winding; p1_360 is used to introduce a winding phase error which varies with the sine of the coarse angle, sinthm.

Then a quadrature signal may be added by making parameter k1 non-zero:

$$sinsig=sinsig+k1*cos(thmf)$$

Finally, amplifier offsets may be introduced:

$$sinsig=sinsig+o1+co1*sinthm$$

where o1 introduces a constant offset; co1 introduces an offset which varies with the sine of the coarse angle.

The cosine winding signal is generated similarly:

$$\begin{aligned}cossig &= g2.*cos(thmf+p2+p2_360*costhm) \\cossig &= cossig+k2*sin(thmf) \\cossig &= cossig+o2+co2*sinthm\end{aligned}$$

From the sine and cosine signal, a readout signal, RO is generated:

$$RO=atan2(sinsig,cossig)$$

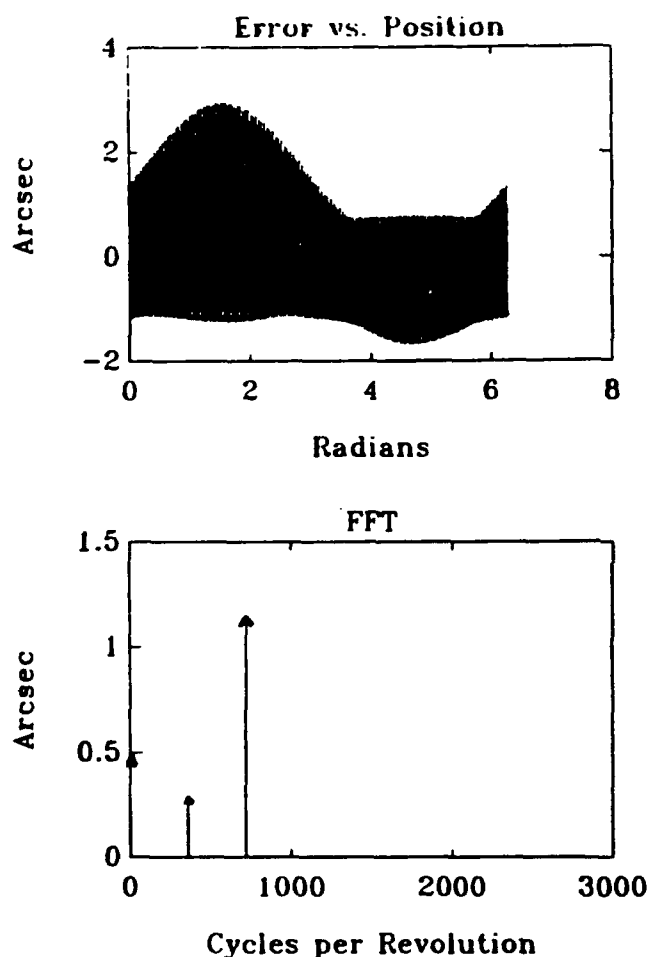
and then used to generate an error signal from a previously computed perfect readout vector in variable "good":

$$er1=RO-good.$$

The first graph, Figure C-1, in this appendix shows the error signal and its FFT using a sample rate of 4096 samples/revolution with all error parameters set to non-zero values. The significant components of this error are listed on the following sheet, Figure C-2. This sheet shows that the signal contains a high amplitude 1/rev error along with significant components at the fine frequency, its second harmonic, and their sidebands.

The second graph, Figure C-3, displays the same information as the first for the same parameters except that the sample rate has been lowered to 128 samples/revolution. The page following lists the significant Fourier coefficients which agree with those in the preceding properly sampled example after adjustments for aliasing are made. For example, the fine fundamental which appears at 24 cycles/rev corresponds to a 360 cycle/sec component with the same amplitude shown, 0.2863, but with a phase opposite to that shown, namely 0.001 radians, which agrees with the component calculated in the previous properly sampled example.

The rest of the graphs show the contribution made by each of the parameters individually. Each graph is followed by a list of the Fourier coefficients - phase is not shown.



Inductosyn Error Simulation
1990 6 12 9 12 53

g1amp	0.999
g1mod	1.0000e-03
k1	1.0000e-03
k2	1.1000e-03
o1	5.0000e-04
c01	1.0000e-03
p1	1.7453e-03
N	4096
p1-360	1.7453e-03
g1-360	1.0000e-03
speed	360

Figure C-1.

signif =

0.0010	0.5002	-1.5708
0.0020	0.0002	-3.1416
0.3580	0.0002	-0.7179
0.3590	0.2865	1.5721
0.3600	0.2963	2.0017
0.3610	0.2963	-1.3695
0.3620	0.0002	-0.7179
0.7180	0.0005	-2.0927
0.7190	0.3792	0.7196
0.7200	1.1392	0.2564
0.7210	0.3792	-2.4220
0.7220	0.0005	-2.0927
1.0780	0.0002	-2.4204
1.0790	0.0007	-3.1370
1.0800	0.0008	1.3981
1.0810	0.0007	0.0046
1.0820	0.0002	-2.4204
1.4380	0.0001	3.0111
1.4390	0.0008	2.5476
1.4400	0.0010	1.8825
1.4410	0.0008	-0.5940
1.4420	0.0001	3.0111

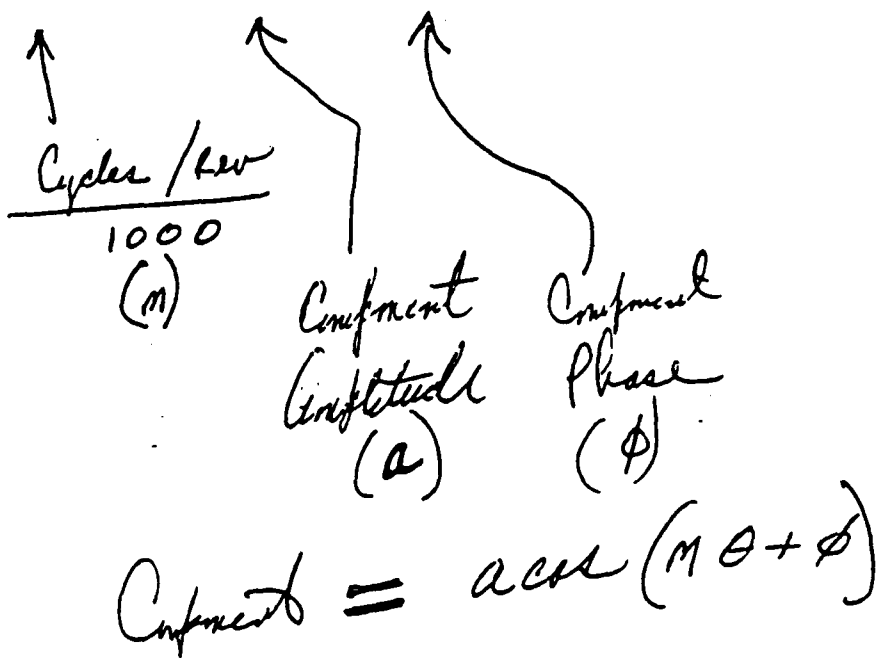
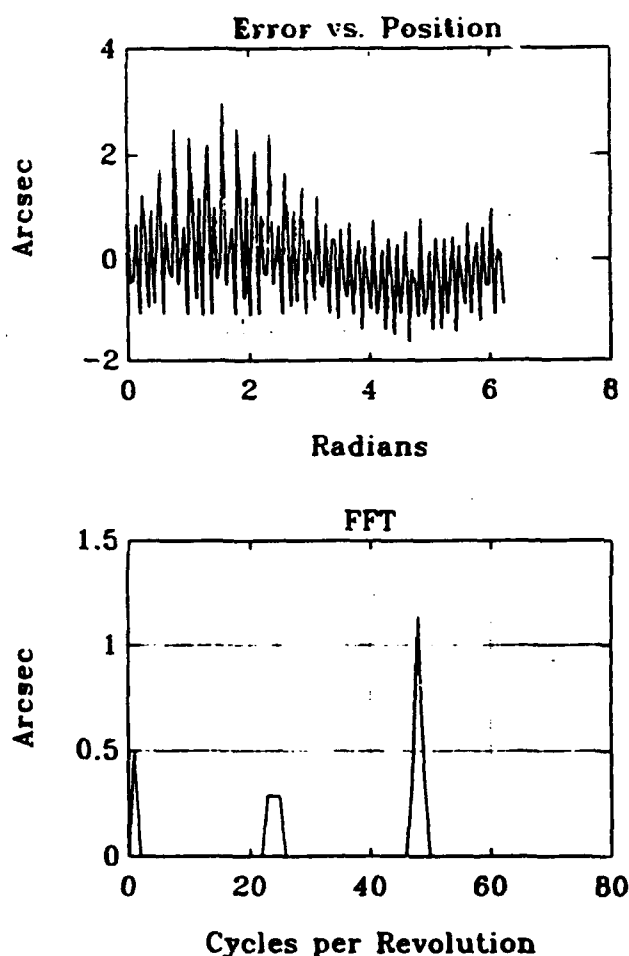


Figure C-2.



Inductosyn Error Simulation
1990 6 12 8 34 13

glamp	0.999
g1mod	1.0000e-03
k1	1.0000e-03
k2	1.1000e-03
o1	5.0000e-04
c01	1.0000e-03
p1	1.7453e-03
N	128
p1-360	1.7453e-03
g1-360	1.0000e-03
speed	360

Figure C-3.

signif =	cycles/sec		
	1000		
0.0010	0.5003	-1.5708	
0.0020	0.0002	-3.1416	2
0.0220	0.0002	0.7179	362
0.0230	0.2865	1.5695	361
0.0240	0.2862	-0.0017	360
0.0250	0.2862	-1.5721	359
0.0260	0.0002	0.7179	358
0.0300	0.0001	3.0111	1438
0.0310	0.0008	2.5476	1435
0.0320	0.0010	1.8825	1440
0.0330	0.0008	-0.5940	1441
0.0340	0.0001	3.0111	1442
0.0460	0.0005	2.0927	722
0.0470	0.3792	2.4220	721
0.0480	1.1392	-0.2564	720
0.0490	0.3792	-0.7196	719
0.0500	0.0005	2.0927	718
0.0540	0.0002	-2.4204	1078
0.0550	0.0007	-3.1370	1079
0.0560	0.0008	1.2981	1080
0.0570	0.0007	0.0046	1071
0.0580	0.0002	-2.4204	1082

Simple at 128/REV

phase inversion
- alias above Nyquist freq.
No phase inversion - always below
Nyquist freq.

phase inversion

No phase inversion



Figure C-4.

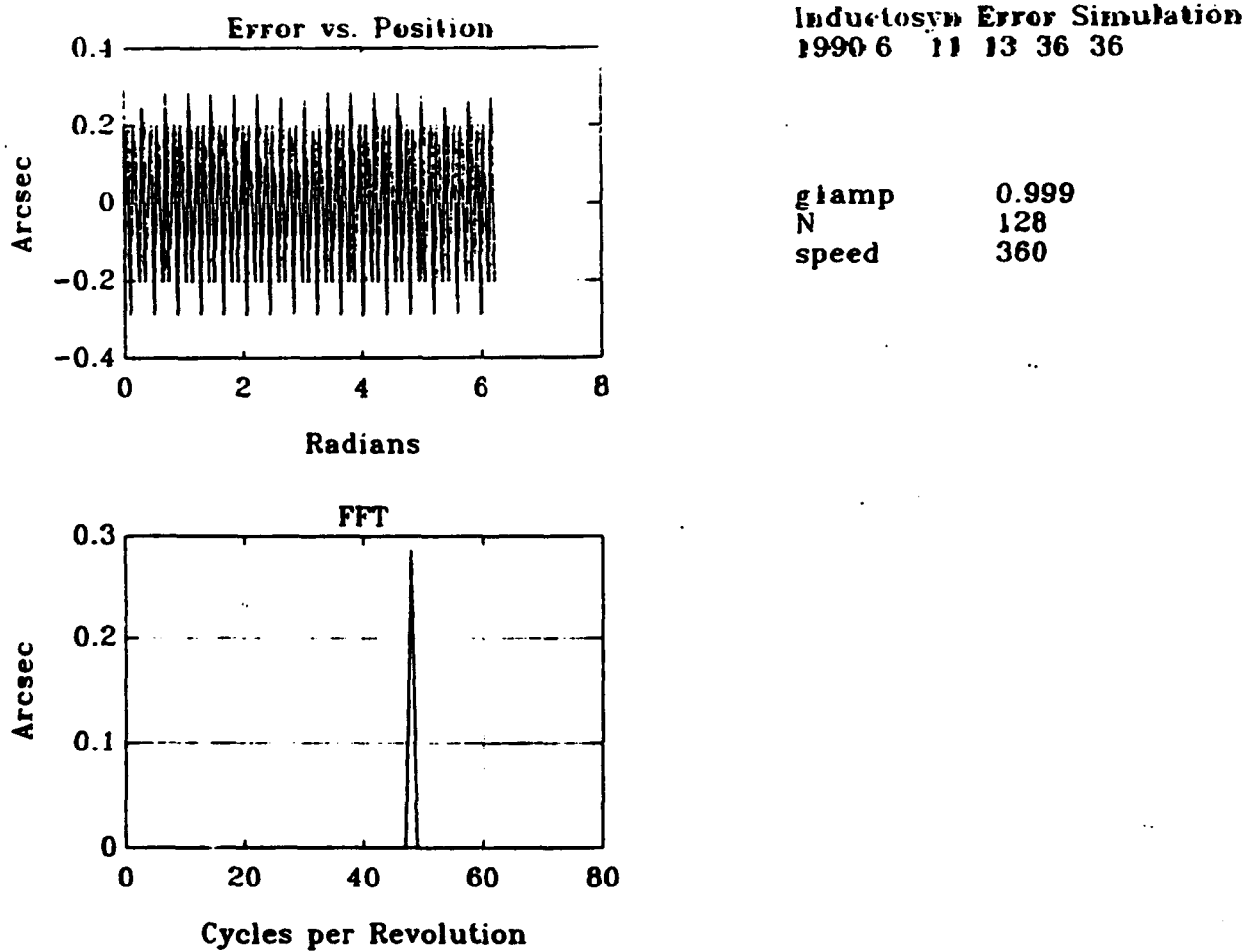


Figure C-5.

We reserve all rights in connection with this document and in the subject matter represented therein. The recipient hereby acknowledges these rights and shall not, without our permission in writing, disclose or divulge this document in whole or in part to third parties or use it for any purpose other than that for which it was delivered to recipient.

ampl =

Columns 1 through 7

0.0000 0.0000 0.0000 0.0000 0.0000 0.0000 0.0000

Columns 8 through 14

0.0000 0.0000 0.0000 0.0000 0.0000 0.0000 0.0000

Columns 15 through 21

0.0000 0.0000 0.0000 0.0000 0.0000 0.0000 0.0000

Columns 22 through 28

0.0000 0.0000 0.0000 0.0000 0.0000 0.0000 0.0000

Columns 29 through 35

0.0000 0.0000 0.0000 0.0000 0.0001
1440 0.0000 0.0000

Columns 36 through 42

0.0000 0.0000 0.0000 0.0000 0.0000 0.0000 0.0000

Columns 43 through 49

0.0000 0.0000 0.0000 0.0000 0.0000 0.0000 0.2866

720/rev

Columns 50 through 56

0.0000 0.0000 0.0000 0.0000 0.0000 0.0000 0.0000

Columns 57 through 63

0.0000 0.0000 0.0000 0.0000 0.0000 0.0000 0.0000

Column 64

0.0000

Figure C-6.

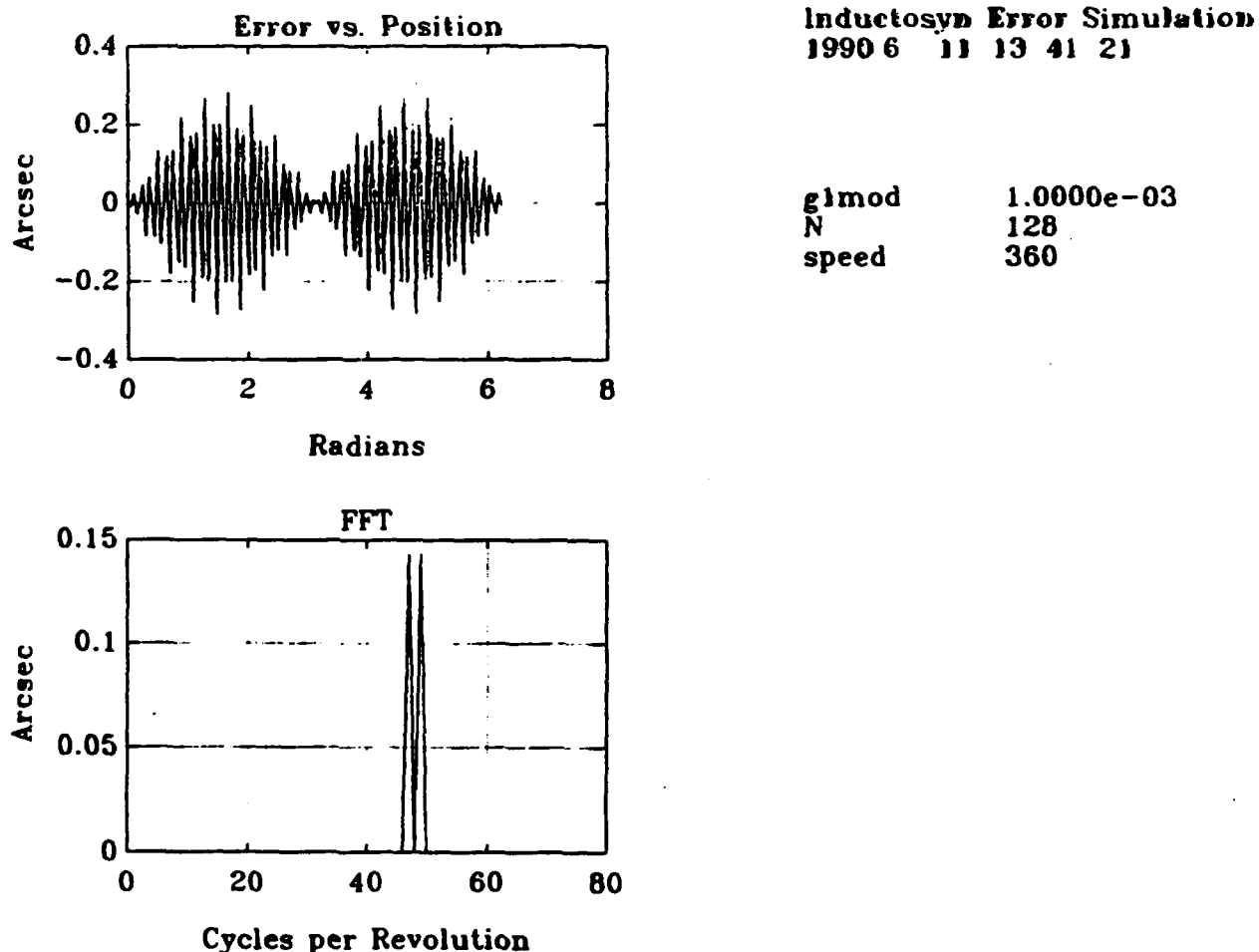


Figure C-7.

We reserve all rights in connection with this document and in the subject matter represented therein. The recipient hereby acknowledges these rights and shall not, without our permission in writing, disclose or divulge this document in whole or in part to third parties or use it for any purpose other than that for which it was delivered to recipient.

ampl =

Columns 1 through 7

0.0000	0.0000	0.0000	0.0000	0.0000	0.0000	0.0000
--------	--------	--------	--------	--------	--------	--------

Columns 8 through 14

0.0000	0.0000	0.0000	0.0000	0.0000	0.0000	0.0000
--------	--------	--------	--------	--------	--------	--------

Columns 15 through 21

0.0000	0.0000	0.0000	0.0000	0.0000	0.0000	0.0000
--------	--------	--------	--------	--------	--------	--------

Columns 22 through 28

0.0000	0.0000	0.0000	0.0000	0.0000	0.0000	0.0000
--------	--------	--------	--------	--------	--------	--------

Columns 29 through 35

0.0000	0.0000	0.0000	0.0000	0.0000	0.0000	0.0000
--------	--------	--------	--------	--------	--------	--------

Columns 36 through 42

0.0000	0.0000	0.0000	0.0000	0.0000	0.0000	0.0000
--------	--------	--------	--------	--------	--------	--------

Columns 43 through 49

0.0000	0.0000	0.0000	0.0000	0.0000	0.1432	0.0001
--------	--------	--------	--------	--------	--------	--------

Columns 50 through 56

0.1432	0.0000	0.0000	0.0000	0.0000	0.0000	0.0000
--------	--------	--------	--------	--------	--------	--------

719 Columns 57 through 63

0.0000	0.0000	0.0000	0.0000	0.0000	0.0000	0.0000
--------	--------	--------	--------	--------	--------	--------

Column 64

0.0000

Figure C-8.

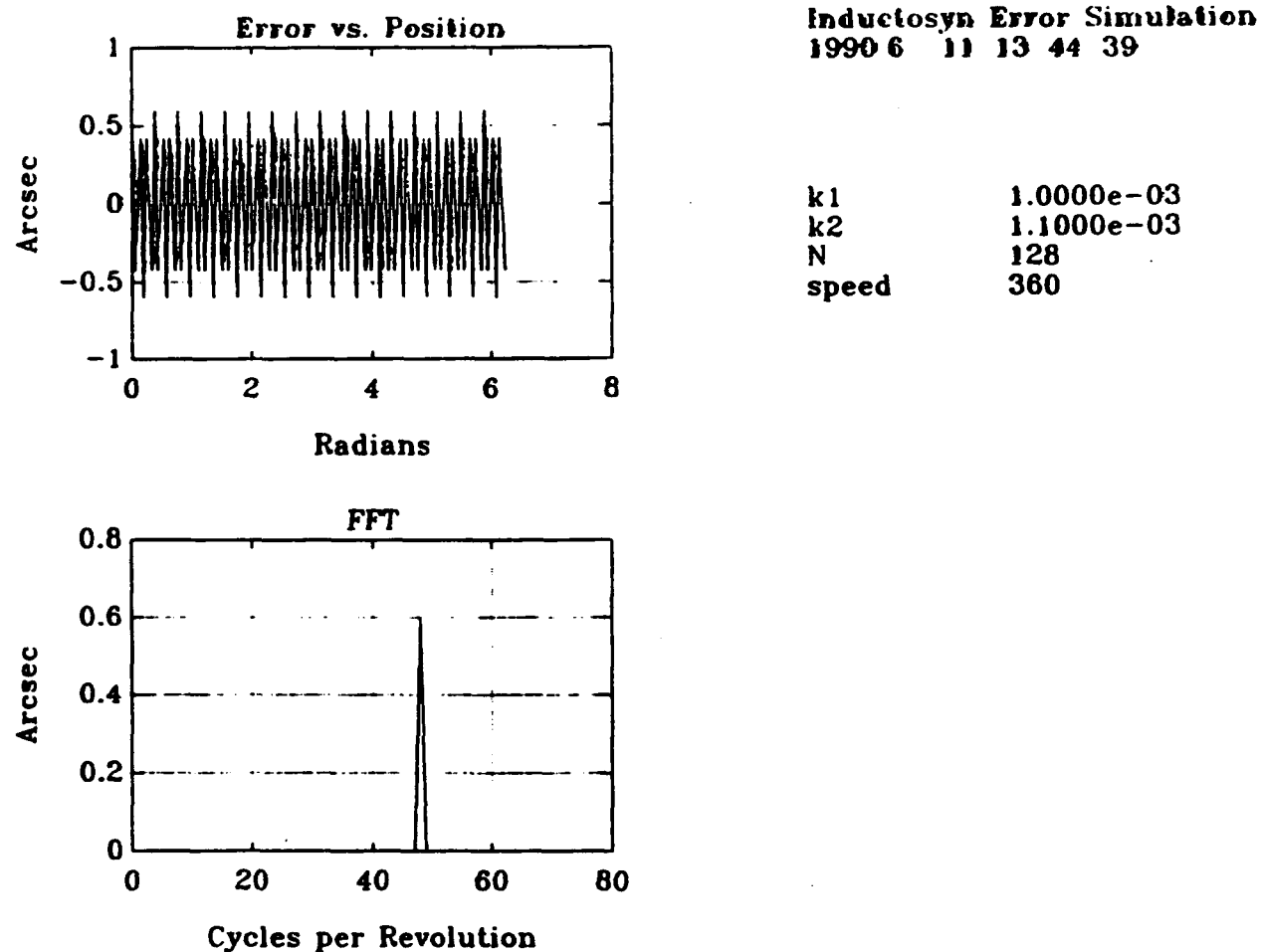


Figure C-9.

We reserve all rights in connection with this document and in the subject matter represented therein. The recipient hereby acknowledges these rights and shall not, without our permission in writing, disclose or divulge this document in whole or in part to third parties or use it for any purpose other than that for which it was delivered to recipient.

ampl =

Columns 1 through 7

0.0000 0.0000 0.0000 0.0000 0.0000 0.0000 0.0000

Columns 8 through 14

0.0000 0.0000 0.0000 0.0000 0.0000 0.0000 0.0000

Columns 15 through 21

0.0000 0.0000 0.0000 0.0000 0.0000 0.0000 0.0000

Columns 22 through 28

0.0000 0.0000 0.0000 0.0000 0.0000 0.0000 0.0000

Columns 29 through 35

0.0000 0.0000 0.0000 0.0000 0.0003
1440

Columns 36 through 42

0.0000 0.0000 0.0000 0.0000 0.0000 0.0000 0.0000

Columns 43 through 49

0.0000 0.0000 0.0000 0.0000 0.0000 0.0000 0.6016

Columns 50 through 56

0.0000 0.0000 0.0000 0.0000 0.0000 0.0000 0.0000

720

Columns 57 through 63

0.0000 0.0000 0.0000 0.0000 0.0000 0.0000 0.0000

Column 64

0.0000

Figure C-10.

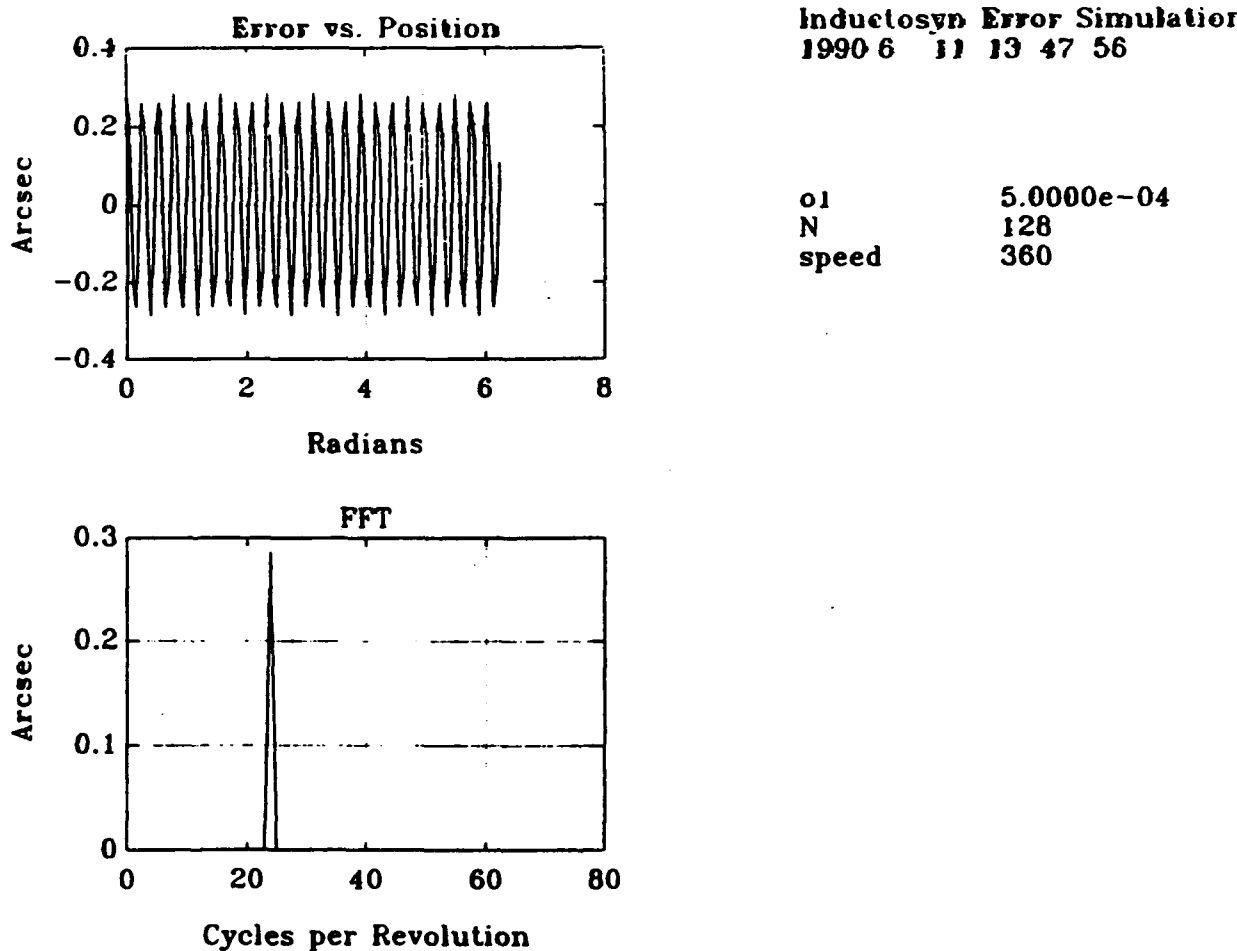


Figure C-11.

We reserve all rights in connection with this document and in the subject matter represented therein. The recipient hereby acknowledges these rights and shall not, without our permission in writing, disclose or divulge this document in whole or in part to third parties or use it for any purpose other than that for which it was delivered to recipient.

ampl =

Columns 1 through 7

0.0000	0.0000	0.0000	0.0000	0.0000	0.0000	0.0000
--------	--------	--------	--------	--------	--------	--------

Columns 8 through 14

0.0000	0.0000	0.0000	0.0000	0.0000	0.0000	0.0000
--------	--------	--------	--------	--------	--------	--------

Columns 15 through 21

0.0000	0.0000	0.0000	0.0000	0.0000	0.0000	0.0000
--------	--------	--------	--------	--------	--------	--------

Columns 22 through 28

0.0000	0.0000	0.0000	0.2865	0.0000	0.0000	0.0000
--------	--------	--------	--------	--------	--------	--------

360

Columns 29 through 35

0.0000	0.0000	0.0000	0.0000	0.0000	0.0000	0.0000
--------	--------	--------	--------	--------	--------	--------

Columns 36 through 42

0.0000	0.0000	0.0000	0.0000	0.0000	0.0000	0.0000
--------	--------	--------	--------	--------	--------	--------

Columns 43 through 49

0.0000	0.0000	0.0000	0.0000	0.0000	0.0000	0.0001
--------	--------	--------	--------	--------	--------	--------

720

Columns 50 through 56

0.0000	0.0000	0.0000	0.0000	0.0000	0.0000	0.0000
--------	--------	--------	--------	--------	--------	--------

Columns 57 through 63

0.0000	0.0000	0.0000	0.0000	0.0000	0.0000	0.0000
--------	--------	--------	--------	--------	--------	--------

Column 64

0.0000

Figure C-12.

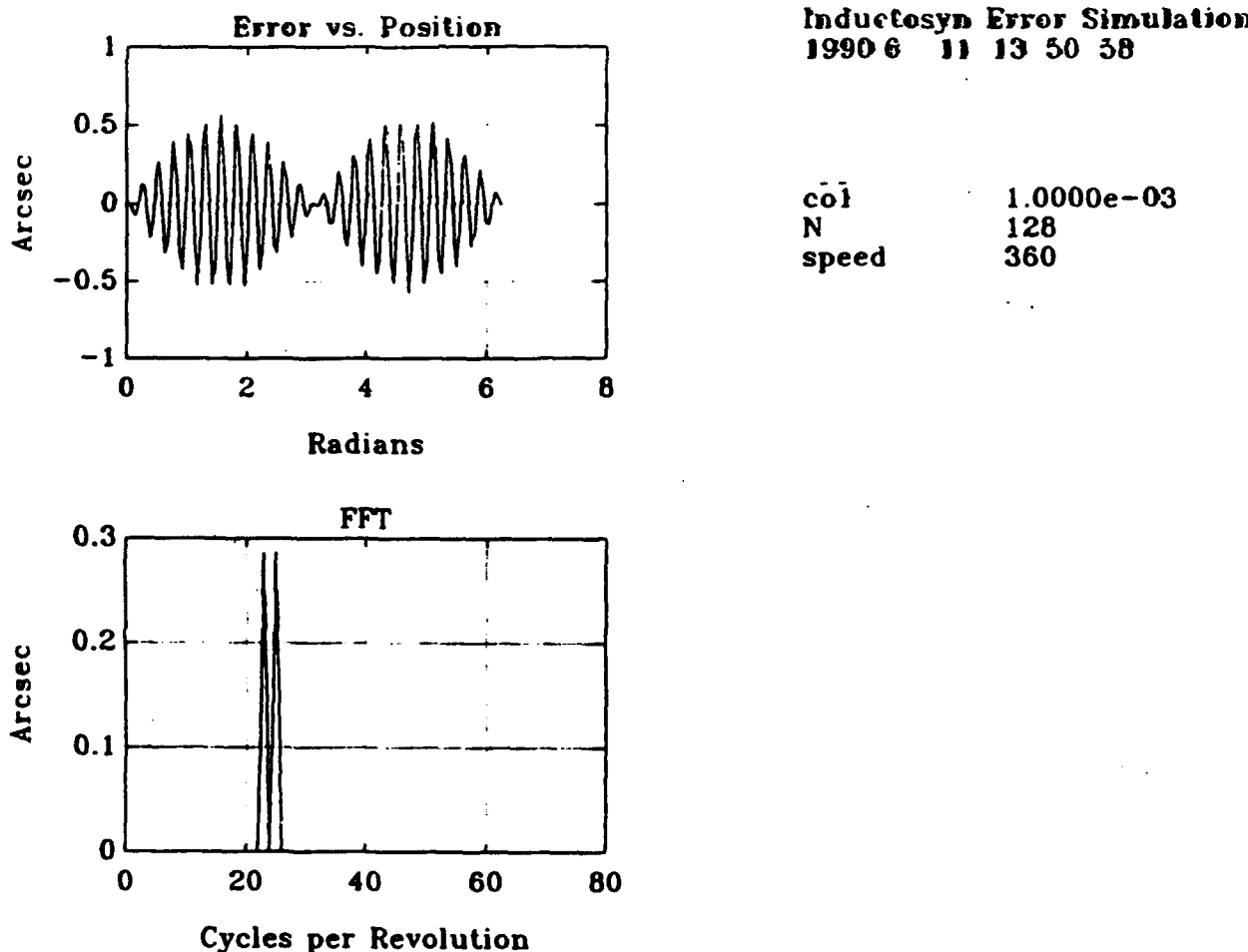


Figure C-13.

We reserve all rights in connection with this document and in the subject matter represented therein. The recipient hereby acknowledges these rights and shall not, without our permission in writing, disclose or divulge this document in whole or in part to third parties or use it for any purpose other than that for which it was delivered to recipient.

ampl *

Columns 1 through 7

0.0000 0.0000 0.0000 0.0000 0.0000 0.0000 0.0000

Columns 8 through 14

0.0000 0.0000 0.0000 0.0000 0.0000 0.0000 0.0000

Columns 15 through 21

0.0000 0.0000 0.0000 0.0000 0.0000 0.0000 0.0000

Columns 22 through 28

0.0000 0.0000 0.2865 0.0000 0.2865 0.0000 0.0000

Columns 29 through 35 36/ 359.

0.0000 0.0000 0.0000 0.0000 0.0000 0.0000 0.0000

Columns 36 through 42

0.0000 0.0000 0.0000 0.0000 0.0000 0.0000 0.0000

Columns 43 through 49

0.0000 0.0000 0.0000 0.0000 0.0001 0.0000 0.0001

Columns 50 through 56 72/ 720

0.0000 0.0001 0.0000 0.0000 0.0000 0.0000 0.0000

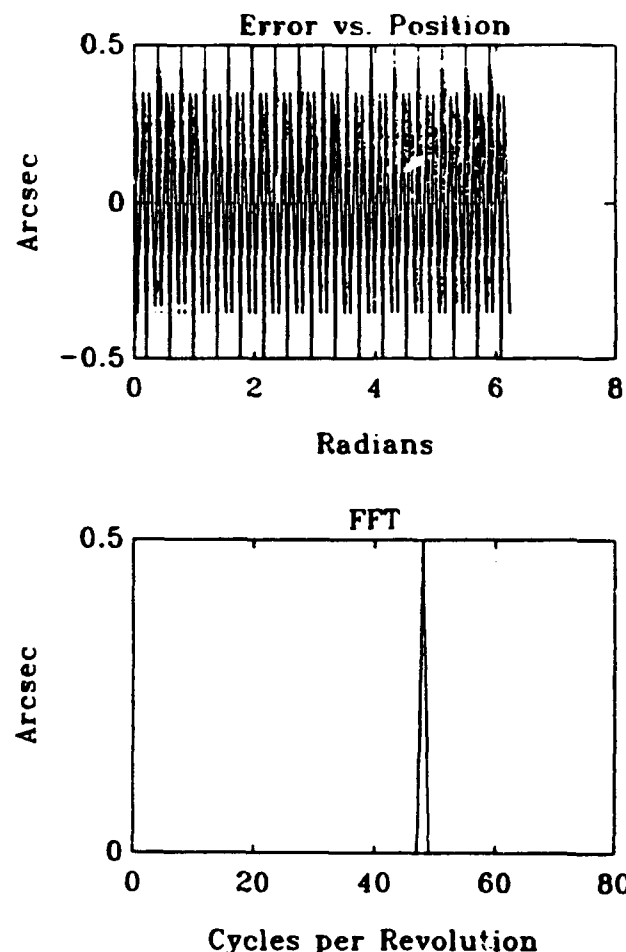
Columns 57 through 63 718

0.0000 0.0000 0.0000 0.0000 0.0000 0.0000 0.0000

Column 64

0.0000

Figure C-14.



Inductosyn Error Simulation
1990 6 12 8 29 8

p1 1.7453e-03
N 128
speed 360

Figure C-15.

ampl =

Columns 1 through 7

0.0000	0.0000	0.0000	0.0000	0.0000	0.0000	0.0000
--------	--------	--------	--------	--------	--------	--------

Columns 8 through 14

0.0000	0.0000	0.0000	0.0000	0.0000	0.0000	0.0000
--------	--------	--------	--------	--------	--------	--------

Columns 15 through 21

0.0000	0.0000	0.0000	0.0000	0.0000	0.0000	0.0000
--------	--------	--------	--------	--------	--------	--------

Columns 22 through 28

0.0000	0.0000	0.0000	0.0000	0.0000	0.0000	0.0000
--------	--------	--------	--------	--------	--------	--------

Columns 29 through 35

0.0000	0.0000	0.0000	0.0000	0.0002	0.0000	0.0000
--------	--------	--------	--------	--------	--------	--------

Columns 36 through 42

0.0000	0.0000	0.0000	0.0000	0.0000	0.0000	0.0000
--------	--------	--------	--------	--------	--------	--------

Columns 43 through 49

0.0000	0.0000	0.0000	0.0000	0.0000	0.0000	0.5000
--------	--------	--------	--------	--------	--------	--------

0.5000

Columns 50 through 56

0.0000	0.0000	0.0000	0.0000	0.0000	0.0000	0.0000
--------	--------	--------	--------	--------	--------	--------

Columns 57 through 63

0.0000	0.0000	0.0000	0.0000	0.0000	0.0000	0.0000
--------	--------	--------	--------	--------	--------	--------

Column 64

0.0000

Figure C-16.

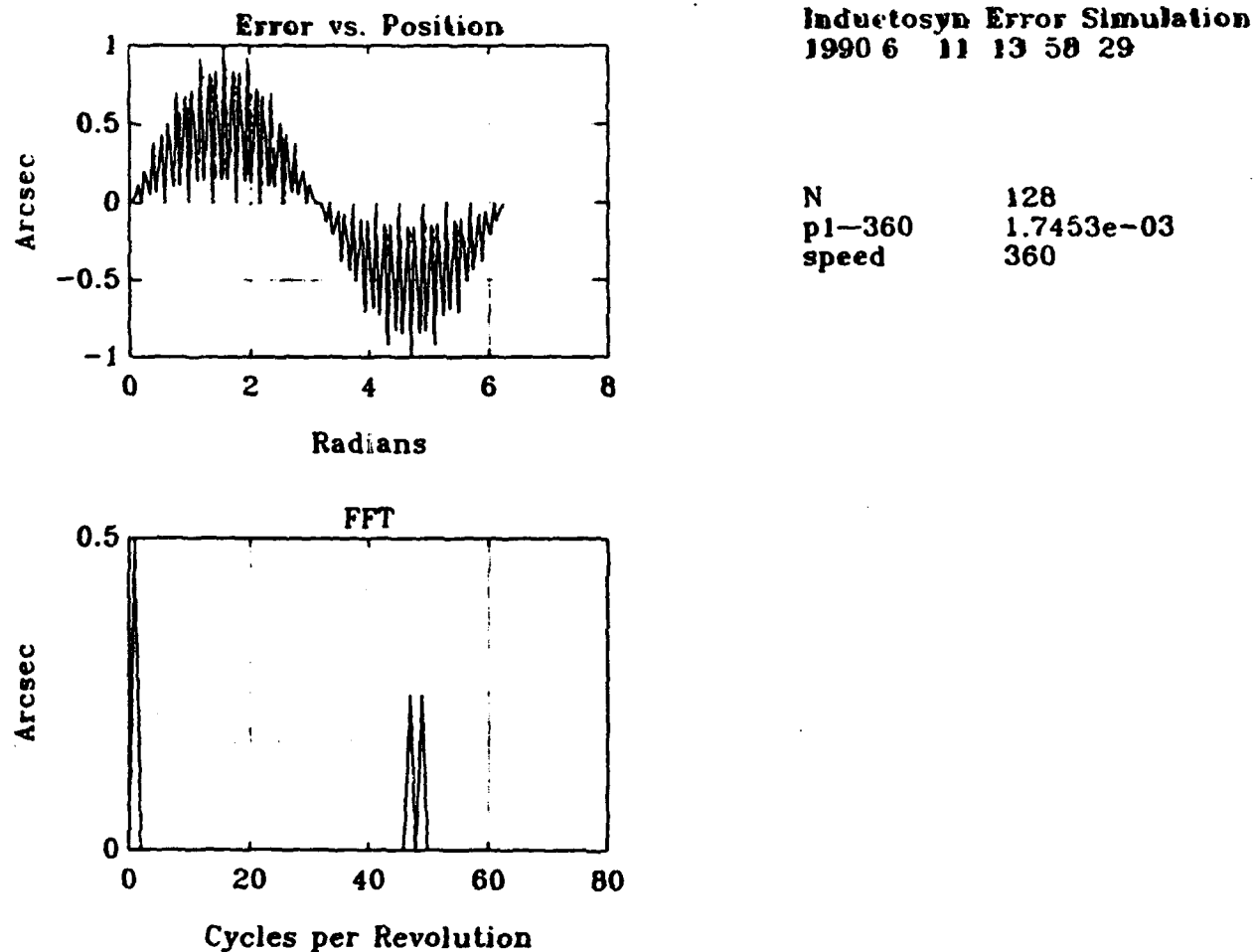


Figure C-17.

We reserve all rights in connection with this document and in the subject matter represented therein. The recipient hereby acknowledges these rights and shall not, without our permission in writing, disclose or divulge this document in whole or in part to third parties or use it for any purpose other than that for which it was delivered to recipient.

ampl =

Columns 1 through 7

0.0000	0.5000 <i>1/L₂V</i>	0.0000	0.0000	0.0000	0.0000	0.0000
--------	-----------------------------------	--------	--------	--------	--------	--------

Columns 8 through 14

0.0000	0.0000	0.0000	0.0000	0.0000	0.0000	0.0000
--------	--------	--------	--------	--------	--------	--------

Columns 15 through 21

0.0000	0.0000	0.0000	0.0000	0.0000	0.0000	0.0000
--------	--------	--------	--------	--------	--------	--------

Columns 22 through 28

0.0000	0.0000	0.0000	0.0000	0.0000	0.0000	0.0000
--------	--------	--------	--------	--------	--------	--------

Columns 29 through 35

0.0000	0.0000	0.0001 <i>1438</i>	0.0000	0.0001 <i>1440</i>	0.0000	0.0001 <i>1442</i>
--------	--------	-----------------------	--------	-----------------------	--------	-----------------------

Columns 36 through 42

0.0000	0.0000	0.0000	0.0000	0.0000	0.0000	0.0000
--------	--------	--------	--------	--------	--------	--------

Columns 43 through 49

0.0000	0.0000	0.0000	0.0000	0.0002 <i>722</i>	0.2500 <i>721</i>	0.0004 <i>720</i>
--------	--------	--------	--------	----------------------	----------------------	----------------------

Columns 50 through 56

0.2500 <i>719</i>	0.0002 <i>718</i>	0.0000	0.0000	0.0000	0.0000	0.0000
----------------------	----------------------	--------	--------	--------	--------	--------

Columns 57 through 63

0.0000	0.0000	0.0000	0.0000	0.0000	0.0000	0.0000
--------	--------	--------	--------	--------	--------	--------

Column 64

0.0000

Figure C-18.

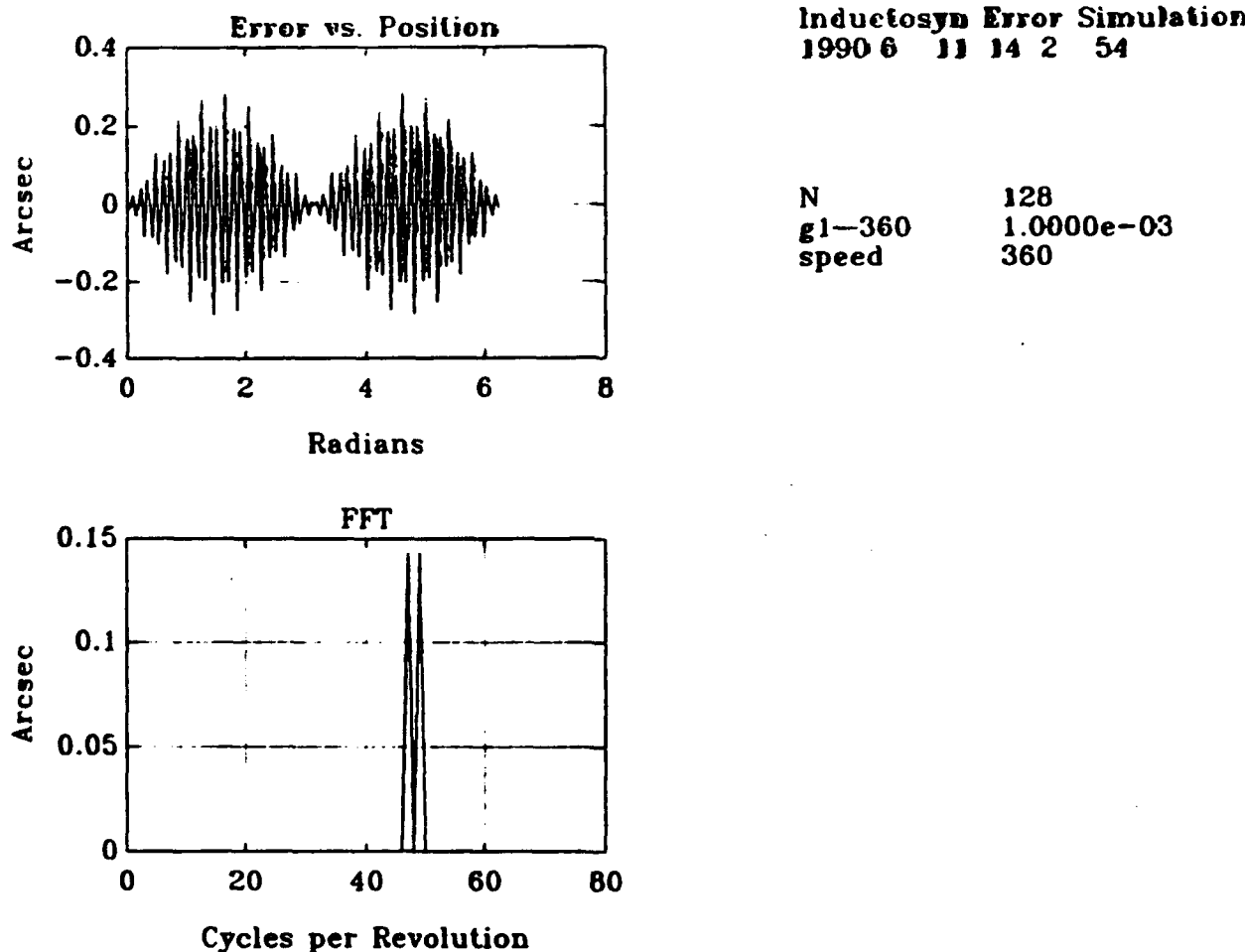


Figure C-19.

We reserve all rights in connection with this document and in the subject matter represented therein. The recipient hereby acknowledges these rights and shall not, without our permission in writing, disclose or divulge this document in whole or in part to third parties or use it for any purpose other than that for which it was delivered to recipient.

ampl =

Columns 1 through 7

0.0000 0.0000 0.0000 0.0000 0.0000 0.0000 0.0000

Columns 8 through 14

0.0000 0.0000 0.0000 0.0000 0.0000 0.0000 0.0000

Columns 15 through 21

0.0000 0.0000 0.0000 0.0000 0.0000 0.0000 0.0000

Columns 22 through 28

0.0000 0.0000 0.0000 0.0000 0.0000 0.0000 0.0000

Columns 29 through 35

0.0000 0.0000 0.0000 0.0000 0.0000 0.0000 0.0000

Columns 36 through 42

0.0000 0.0000 0.0000 0.0000 0.0000 0.0000 0.0000

Columns 43 through 49

0.0000 0.0000 0.0000 0.0000 0.0000 0.1432 0.0001
719 72/ 720

Columns 50 through 56

0.1432 0.0000 0.0000 0.0000 0.0000 0.0000 0.0000
719

Columns 57 through 63

0.0000 0.0000 0.0000 0.0000 0.0000 0.0000 0.0000

Column 64

0.0000

Figure C-20.

APPENDIX C

ITATT BEARING AND AXIS CONTROLS SYSTEMS ANALYSIS A MULTI-AXIS PERSPECTIVE

We reserve all rights in connection with this document and in the subject matter represented therein. The recipient hereby acknowledges these rights and shall not, without our permission in writing, disclose or divulge this document in whole or in part to third parties or use it for any purpose other than that for which it was delivered to recipient.

DYNAMIC AND CONTROL CONSIDERATIONS FOR THE ITATT

The present ITATT axes control system "separates" the axis orientation from the axis rotation thus separating the magnetic bearing control problem from the Inductosyn feedback positioning problem. The magnetic bearing locates the axis in 5 degrees of freedom while the axis position controller locates the axis in rotation (i.e., the remaining sixth degree of freedom). This ignores the torque coupling from axis to axis and can only work if the coupling is weak or if the bearing servo bandwidth is sufficiently high relative to the position loop bandwidth to reject coupling torque disturbances. The bearing control system must also reject gravity force disturbances caused by axis rotation while maintaining axis relative orientation; this may require a co-ordinated control of the bearing systems on each end of the gimbal.

TORQUE COUPLING

The present system has only one gimbal and cannot adequately measure the coupling effect. The figure below shows the coupling due to rotational dynamics:

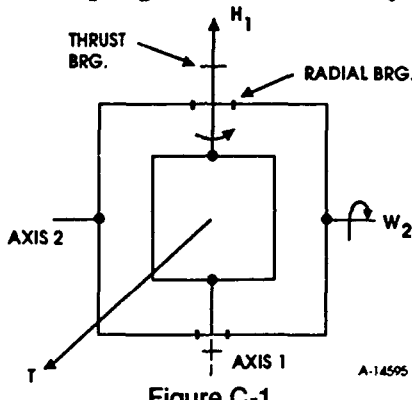


Figure C-1.

As axis 1 spins at high rate it will produce a momentum vector H_1 . A rotation of axis 2 (w_2) will produce a torque (T) on axis 1 which will produce equal and opposite forces on the radial bearings of axis 1, i.e.

$$T = (H_1) \times (w_2)$$

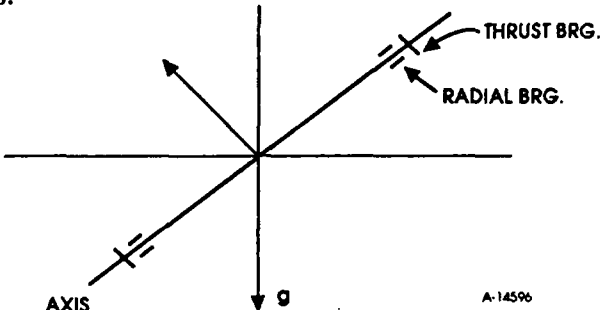
Additionally, any inertial torque on axis 2 produced by axis 2 motor will also produce equal and opposite forces on the radial bearings of axis 1. These disturbance forces must be rejected by the magnetic bearing control system.

Coupling also comes from the opposite direction. Any disturbance (noise fluctuations, for example) in the force produced by the magnetic bearings of axis 1 will disturb the rotational position control of the axis 2 servo. These disturbance torques must be rejected by the axis 2 position servo.

The amount of cross coupling motion will depend on the servo structure and performance of both bearings and axis positioner.

GRAVITY COUPLING

As axis 1 is rotated in the field of gravity the radial and thrust bearings of axis 1 see varying sinusoidal amounts of torque feedback as a function of axis 2 angular position. The figure below illustrates this:



A-14596

Figure C-2. Control Issues

The above issues concerning the dynamic coupling, stability and performance of the various magnetic bearing control loops must be addressed before we can make any predictions about the behavior of the overall system.

We must consider each gimbal as a free rigid body suspended by the action of five magnetic bearings and rotated by a torque motor.

Each magnetic bearing has a control loop driven by the variations in its gap. However, these gap variations represent the relative displacements of the successive gimbals. Therefore the state of motion of all the gimbals affects the signals that drive the control loops of the magnetic bearings. This brings about a feedback control coupling of all the magnetic bearing loops.

These interactions can be considered as disturbance to be rejected by the control loops but, in fact, they can have a destabilizing effect because they act along close-loop paths.

The dynamic and control feedback interaction paths for a pair of gimbals is schematically shown in Figure 1.

The relevant tasks in this investigation can be broken down as issues concerning a single magnetic bearings on a single gimbal and issues concerning the interactions of the magnetic bearings on all the gimbals at once.

1. Behavior of a single axis magnetic bearing control:

The relevant issue here is the stability and disturbance rejection characteristics of the bearing at various of the gap away from the nominal value. Also of interest is the ability to account for a variation in the steady-state weight that the bearing is supporting.

2. Control of the magnetic bearings on a single gimbal:

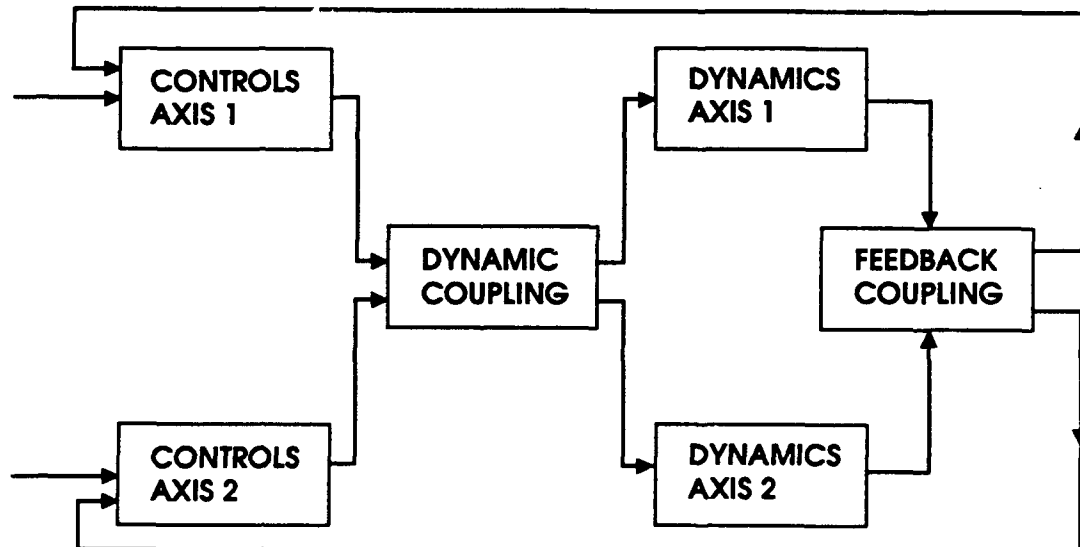
The question must be answered as to whether it is sufficient to control each magnetic bearing on a gimbal independently or whether they must be coordinated to control the definition of the instantaneous axis. This again depends on whether the independent magnetic bearing controls are adequate for the desired axis definition or whether the axis definition should be the primary control objective.

It is possible that some of these questions may be settled or partially answered by measurement data on the Phase 1 system.

3. The next issue concerns gimbal rotational and cascaded body dynamic interactions and feedback coupling:

A dynamic and control simulation model must be developed to study the extend of such dynamic interactions on the controllers (assumed independent). The stability of the overall system will be instigated for the types of per axis desired bandwidths. These interactions will also affect the degree of axis orthogonality that can be achieved under dynamic operating conditions.

4. If the results of items 3 are not satisfactory an additional investigation of coupled control approaches may be necessary to achieve overall system performance. As a minimum bandwidth limits should be established within which the overall system has an acceptable stable response.



A-14597

Figure C-3.

APPENDIX D

HONEYWELL REPORT 5000-112892 ON THE INNER AXIS ROLL RING ASSEMBLY

We reserve all rights in connection with this document and in the subject matter represented therein. The recipient hereby acknowledges these rights and shall not, without our permission in writing, disclose or divulge this document in whole or in part to third parties or use it for any purpose other than that for which it was delivered to recipient.

Final Report No. 5000-130801
13 August 1990

Inner Axis Roll Ring Assembly
PN 5000-112892

for

Contraves Goerz Corporation

Improved Three Axis Test Table

under

Contract Number FO8635-89-C-0297

and

Statement of Work TR-27405, Aug'89

Honeywell, Inc.
Satellite Systems Operation, Glendale, AZ

Index

<u>Paragraph</u>		<u>Page</u>
Summary		1
Discussion		2
Manufacturing		2
Assembly		3
Test		4
Physical Requirements		4
Insulation Resistance		4
Isolation		4
Static Resistance		4
Dynamic Resistance		4
Torque		6
Speed Capability		6
Conclusions/Recommendations		7/8
Appendix A, Flexure Design Details		9
Appendix B, Flexure Insertion Tool Details		11
Appendix C, Acceptance Test Plan/Data Sheets		13
Appendix D, Noise Resistance Data		33

Summary

The first 120 circuit roll ring assembly has been designed, fabricated, assembled and tested. The ultimate application for this evaluation unit is an advanced 0.1 arc sec Contraves Goerz Corporation Three Axis Test Table. Advantages provided by the roll ring technology are minimal torque, low maintenance, long life and minimal wear debris. The unit developed under this contract met all of the performance objectives for isolation, insulation and noise resistance except for a low insulation resistance to ground on one circuit and the possibility of torque perturbations (introduced by the bearings) which were 50 percent greater than the 0.2 oz-in requirement.

Discussion

This report covers the fabrication, assembly and test of the 120 circuit roll ring evaluation unit developed under contract FO8635-89-C-0297 for the Contraves Goerz Corp. This section will cover the high lights of the unit build and test.

Manufacturing

Electro-Tec was selected to fabricate the Inner and Outer Ring Housing Assemblies and to plate the Flexures. One problem encountered during the Housing fabrication was an out of spec surface finish on the Inner Ring grooves. This problem was eventually corrected with process changes at Electro-Tec. A second problem consisted of a loss of the gold plating (by adhesion failure) on the Rotor connector female sockets. These sockets were manufactured by Mill-Max Manufacturing Company. (Their PN 0348-0-33-(TBD)). The correction to this problem on this unit was to solder the lead wires to the connector body.

The design of the Flexures was based on a set of acceptable design parameters related to bending stress, deflection, contact force, stiffness, dynamic stability and current density. The final results of the analysis are shown in Appendix A which identifies the most important design and application parameters.

The Flexures were manufactured by a local machine shop by a numerically controlled procedure. The drop-out of these components was approximately 10 percent. Reasons for rejection included out of print radial thickness and axial width. It is probable that some of the Flexures (including those installed in the unit) were also under or over the diameter range. Since no inspection tooling for diameter and roundness is available nor included in this contract all inspection was performed visually. The wall thickness and width was checked in 2 or 3 locations with a pinch micrometer. (Refer to the "Recommendation" section). The Flexure manufacturer had a continual improvement of quality and yield as experience was gained.

Flexure plating was a major issue on this program. Approximately 30 percent of the 140 pieces which were plated were unacceptable for use because of exposed copper after plating. These areas of incomplete plating were at the holding fixture contact points on the ID. If the Nickel alone was exposed, the units were used. Exposed copper is unacceptable because of the possibility of copper migration to the contact tracks and subsequent resistive oxidation film formations.

Assembly

The assembly process was rather straight forward with the exception of the Rotor (inner ring) leads. The shielded leads tended to twist and wind together inside the housing ID. This "bunching" of the leads introduced moment loads across one bearing and resultant torque changes. A request was made to CGC to reduce the diameter of the central bore from 0.875 to 0.500 inches to facilitate the channeling of these wires. This request was granted and relieved the congestion somewhat. Future units would impose less problems during assembly if wire routing grooves were formed into the inner mounting tube.

A connection terminal broke in two inside the plastic matrix on the Inner Ring Assembly. This terminal (on circuit 115) was repaired by carefully clearing the area around the broken stud and butt soldering a new connecting pin to the remaining terminal. The terminal appeared to be faulty.

The Flexures were originally assembled into the annulus space of the Inner and Outer Rings with a tool one at a time. This tool stretched the Flexures along one diameter such that they could be inserted in the space. When the tool relaxed the deformation of the Flexure, it seated into the proper pair of grooves. The tool has built-in stops to control the stress of the Flexures during this process. It is determined during assembly, test and disassembly stages of the build process, however, that some of the Flexures had been over stressed and had a small out-of-round condition. When they could be located, these faulty/damaged Flexures were discarded and others used in their place. Subsequent rebuilds of some of the modules pointed up a requirement for an alternate means of assembling the Flexures. A tool was designed which inserts all 20 Flexures in a given module in one operation and does so without deforming the Flexures during the process. This tool is detailed in Appendix B. It was used successfully for the last 2 builds of the unit and proved to be efficient for safe installation of the Flexures.

All of the Flexures which were suspected of having deformation or other handling damage were replaced within the available budget of the program. Complicating this situation is the fact that no inspection tools are available to properly inspect the Flexures for diameter, wall thickness and stiffness. The build of this unit has pointed vividly to the fact that these tools are required for future builds. Since the contact resistance across the rings is not strongly dependent upon preload, resistance alone is not a viable replacement for proper geometric gages.

Test

All acceptance testing was conducted in accordance with the requirements of PN 5000-112892 as approved.

a. Physical Requirements

The unit (SN 001) met all of the physical requirements with the exception of the central tube bore of 0.50 inches which had been specified as 0.875, (Refer to previous text.) The inspection data is compiled on Page 1 of the data sheets.

b. Insulation Resistance

All of the circuits passed the high voltage insulation requirements for lead-to-lead, lead-to-ground and lead-to-shield resistance except for the lead-to-ground resistance of circuit number 120. This circuit had a resistance of 13 meg ohms at 500 volts. The insulation resistance ranges are summarized on Page 2 of the data pages of the Acceptance Plan. The dielectric of the molding material was too thin to provide the required higher insulation resistance. Subsequent builds would require an increase in allowable unit length to improve this condition.

c. Isolation

The circuit-to-circuit isolation was well within the specification requirements when measured at the module terminals. The isolation test results are summarized on Page 2 of the Data in the Plan.

d. Static Resistance

There were no specified requirements for this parameter. The resistance was monitored, however, to check for Flexures which may be faulty. These "faults" which could include improper preload/stress would be captured prior to assembly if inspection tooling were available. The static resistance measurements did not reveal any faulty circuits. Two such circuits were identified, however, during the noise resistance tests which followed. As can be derived from the data sheets on Pages 3 and 4, the lead wire resistance translates to 205 milli ohms or so and the terminal-to-terminal resistance is a nominal 25 milli ohms.

e. Dynamic Resistance

The noise resistance of each circuit and of adjacent circuit pairs was measured and recorded on a Gould strip chart recorder Model 2200S. The measurements were taken with the spin axis vertical at a test speed of approximately 200 deg/sec. (Speed was difficult to maintain due to the direct drive motor configuration.)

An exception was made to the procedure delineated in the Plan in that the return leads were not parallel sets of 4 leads as specified in the plan but a twisted single wire. This wire was configured to coil and uncoil during data taking.

This approach to test provided lower noise and more precise and dependable test signals.

All of the Strip chart test data (Refer to appendix C) was reduced to numerical form and compiled on Page 5 of the Data Sheets. As can be seen in the data 99 of the 120 single circuits had performance which met the 100 milli ohm design goal. As can be seen in the strip chart data, the inherent integrity of the various circuits is evident in the data. This noise resistance is defined as the peak noise spikes over several revolutions. The background or mean noise magnitude is always less than the peak value. Circuits number 97 and 101 are not acceptable from the stand point of over-all noise characteristics. Since there is no inspection data on these components, the exact cause of the unacceptable noise behavior is unknown. It is likely that these two circuits have undersized Flexures and extremely low preload. This type of performance anomaly can be avoided by proper inspection of the geometrics of the Flexures during the manufacturing process. (Flexure size and other geometric properties would be certified before the plating process.)

The noise resistance of parallel pairs was taken with sequential pairing of circuits. The resultant noise resistances resulted in 53 of the pairs being in spec. If the pairing is chosen based upon low and high spike circuits being paired, the resultant 60 pairs would meet the design goal for resistance. As an example, instead of pairing A1 with A2 and A3 with A4, a more optimum arrangement would be to pair A1 with A3 and A2 with A4. This latter grouping would bring the A1/3 pair into spec without causing A2/4 to go beyond the specified value. Instead of pairing F1 with F2 and F3 with F4, an alternate arrangement would be to pair F1 with F3 and F2 with F4.

A fixture related problem which didn't affect the data, but which increased the test time, was the direct drive motor which made it difficult to set a specific test speed.

The lead wire resistance and, hence, the lead length, influences the noise resistance. Additionally, the tie point where the leads are wired in parallel has an influence on the noise resistance. The equivalent resistance of a parallel circuit is related to the lead wire resistances. If the rotor and stator lead wires were connected at their outer ends, a noise resistance on one circuit of 0.7 ohms would produce a 0.1 ohm change on the pair. If the leads were tied at the ends on the rotor and at the terminals on the stator, a resistance spike of 1.7 ohms would be required on one circuit to produce the same 0.1 ohm change on the pair.

All of the "paired" circuit test data was taken with the circuits tied together at the lead wire ends. The strip chart data in Appendix "C" has a ± 0.5 mm (smallest division) deviation over several runs which is a result of a mechanical tracking problem in the recorder. The test data is grouped with circuits 1 through 120 first followed by the 60 pairs. The test data is the recording on the left hand side of each chart. When a resistance indication occurs on the test data if a

matching change occurs on the right-hand chart, that particular change is invalid. The chart speed was 10 mm/sec which translates to one revolution of the unit per 18 mm (small divisions). The cross axis represents circuit resistance at a scale factor of 1 mm (division) per 10 milli ohms.

f. Torque

Starting and running torque proved to be quite difficult to measure. Assembly of the unit without cables and roll rings indicated a small performance margin to the required torque specification in the horizontal axis and torque peaks up to 50 percent over spec in a vertical axis. The housing pendulosity introduced uncertainty into the torque measurements in the horizontal axis. After the unit was assembled with roll rings and cables attached, the torque measurements were even more difficult to obtain. The rotor lead wires applied radial loads on the inner sleeve which resulted in reaction moments applied to the bearing. These reaction moments introduced regions of over-spec torque peaks. Replacement of the tube with another smaller tube reduced the torque peaks to an acceptable level.

g. Speed Capability

The unit was operated at the 200 rev/min upper speed requirement by spinning the Outer Housing Assembly with the rotor secured to a base plate. The test was not repeated with the rotor rotating because of the difficulty protecting the lead wires. A special fixture would be required to measure the unit torque levels after full assembly is complete.

Conclusions

The following conclusions were derived from the build and test of this evaluation unit.

1. A number of fabrication, plating and assembly processes were worked out on this study. These will enhance the build of future units.
2. The basic design of the evaluation unit is very efficient. The configuration is also flexible such that alternate numbers of circuits are possible.
3. At least one Flexure plating vendor is now qualified to produce reliable components on a predictable schedule.
4. It is evident that additional inspection tools are required to eliminate faulty Flexures from finding their way into the completed unit and into the test phase.
5. An inspection tool is required to measure the Flexure space between the Inner (Rotor) and Outer (Stator) ring grooves.

Recommendations

1. It is recommended that inspection tools be developed to accomplish the following measurements prior to initiating the build of additional units:
 - a. Flexure diameter gage (100% inspection)
 - b. Flexure wall thickness gage (100% inspection)
 - c. Flexure diametral stiffness (at specific deflection) fixture.
 - d. Flexure contact profile gage
 - e. Ring annulus gage
2. The Inner Ring mounting tube should be modified by adding wire channels which will minimize "bunching" of the cables.
3. The circuits should be separated into stand-alone modules of approximately 20 circuits each. This will simplify the assembly process and add barriers between the groups of circuits.
4. The test fixture should be modified to provide a rotationally stable variable drive speed.
5. The test fixture should be modified to provide a "zero" (<2 milli ohm) noise return path with unlimited rotational capability.

Final Report
No. 5000-130801

Appendix A

Flexure Design Details

CG/PROTO2
INPUTS FROM :

12:05:18

11/28/1989

***** PROGRAM INPUTS *****

OUTER GROOVE RADIUS (IN)	=	1.73800
INNER GROOVE RADIUS (IN)	=	1.08800
OUTER GROOVE TRANSVERSE RADIUS (IN)	=	0.02000
INNER GROOVE TRANSVERSE RADIUS (IN)	=	0.02000
FLEXURE CORNER TRANSVERSE RADIUS (IN)	=	0.01500
FLEXURE INSIDE DIAMETER (IN)	=	0.65800
FLEXURE WALL THICKNESS (IN)	=	0.00575
FLEXURE WIDTH (IN)	=	0.02700
AXIAL SPAN BETWEEN FLEXURE RADIUS AND GROOVE RADIUS CENTER (IN)	=	0.00250
RADIAL SPAN BETWEEN FLEXURE I.D. AND FLEXURE CORNER RADIUS CENTER (IN)	=	0.00900
THICKNESS OF PLATING ON RING (IN)	=	0.00020
THICKNESS OF PLATING ON FLEXURE (IN)	=	0.00020
ELASTIC MODULUS OF FLEXURE MATERIAL (PSI)	=	1.9000E+07

***** FLEXURE GEOMETRIES *****

FLEXURE CROSS SECTIONAL AREA (SQ IN)	=	1.3920E-04
SECTION INERTIA ABOUT NEUTRAL AXIS (IN**4)	=	3.9660E-10
RADIUS TO NEUTRAL AXIS OF UNLOADED FLEXURE (IN)	=	0.331519
INBOARD RADIUS INTERCEPT ANGLE OF FLEXURE (DEG)	=	10.40598
OUTBOARD RADIUS INTERCEPT ANGLE OF FLEXURE (DEG)	=	47.46310

***** INTERFACE *****

CONTACT ANGLE (DEG)	=	32.92073
TOTAL DEFLECTION OF FLEXURE AT CONTACT (IN)	=	0.022277
TOTAL DEFLECTION OF FLEXURE AT FREE LOOP (IN)	=	-0.020457
EFFECTIVE CONTACT RADIUS OF OUTER RING (IN)	=	1.734621
EFFECTIVE CONTACT RADIUS OF INNER RING (IN)	=	1.091379
EFFECTIVE FREE DIAMETER OF FLEXURE AT THE CONTACT (IN)	=	0.665518
RADIUS OF CURVATURE AT CONTACT OF LOADED FLEXURE (IN)	=	0.388424
FLEXURE TRACKING STABILITY RATIO	=	0.061538

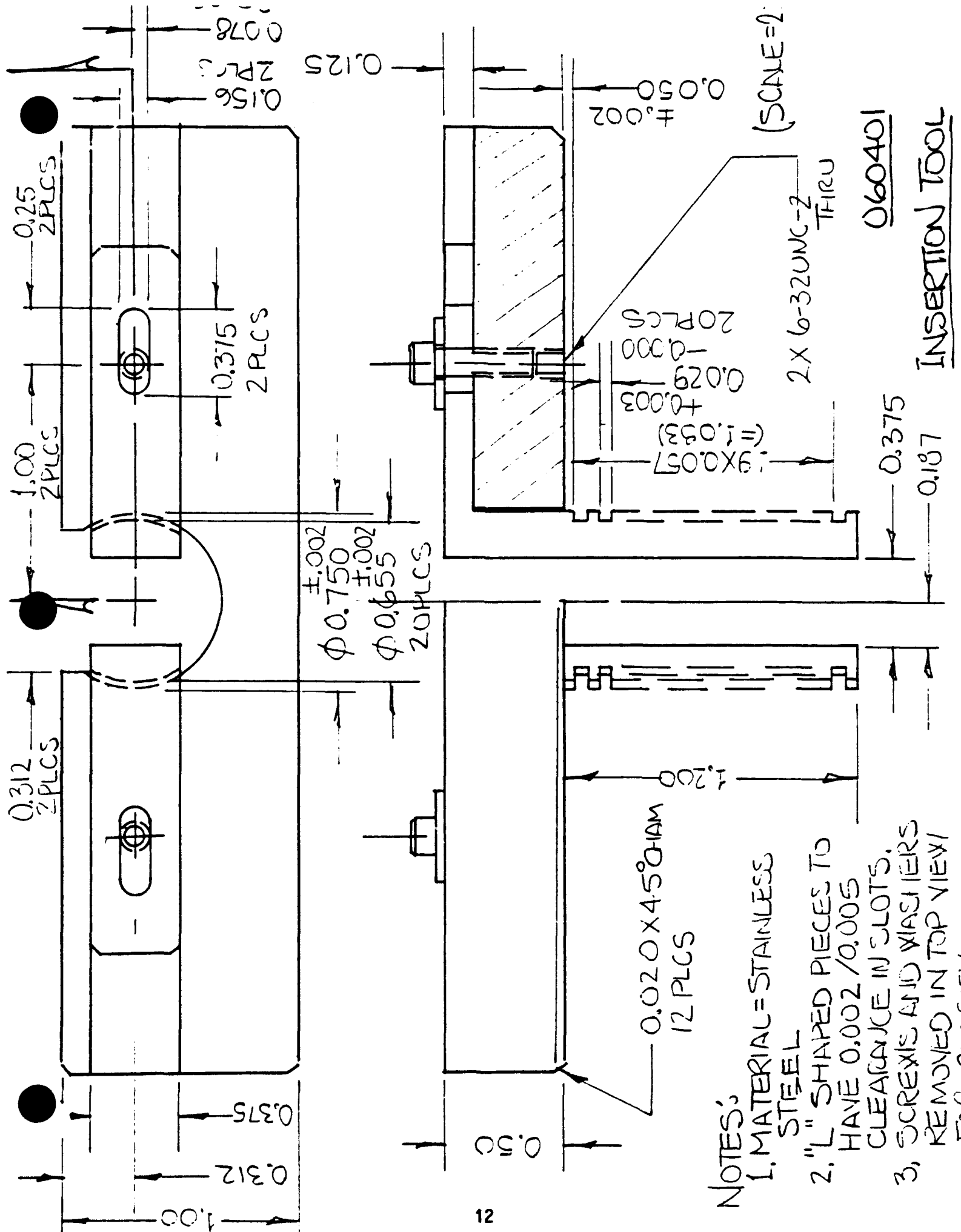
***** LOADS & STRESSES *****

RADIAL PRELOAD (LBS)	=	0.0310
FLEXURE STIFFNESS (LBS/IN)	=	1.3901
STRESS AT OUTER FIBER AT CONTACT (PSI)	=	-28245.3
STRESS AT INNER FIBER AT CONTACT (PSI)	=	22379.4
STRESS AT OUTER FIBER AT FREE LOOP (PSI)	=	16054.3
STRESS AT INNER FIBER AT FREE LOOP (PSI)	=	-12910.6
NORMAL CONTACT FORCE (LBS)	=	0.018446

**Final Report
No. 5000-130801**

Appendix B

Flexure Insertion Tool Details



Final Report
No. 5000-130801

Appendix C

*Acceptance Test Procedure
and Data Sheets*

5000-112892

15 May 1990

Acceptance Test Plan

for

Contraves Goerz

Inner Axis Roll Ring Assembly

PN 5000-112892

**HONEYWELL, INC.
Satellite Systems Operation, Glendale**

5000-021211

**12 February 1990
Revised 27 April 1990**

Acceptance Test Plan

5000-021211

Approved this 15th day of May 1990.

Contraves Goerz Corporation

by: David Henderson
(Name)

Program Manager
(Title)

TABLE OF CONTENTS

<u>SECTION</u>		<u>BEGINS ON PAGE NUMBER</u>
Introduction	2
Requirements	
Physical	3
Performance	4
Verification	
Physical	5
Performance	6
Appendix A, Data Sheets	8

1. Introduction

The objective of this Acceptance Plan is to delineate the performance requirements and related test procedures applicable to the Improved Three Axis Test Table (ITATT) Inner Axis Roll Ring Assembly (IARRA) Part No. 5000-112892. The basis for these requirements are those specified in Contraves Goerz Statement of Work TR-27405 dated Aug, 1989 and related "Roll Ring Assembly" drawing 903989 revision C and by written communications between C.R. Greenhill and E. M. Frazier dated 19 and 29 Jan '90.

2. Physical and Performance Requirements

The referenced control documents establish the following requirements which form the basis for IARRA unit evaluation.

2.1 Physical - These parameters are not all inclusive. All dimensions specified on 903989 A will be verified prior to accepting the unit.

2.1.1 Max Envelope (Includes cables)

a.	Diameter (In)	4.375
b.	Length of Stator Housing (In)	8.210
c.	Length of Rotor Housing	9.210

2.1.2 Mounting Diameters

a.	Stator/Both Ends (In)	3.749 ^{+0.000} _{-0.001}
b.	Rotor/Both Ends (In)	2.187 ^{+0.001} _{-0.000}

2.1.3 Number of Circuits

120

Note: Cables may be tied in 60 pairs at outer end.

2.1.4 Min Continous Current Capacity/All circuits (Amps)

3.0

2.1.5 Operating Environment

a.	Temperature (°F)	70 ± 15
b.	Humidity (%)	10 to 85

2.1.6 Cables

a.	Size (AWG No.)	24
b.	Insulation	White Ethylene Copolymer
c.	Min Length (In)	84
d.	Shield	Req'd.
e.	Strain Relief	Req'd.
f.	Labels	Req'd.

2.1.7 Insulation Resistance (M ohms)

a.	Lead-to-Lead	1K
b.	Lead-to-Ground	1K
c.	Lead-to-Shield	1K

2.1.8 Min Isolation into 50 ohm load at 1 KHz (db)

a.	Terminal-to-Terminal	-70
b.	Lead-to-Lead	TBD

Note: since two adjacent 84 inch long shielded leads alone will not meet this specification this isolation requirement will be assumed to apply to the unit, terminal-to-terminal, on adjacent circuits.

2.2 Performance

2.2.1 Static Resistance (milli ohms)

a.	Each Circuit/Terminal-to-Terminal	ND
b.	Each Circuit/Lead-to-Lead	ND
c.	Circuit Pair/Lead-to-Lead	ND

Note: "ND" = Not defined

2.2.2 Max Dynamic Resistance (milli ohms)

a.	Each Circuit @ 200 deg/sec	ND
b.	Circuit Pair @ 200 deg/sec	100

Note: Requirement 2.2.2b is a design goal

2.2.3 Max Total Unit Torque (Oz In)

a.	Starting	0.2
b.	Running	0.16

2.2.4 Continous Speed Capability (Rev/Min) 200

2.2.5 Min Rotational Life (revs) 10^7

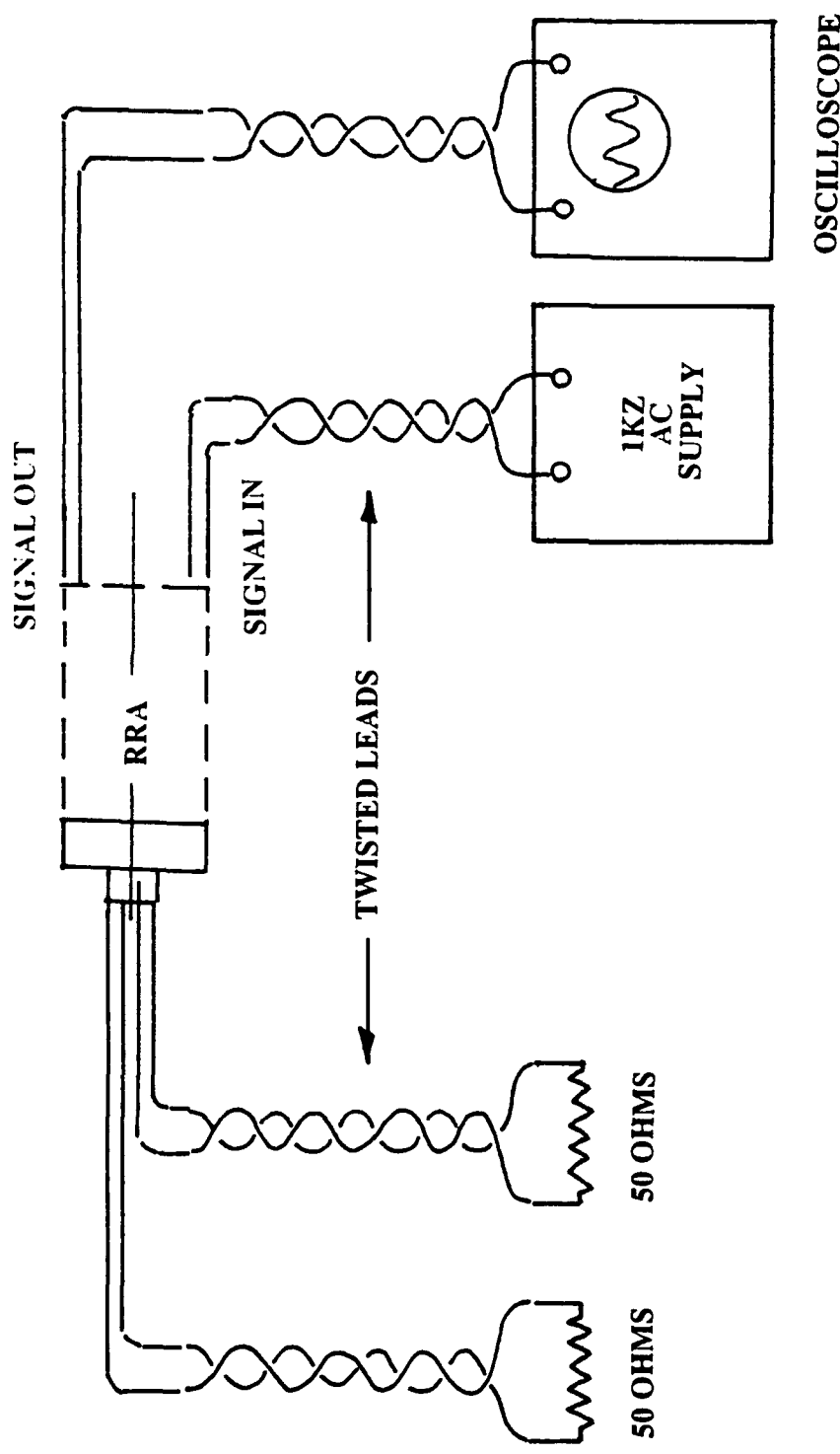
Note: Unit performance at 10^7 revs is "ND". Life verification is not required.

3.0 Physical Verification

The following procedure will be used to verify the conformance of the unit to the requirements of Section 2.1. The results of this verification will be recorded on the data sheets displayed in Appendix A.

<u>Parameter</u>	<u>Verification Technique</u>
2.1.1 Envelope	Measure on completed unit
2.1.2 Mounting Diameters	Measure on applicable detail parts
2.1.3 Number of Circuits	Verify on completed unit
2.1.4 Current Capacity	Confirm at 125% capacity with DC voltage and resistive load
2.1.5 Operating Environment	Measure all performance at $75 \pm 10^\circ\text{F}$ and $20 \pm 10\%$ RH (Range not to be evaluated)
2.1.6 Cables	Measure and verify on completed unit
2.1.7 Insulation Resistance	
a. Lead-to-Lead	A Megohmeter will be used to verify at 500 V DC the minimum lead-to-lead insulation resistance by checking each Stator lead against all other stator leads.
b. Lead-to-Ground	A Megohmeter will be used to verify at 500 V DC the minimum lead-to-ground insulation resistance by checking each Stator Lead against the unit ground or frame.
c. Lead-to-Shield	A Megohmeter will be used to verify at 500 V DC the minimum lead-to-shield insulation resistance by checking each Stator and Rotor lead against it's own shield.
2.1.8 Isolation	
a. Terminal-to-Terminal	Each Adjacent pair of terminals of each module will be connected into the circuit of Figure 1 (using twisted leads) after the Module is assembled but prior to assembly of the Module into the transfer unit. The circuit isolation will be measured at 1 KHz using a 50 ohm load impedance.
b. Lead-to-Lead	The testing procedure for paragraph 2.1.8a will be repeated after the module is assembled into the transfer unit and lead wires have been attached. This second set of tests will include the influence of the shielded leads on circuit coupling.

FIGURE 1



CIRCUIT ISOLATION MEASUREMENT SCHEMATIC

4.0 Performance Verification

The following procedure will be used to verify the performance conformance of the unit to the requirements of Section 2.2. The results of this verification will be recorded on the data sheets displayed in Appendix A.

<u>Parameter</u>	<u>Test and Verification Technique</u>
2.2.1 Static Resistance	
a. Each Circuit	
• Terminal-to-Terminal	The resistance of each circuit will be measured in a static mode with a 3 lead milliohmeter (HP 4328A) at the terminals of each module prior to attaching the lead wires.
b. • Lead-to-Lead	The resistance of each circuit will be measured in a static mode with a 3 lead milliohmeter (HP 4328A) on a completed unit at the lead wire ends.
c. • Circuit Pair	The resistance of each circuit will be measured in a static mode with a 3 lead milliohmeter (HP 4328A) on a completed unit at the lead wire ends. Adjacent circuits will be paired at the cable ends on both rotor and Stator.
2.2.2 Dynamic Resistance	
	The completed unit will be run in at 200 ± 25 deg/sec for a minimum of 12 hours prior to conducting performance testing. A portion of this run-in period will be at 200 rev/min.
a. Each Circuit	The unit will be mounted in the test fixture such that a continuous rotational speed of 200 deg/sec can be maintained during performance testing. Each circuit will be sequentially connected to the load circuit as shown in Figure 2. A minimum of 4 parallel circuits will be used to provide a low resistance return path for the load current. A strip chart recorder will be used to monitor the electrical noise resistance across the circuit at a DC load current of 1 amp. The voltage drop across the test unit will be recorded and the noise resistance will be derived from the voltage drop. "Average noise" will be derived from the steady state background voltage level and "peak noise" will be derived from the maximum recorded peak over a 20 sec (11 rev) interval.

ELECTRICAL NOISE MEASUREMENT SCHEMATIC

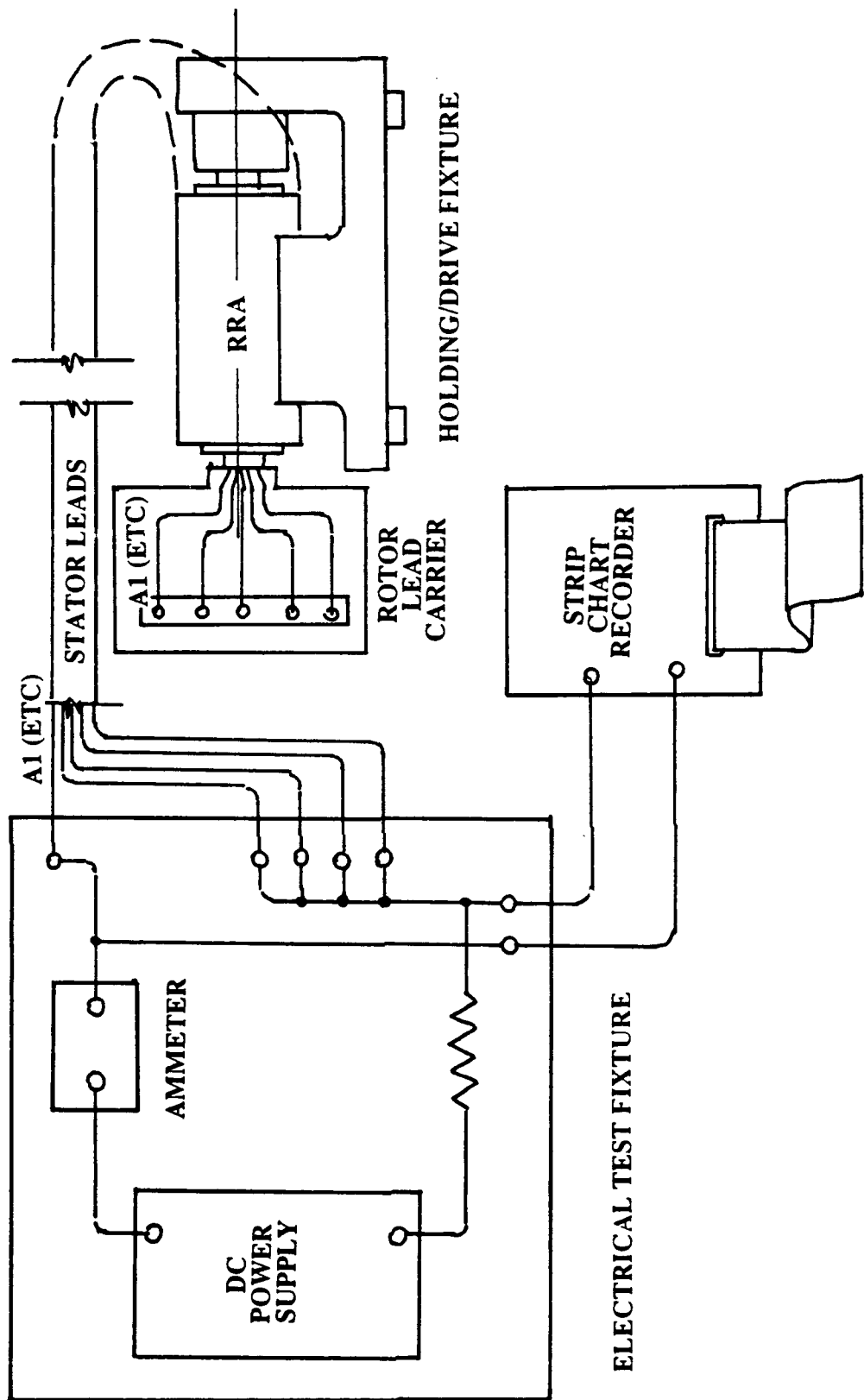


FIGURE 2

<u>Parameter</u>	<u>Test and Verification Technique</u>
	The resolution of the strip chart recorder shall be such as to determine the voltage drops across each circuit to a resolution of 10 mv (10 milliohms) or better.
b. Circuit Pair	The procedure of paragraph 2.2.2a will be repeated with adjacent pairs of circuits. This pairing will result in electrical noise resistance determinations for 60 total pairs.
2.2.3 Torque	All torque readings will be made using a torque watch and adapter which drives the Rotor relative to a fixed Stator. The complete unit will be utilized for this test with all six circuit modules assembled. Readings will be taken in a horizontal orientation which represents the application.
a. Starting	Measurements will be made of the unit break-away or starting torque in both a clockwise and a counterclockwise direction of rotation.
b. Running	The unit running torque will be measured at a rotational speed of 200 deg/sec for both clockwise and counterclockwise directions of rotation. The peak hold needle will be monitored to obtain these torque levels after resetting the needle after break-away has occurred.
2.2.4 Speed Capability	Since the unit run-in will include rotation at the specified maximum operating speed of 200 rev/min this requirement will be established as met after the unit testing is complete.
2.2.5 Rotational Life	Verification of this parameter is not included in the contract. It is included, however, as a design requirement.

APPENDIX A

Data Sheets

DATA SHEET1 of 6

The Physical and Performance data listed on these sheets is applicable to Inner Axis Roll Ring Assembly PN 5000-112892.
 (CGC 903989)

Unit S/N 001

Date 14 Jul '90 to 20 Jul '90

Tester O. Jacobsen

PHYSICAL PARAMETERS

<u>PARAMETER/DIMENSION</u>	<u>REQUIREMENT</u>	<u>ACTUAL</u>
Length	8.200 ± 0.010	<u><8.20</u>
Envelope Diameter	$4.375^{+0.000}_{-0.010}$	<u><4.375</u>
Mounting Diameter, Stator, Right	$3.749^{+0.000}_{-0.001}$	<u>3.7485</u>
Mounting Diameter, Stator Left	$3.749^{+0.000}_{-0.001}$	<u>3.749</u>
Land, Right	0.250 ± 0.005	<u>0.252</u>
Land, Left	0.250 ± 0.005	<u>0.251</u>
Mounting Diameter, Rotor, Right	$2.187^{+0.001}_{-0.000}$	<u>2.1875</u>
Mounting Diameter, Rotor, Left	$2.187^{+0.001}_{-0.000}$	<u>2.187</u>
Recess, Right	0.156 ± 0.005	<u>0.156</u>
Recess, Left	0.156 ± 0.005	<u>0.161</u>
Bore (NOTE 1)	$0.875^{+0.005}_{-0.000}$	<u>0.50</u>
Extension OD (NOTE 1)	$1.000^{+0.000}_{-0.010}$	<u>0.623</u>
Extension Length	1.000 max	<u><1.00</u>
Mounting Pattern, Rotor, Right (NOTE 1)	#4-40, 6 plcs, 1.68	<u>CONFORMS</u>
Mounting Pattern, Rotor, Left	#4-40, 4 plcs, 1.68	<u>CONFORMS</u>
Mounting Pattern, Stator, Right	#4-40, 6 plcs, 3.12	<u>CONFORMS</u>
Mounting Pattern, Stator, Left	#4-40, 6 plcs, 3.12	<u>CONFORMS</u>
Number of Windows	4	<u>4</u>
Inner Radii	0.75 ± 0.005	<u>0.75</u>
Outer Radii	1.03 ± 0.005	<u>1.035</u>
Number of Circuits	120	<u>120</u>

2 of 6DATA SHEETPHYSICAL PARAMETERS (Cont.)

<u>PARAMETER/DIMENSION</u>	<u>REQUIREMENT</u>	<u>ACTUAL</u>
Insulation Resistance (M ohms)		
Lead-to-Lead	>1,000	<u>10^4</u> min/ <u>$>10^6$</u> max
Lead-to-Ground	>1,000	<u>20K</u> min/ <u>200K</u> max ₁
Lead-to-Shield	>1,000	<u>20K</u> min/ <u>2×10^6</u> max ₃
Isolation (db)		
Terminal-to-Terminal	-70	<u>90</u> min/ <u>100</u> max
Lead-to-Lead	ND ₂	<u>NA</u> min/ <u>NA</u> max
Current Capacity	<u>3</u> Amps For	<u>1</u> Minute

Laboratory Environment 75 TO 85 °F 25 TO 40 RH

Cables

Size 24 AWG Length 94 inches (TO TERMINALS)Insulation Type WHITE ETHYLENE COPOLYMERShields ALL LEADS Lables 1 TO 120 ROTOR & STATOR
(FLOATING)

NOTES:

1. CIRCUIT NO 1 HAD RESISTANCE OF 1.4K MEG Ω;
NO. 120 HAD RESISTANCE OF 13 MEG OHMS.
2. CIRCUIT NO. 13 HAD RESISTANCE OF 2K MEG Ω.

PERFORMANCE PARAMETERS (cont.)PARAMETER/DIMENSION REQUIREMENT

Dielectric Resistance (Milliohms) ND

c. Circuit Pair/Lead-to-Lead

Module 3

	A	B	C	D	E	F
1	>218	—	—	—	—	—
2	—	—	—	—	—	—
3	>	—	—	—	—	—
4	—	—	—	—	—	—
5	>	—	—	—	—	—
6	—	—	—	—	—	—
7	>	—	—	—	—	—
8	—	—	—	—	—	—
9	>	—	—	—	—	—
10	—	—	—	—	—	—
11	>	—	—	—	—	—
12	—	—	—	—	—	—
13	—	—	—	—	—	—
14	>	—	—	—	—	—
15	—	—	—	—	—	—
16	>	—	—	—	—	—
17	—	—	—	—	—	—
18	>	—	—	—	—	—
19	—	—	—	—	—	—
20	>	—	—	—	—	—

NOTE: ONLY ONE READING WAS TAKEN SINCE THIS
DATA CAN BE DERIVED FROM DATA ON PAGE 3.

DATA SHEETPERFORMANCE PARAMETERS (cont.)PARAMETER/DIMENSION REQUIREMENTDynamic Resistance₄ (milliohms) ND/ND

a. Circuit (Ave/Peak)

PARAMETER/DIMENSION REQUIREMENTDynamic Resistance₄ (milliohms) <100/<100

b. Circuit Pair (Ave/Peak)

Module 3

Circuit N.	A	B	C	D	E	F
1	20 2500	150 500	20 40	20 240	30 160	70 500
2	20 80	10 10	40 50	10 40	20 40	50 450
3	5 10	20 30	10 30	20 30	10 30	20 40
4	10 60	20 150	10 40	20 40	10 20	15 60
5	10 40	20 380	10 30	10 20	10 25	30 330
6	20 40	5 30	5 20	10 30	10 30	10 20
7	10 40	10 30	5 30	20 30	5 20	20 500
8	10 120	10 30	10 30	10 450	10 70	20 40
9	20 50	5 25	10 30	20 40	5 15	5 25
10	5 20	5 40	10 30	10 500	20 40	10 20
11	20 370	10 50	10 30	10 30	20 60	20 500
12	10 30	10 60	10 450	15 30	20 50	10 25
13	5 30	20 70	20 50	5 10	20 40	40 60
14	10 35	10 25	10 30	10 30	30 500	20 40
15	10 30	10 30	10 50	10 30	50 500	20 50
16	5 20	10 40	20 70	5 20	50 300	15 20
17	5 20	5 30	20 40	10 30	150 400	20 40
18	5 20	5 20	10 40	15 30	30 100	20 60
19	10 35	10 30	10 50	10 30	30 150	30 60
20	20 90	20 80	10 70	10 40	10 20	20 62

Module 3

Circuit Number	A	B	C	D	E	F
1	X 10 110	30 140	10 60	5 20	10 100	10 15
2						
3	X 5 10	10 50	5 10	2 5	2 5	2 10
4						
5	X 2 5	5 100	2 25	2 5	5 20	5 10
6						
7	X 5 10	2 10	3 7	2 10	2 10	5 14
8						
9	X 5 15	2 5	2 5	10 130	2 5	2 10
10						
11	X 5 80	2 5	5 60	2 5	5 10	2 13
12						
13	X 2 5	2 5	5 20	5 10	20 90	2 10
14						
15	X 2 5	2 5	5 10	2 45	30 100	2 10
16						
17	X 2 5	2 10	5 40	5 10	40 60	5 15
18						
19	X 5 80	2 10	10 80	2 5	5 20	5 10
20						

NOTE: DEFECTIVE CIRCUITS 97 (17/E) AND 101 (1/F) SHOULD NOT BE USED.

DATA SHEET
PERFORMANCE PARAMETERS (Cont.)

6 of 6

<u>PARAMETER/DIMENSION</u>	<u>REQUIREMENT</u>	<u>ACTUAL</u>
Torque (Oz In)		
a. Starting	<0.2	<u>0.18 TO 0.35</u>
Clockwise (NOTE BELOW)		<u>0.18 TO 0.38</u>
Counter Clockwise (NOTE BELOW)		
b. Running	<0.16	<u>0.14 TO 0.20</u>
Clockwise (NOTE BELOW)		<u>0.14 TO 0.20</u>
Counter Clockwise (NOTE BELOW)		
Speed Capability (Deg/sec)	1000	<u>OK</u>
Rotational Life (Revs)	$>10^7$	<u>TBD</u>
Total During Testing	$\approx 3,000$	

COMMENTS/OBSERVATIONS THE TORQUE READINGS WERE EFFECTED BY STATOR PENDULOSITY AND LEADS TO AND UNKNOWN AMOUNT. READINGS INCLUDE TERMS NOT APPLICABLE TO USE.

THE 0.875 TO 0.905/-0.000 BORE WAS REDUCED TO 0.500 TO 0.005/-0.000 AND THE EXTENSION OD WAS REDUCED FROM 1.000 TO 0.800/-0.000 TO 0.675 TO 0.000/-0.010 AS AUTHORIZED BY CGC.

TWO OF THE 6 4-4AWG TAPPED HOLES HAVE STEEL INSERTS

NOTES:

1. "Right" end of unit is defined as that at which Stator Leads exist.
2. "ND" = Not Defined
3. Modules and circuits progress left-to-right. (i.e. Circuit "A1" is on extreme left end of unit.)
4. All electrical noise resistance data is included in the data package as noise voltage against time (rotations) on strip charts.
6. Rotation sense is defined as looking into "right" end of unit.

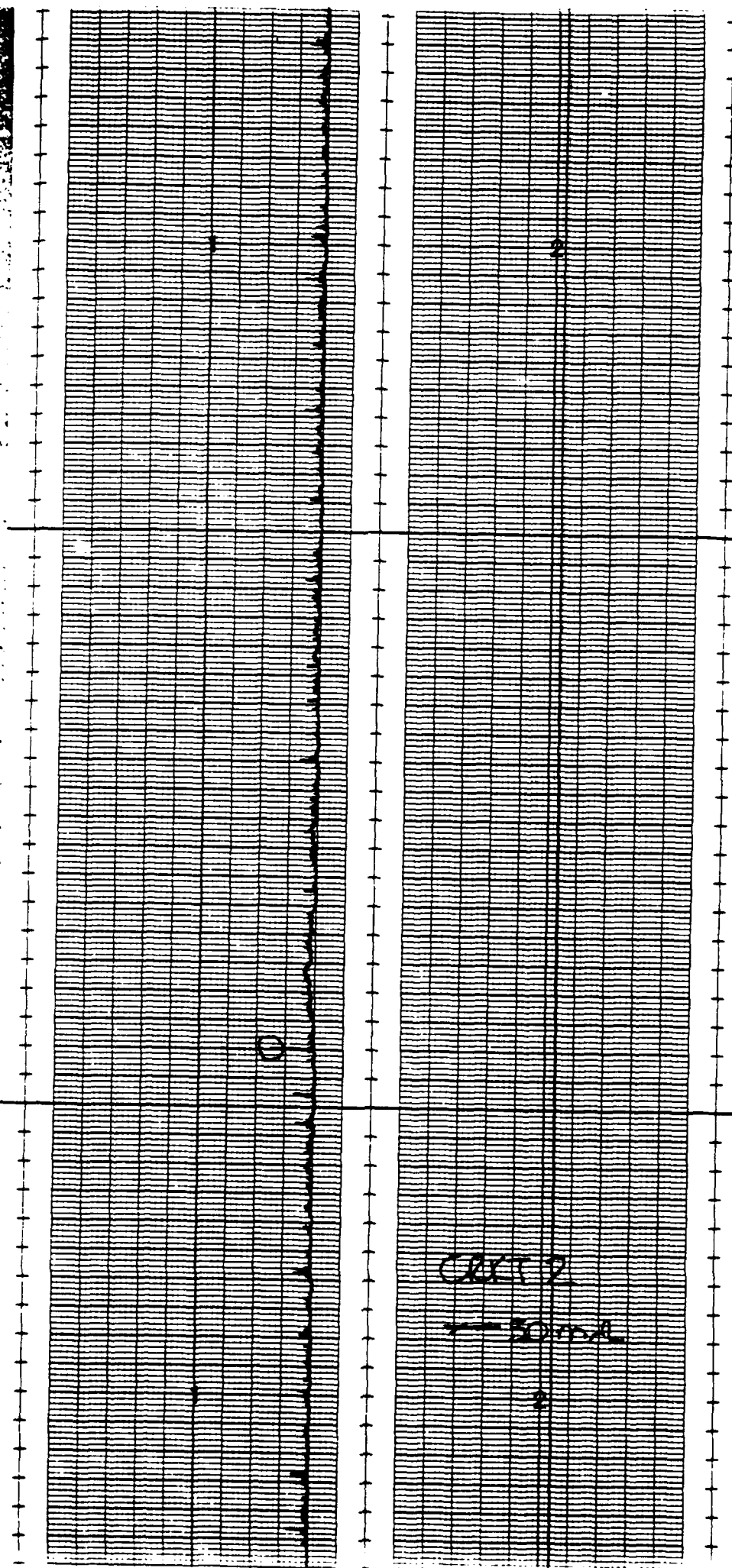
**Final Report
No. 5000-130801**

Appendix D

Noise Resistance Data

ACCUCHART® Gould Inc. Printed in U.S.A.
Cleveland, Ohio

CRX-1
Done



Printed in U.S.A.

ACCUCHART® Gould Inc. Cleveland, Ohio

CHART 3
50mV

CRKT 4

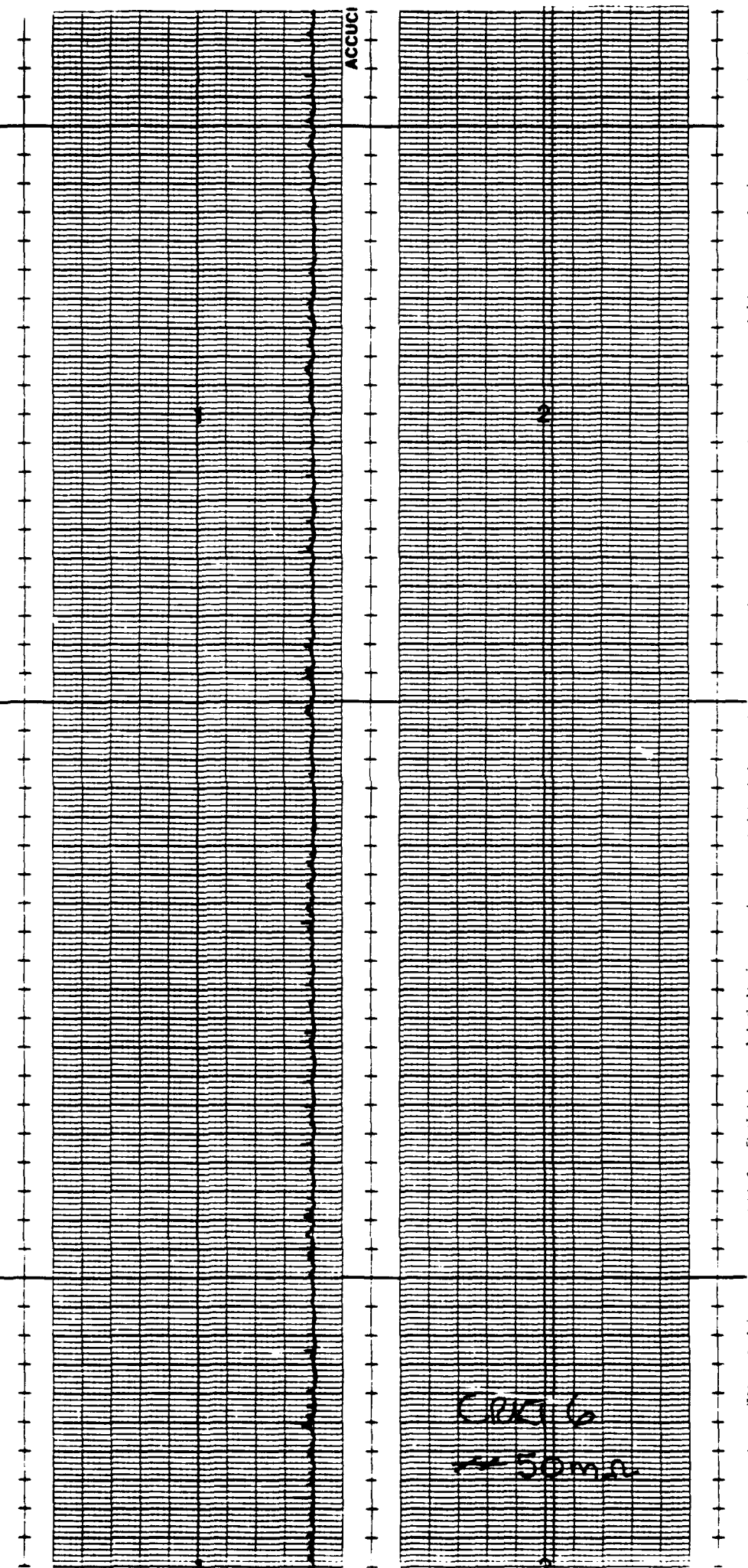
— 50mL

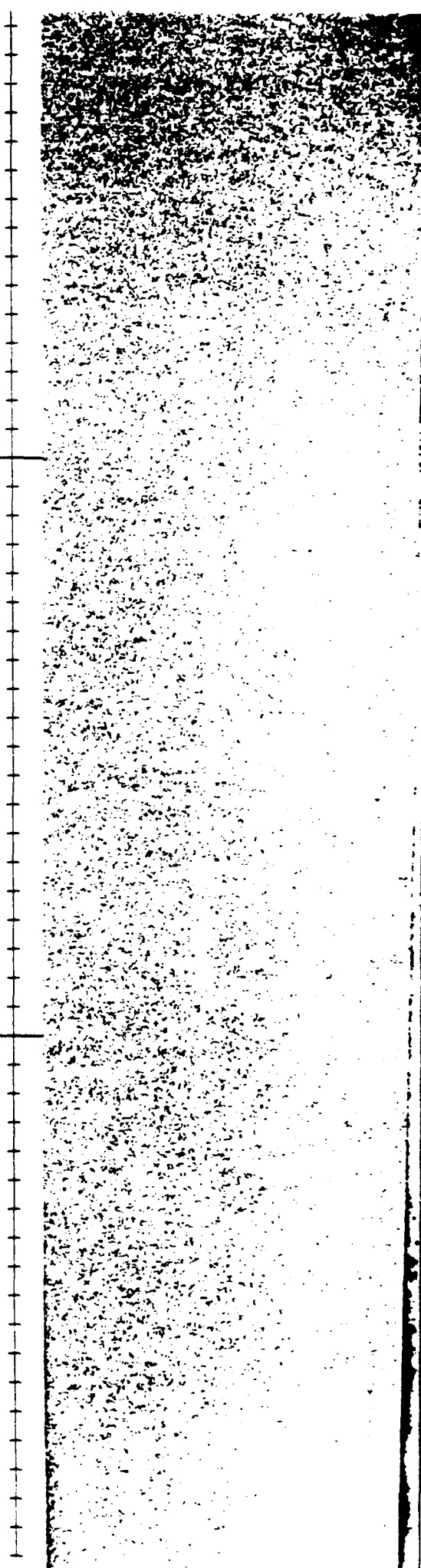
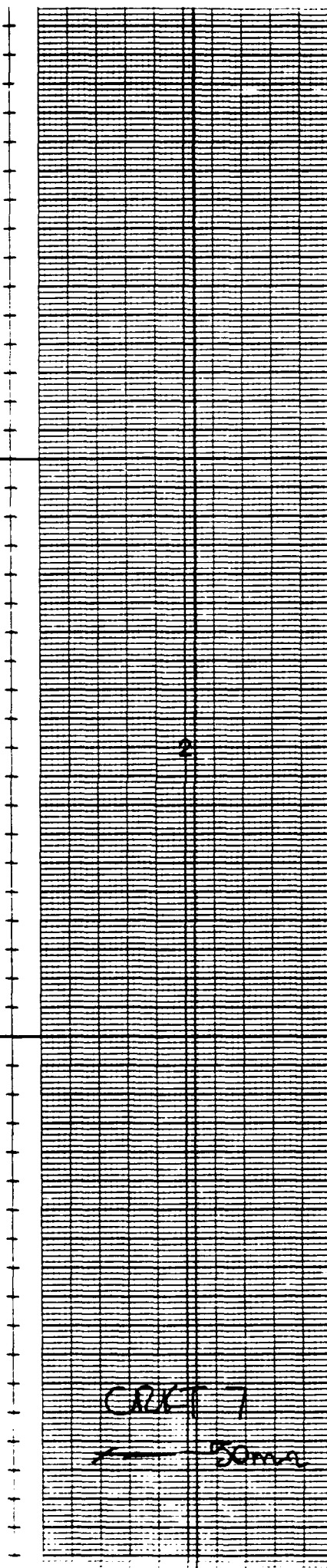
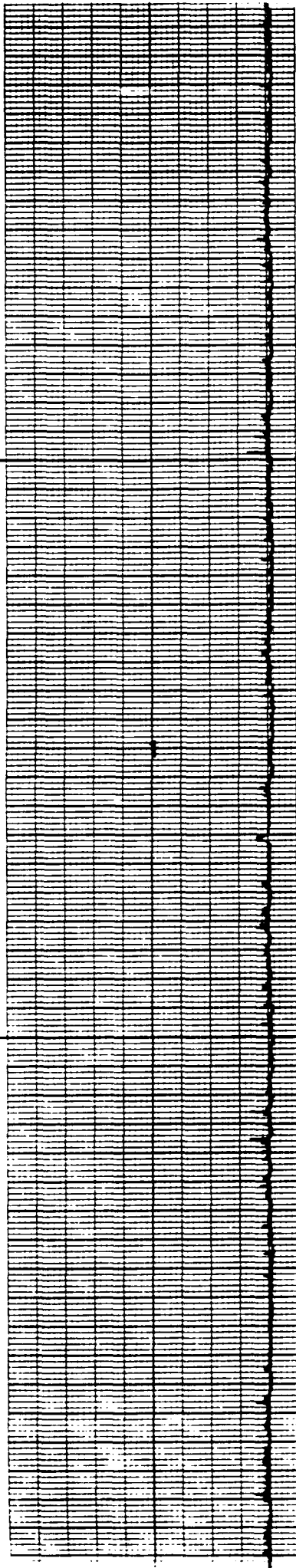
Printed in U.S.A.

Cleveland, Ohio

Inc.

CRCT 5
→ 50m²





Printed in U.S.A.

Cleveland, Ohio

Gould Inc.

ACCUCHART®

CHART 5

— 50 mm

ACCUCHART®

COCT 9

→ 10mV

C

Gould Inc.

ACCUCHART®

COXIT 10

— 20mV

10

Printed in U.S.A.
Land, Ohio

CACI

2000

ACCUCHART® Gould Inc. Cleveland

COVIT 12
SOMA

ACCUCHART®

Gould Inc.

Cleveland, Ohio

Printed in U.S.A.

CACT 13
100000

CRCI 14

CAT 15

— Donk

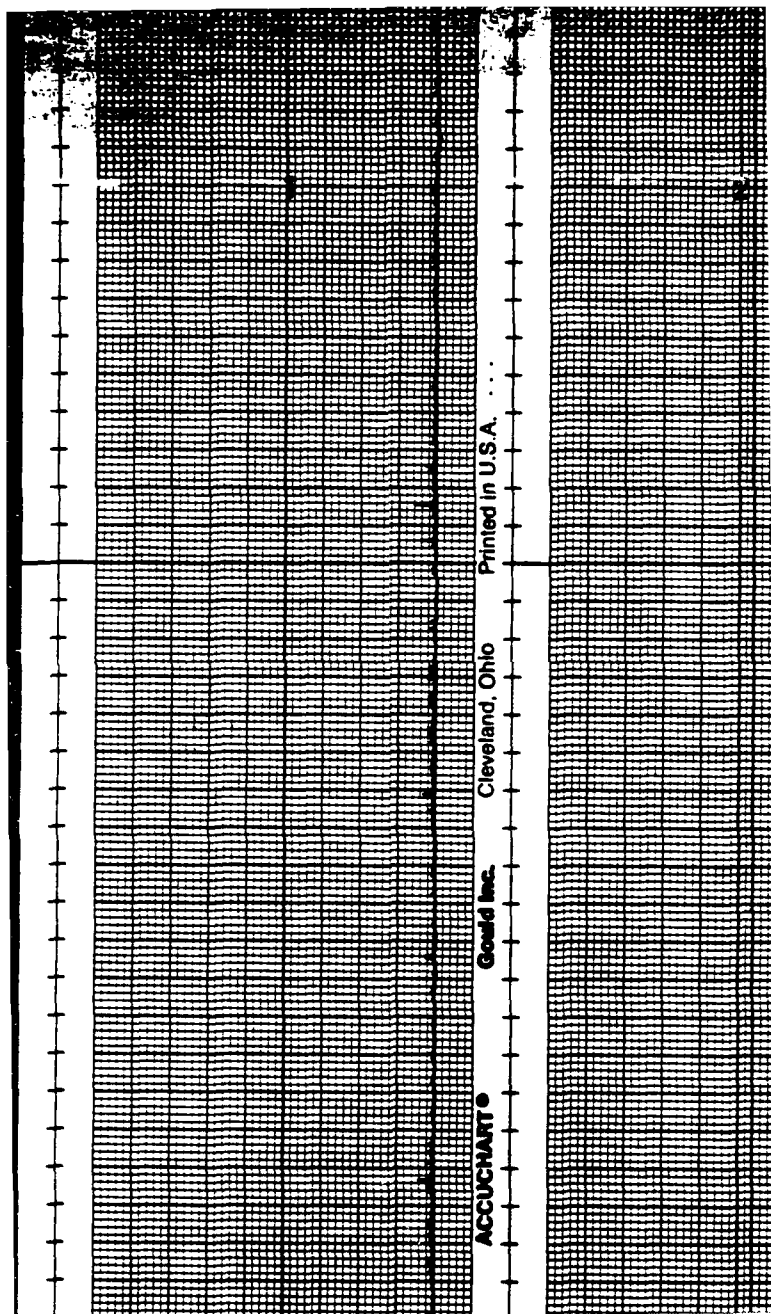
RT • Gould Inc. Cleveland, Ohio Printed in U.S.A.

CART No

750m

CRK 17

— 20m.



ACCUCHART®

Gould Inc.

Cleveland, Ohio
Printed in U.S.A.

Chart 14

— 5 mm/sec —

ACCUCHART®

Gould Inc. Cleveland, Ohio

Printed in U.S.A.

CART 26

20000

ACCUCHART®

Gould Inc. Cleveland, Ohio

Printed in U.S.A.

CART 2
13mm

Oct 27

3000

ACCUCHART® Gould Inc. Printed in U.S.A.

Cleveland, Ohio

025723

50000

Oct 24

100m a

ACCUCHART®

CH00205

20 mm. Q

COT 26

* * Sams.

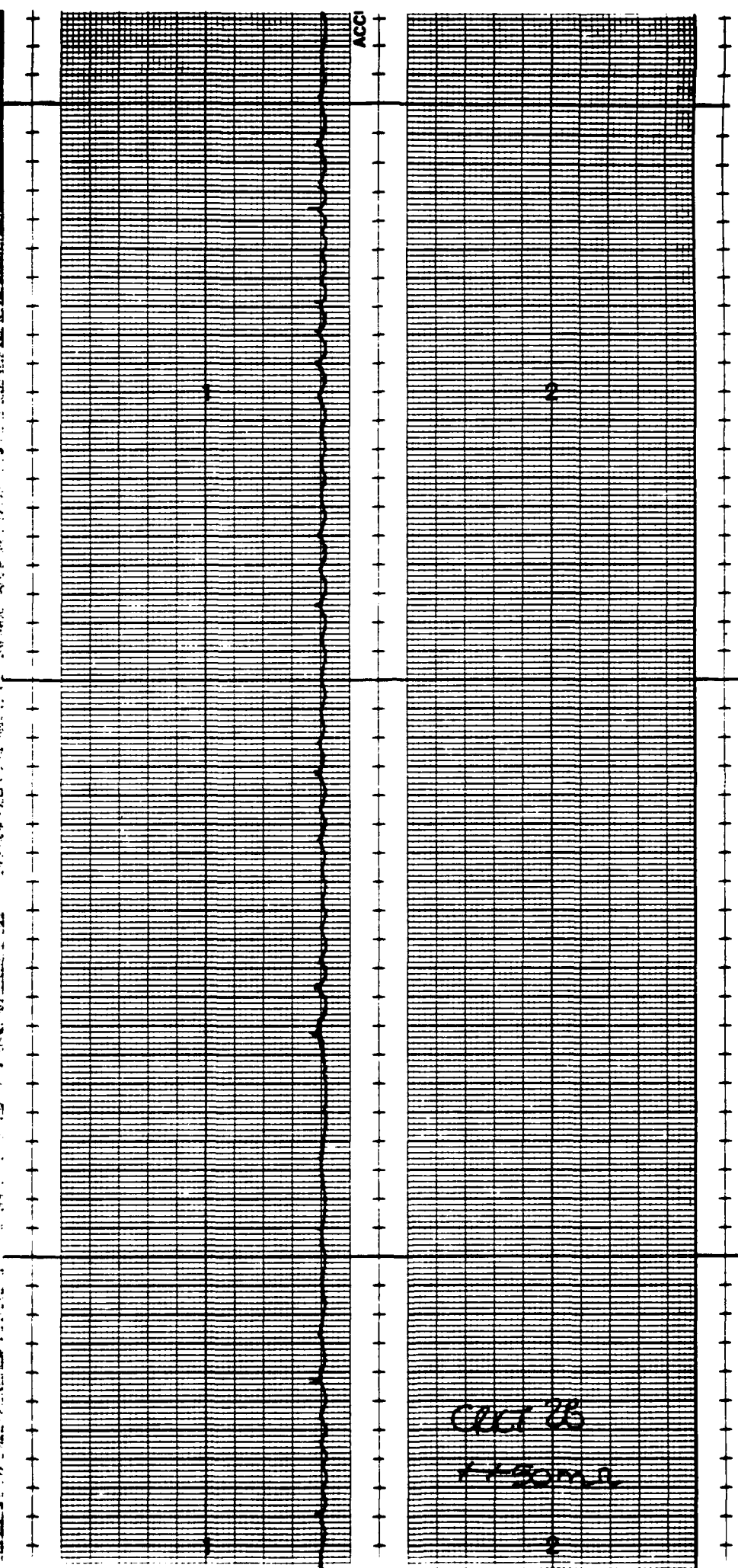
Printed in U.S.A.

Cleveland, Ohio

Gould Inc.

OCT 21

50m/s



ACCUCHART®

Gould Inc.

Printed in U.S.A.

Cleveland, Ohio

CPG 29

* - 50 mm

Printed in U.S.A.

Cleveland, Ohio

Chart 30

7 x 50 mm

CPKT 31

— 50 m.s.

Pin
Cleveland, Ohio
Gould Inc.
ACCUCHART®

Cat 38

1-5mV

Chart 33
1150m.s

Cleveland

Gould Inc.

ACCUCHART®

CHART 34

15 mm/sec

04735

1000000000

Gould Inc. Cleveland, Ohio Printed in U.S.A.

Cat Bl

14500

CART 37

7450m.s

ACCUCHART™

Gould Inc.

Printed in U.S.A.
Cleveland, Ohio

OCT 36
X X 5 mm

Printed in U.S.A.

Cleveland, Ohio

Chart 39

ACCUCHEAR

CERT 40

T ~50 ms

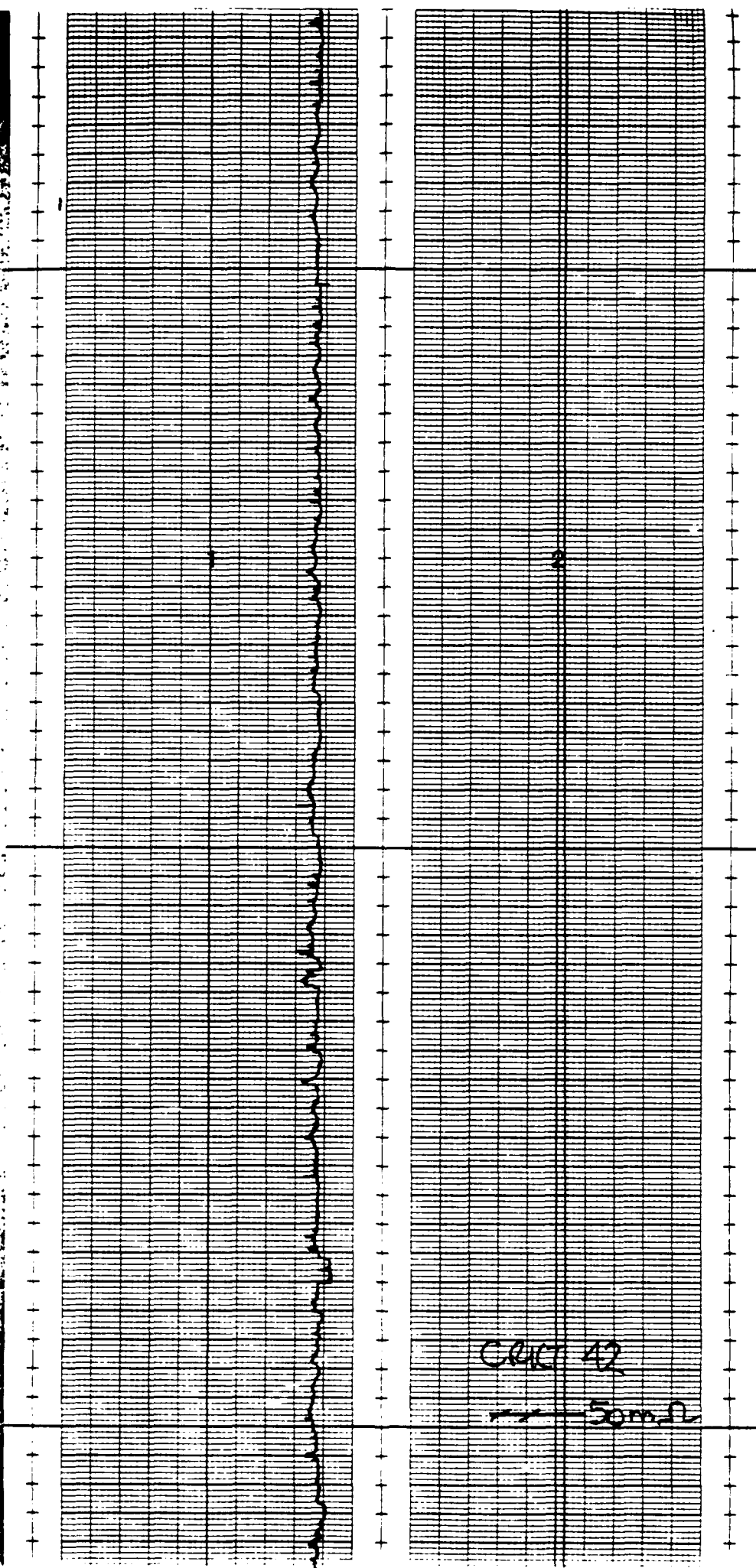
ACCUCHART®

Gould Inc.

Printed in U.S.A.
Cleveland, Ohio

CUT 41

50m²



Cleveland, Ohio

Printed in U.S.A.

Chart 43

Some

CHART 45

20m/s

CART 45

50m/s

Printed
Gould Inc. Cleveland, Ohio

ACCUCHART®

CO-OP 100

50000

CRUFT 48

50m²

Gould Inc.

Cleveland, Ohio

Printed in U.S.A.

Chart 49

← →

50 mm

CERT 20

— 50m

17

Gould Inc. Cleveland, Ohio Printed in U.S.A.

CRCT 5

50mV

Printed in U.S.A.

Gold Inc.,
Cleveland, Ohio

CRU 52

50m2

ACCUCHART™

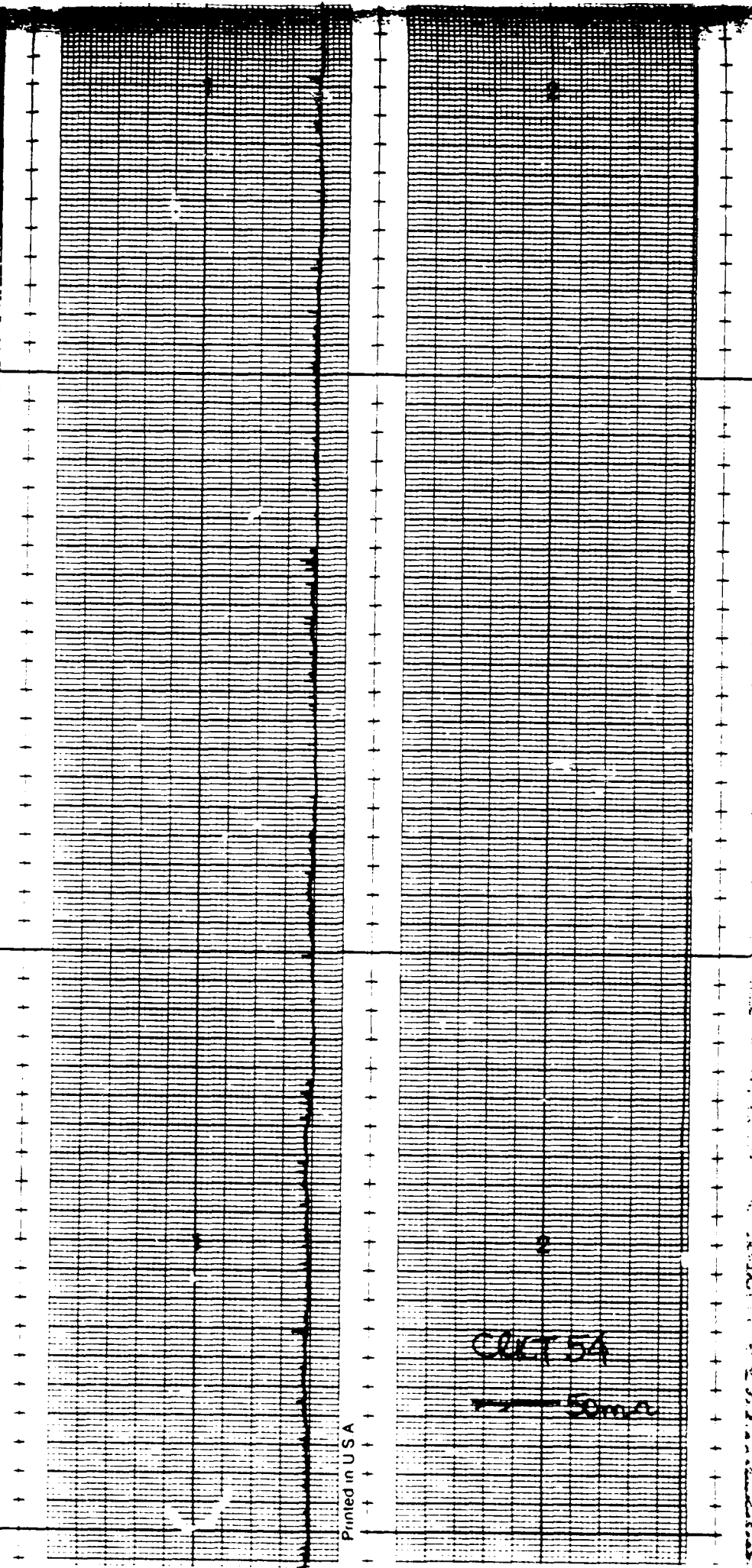
Gould Inc.

Printed in U.S.A.

Cleveland, Ohio

CR407 53

Tomn



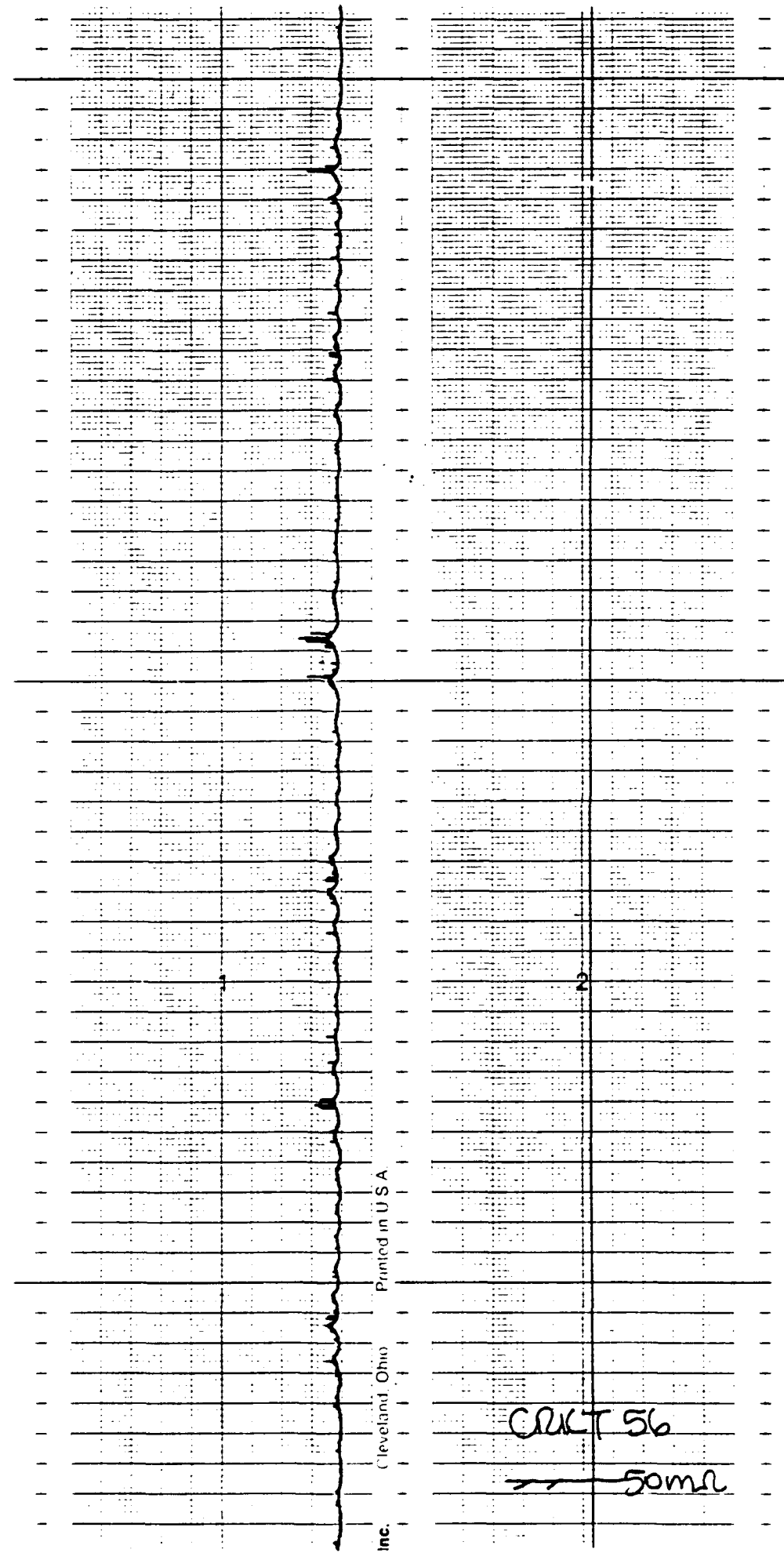
Print

Cleveland, Ohio

Gould Inc.

ACCUCHART®

CRV 55



Inc. Cleveland, Ohio

CRKT 56

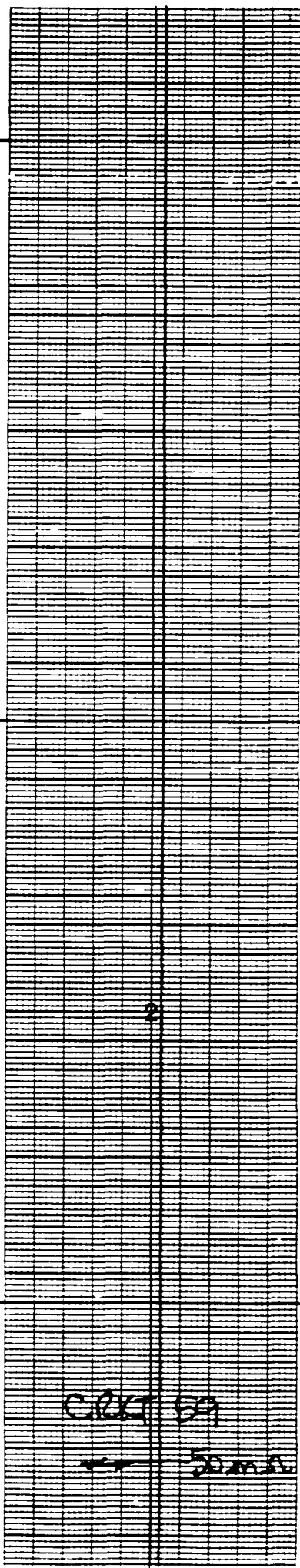
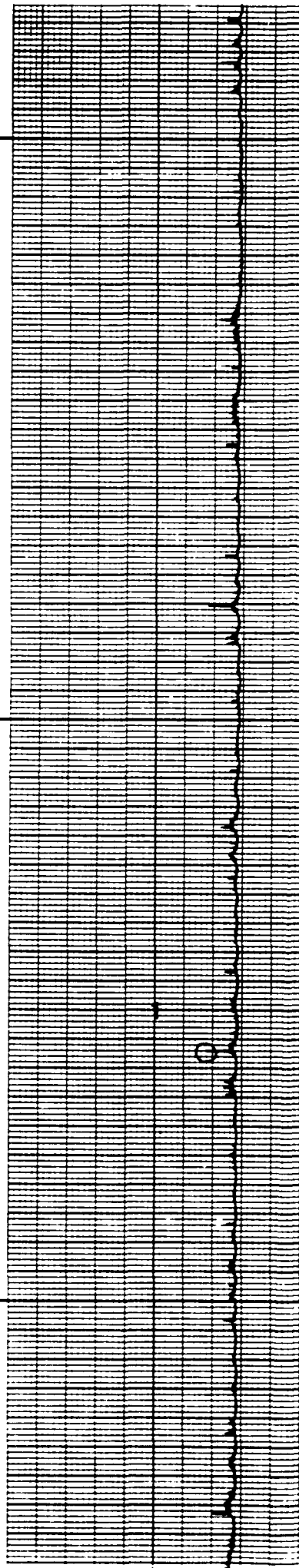
50mL

P
Cleveland, Ohio

ACCUCHART® Gould Inc.

CAT 5B

— 5m/s



CRT 50

50 m/s

ACCUCHART®

Gould Inc.

Cleveland, Ohio
Printed in U.S.A.

Chart 60

50mm/s

Q

Cleveland, Ohio
Printed in U.S.A.

CUT 61

8000

Printed in U.S.A.

Cleveland, Ohio

Gould Inc.

ACCUCHART™

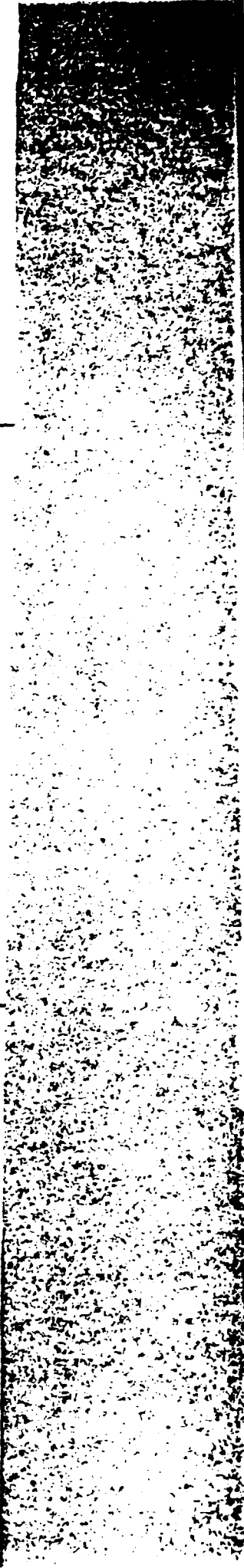
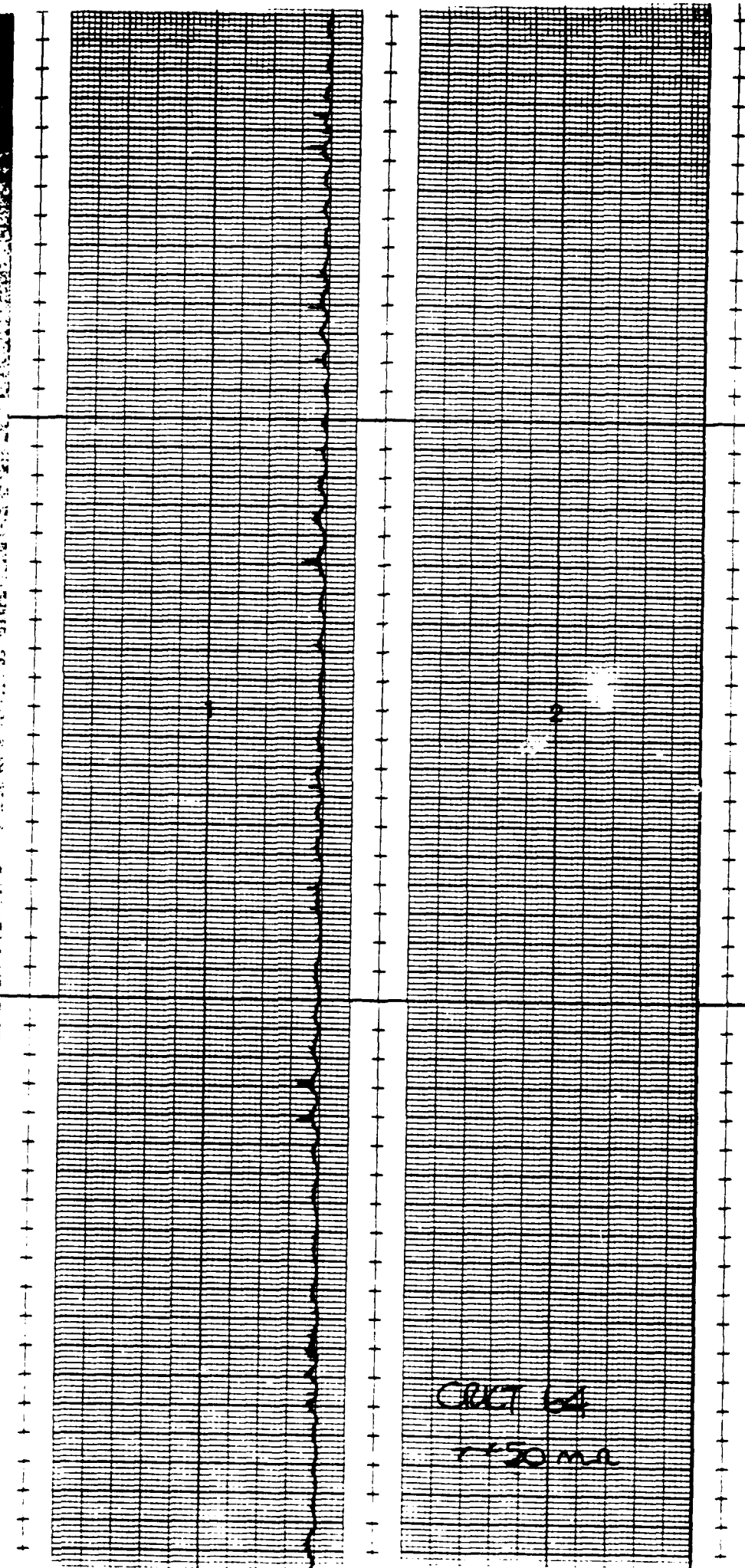
CRIT 62

7 X 50mR

ACCUCHART® Gould Inc. Cleveland, Ohio Printed in U.S.A.

C007 63

- 30m



CRST 65

— 30m.s

Eduard Inc.

Printed in U.S.A.

Cleveland, Ohio

Chart 6a

50mL

ACG

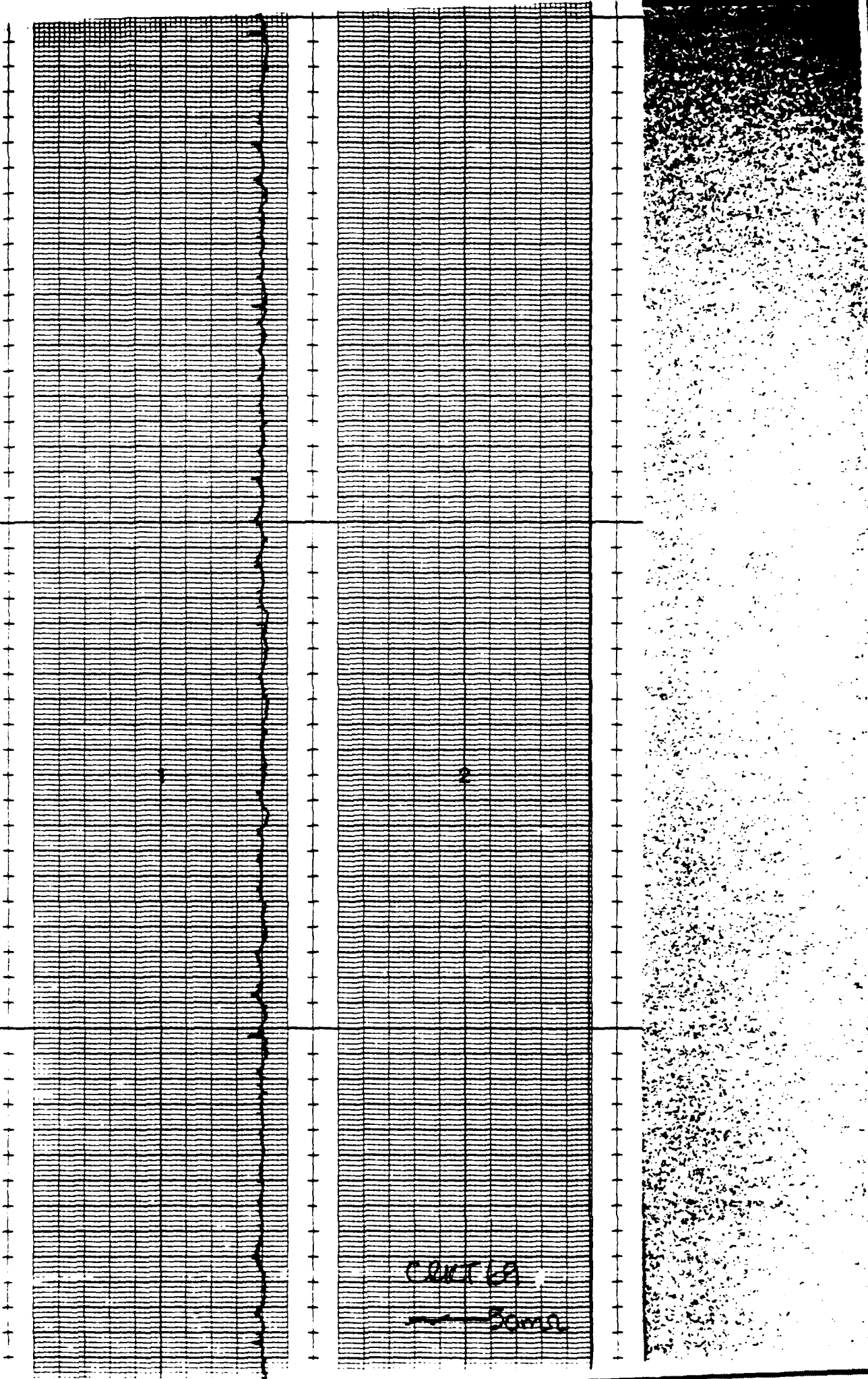
Chart 67

UCHART®

Gould Inc. Cleveland, Ohio

Printed in USA

OCT 68
150m.s



ACCUCHART®

Gould Inc. Cleveland, Ohio Printed in U.S.A.

Chart 70

— 50mA

ACCUCHART®

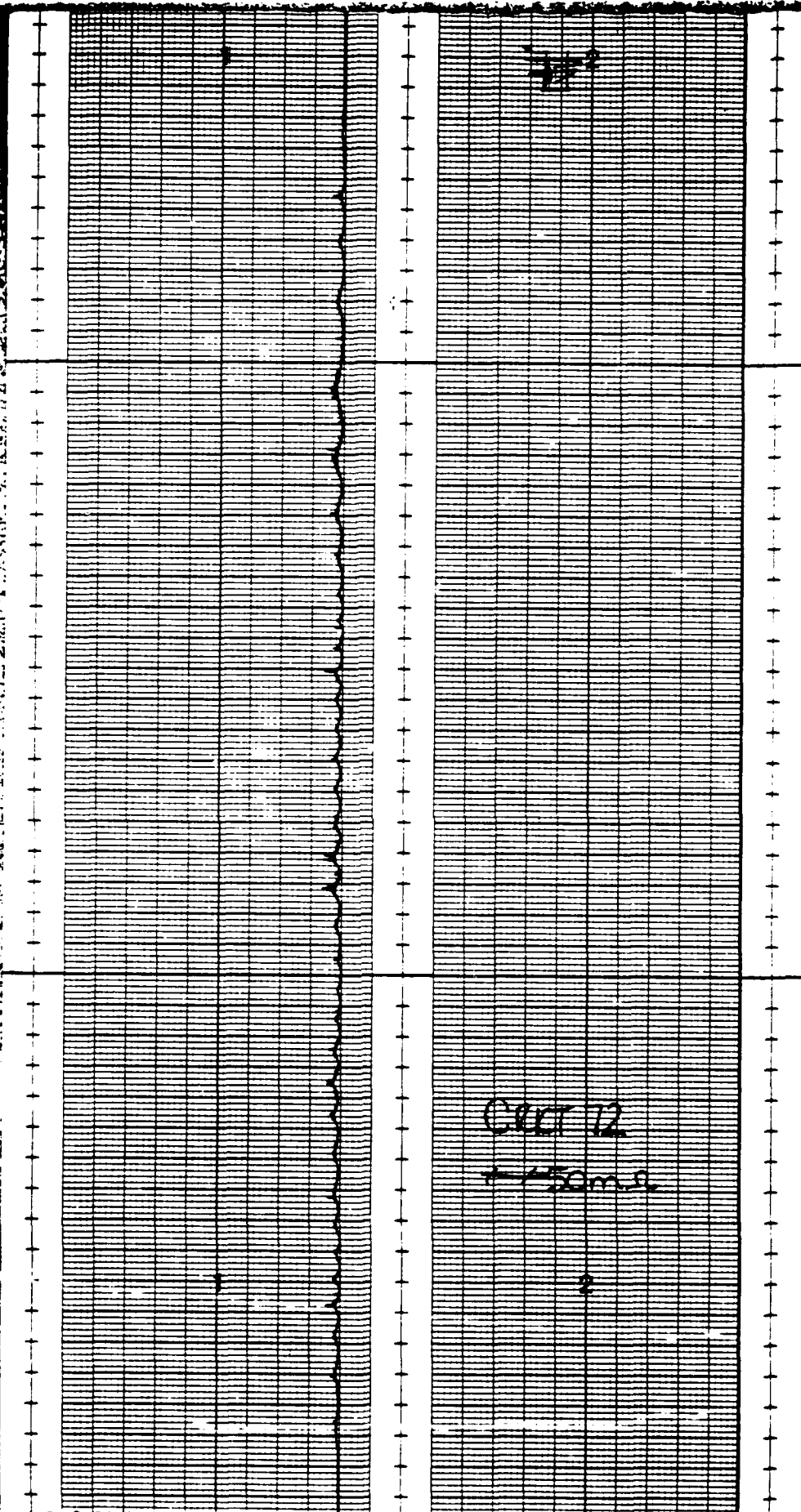
Gould Inc.

Printed in U.S.A.

Cleveland, Ohio

Oct 71

→ 5Ωm



CRD 73

CL&C 74

→ 50m/s

2

ACCUCHART®

CHART 15

→ 50m/s

CERT No

1-Some

Printed in U.S.A.

Cleveland, Ohio

Chart T7

→ 5 mm

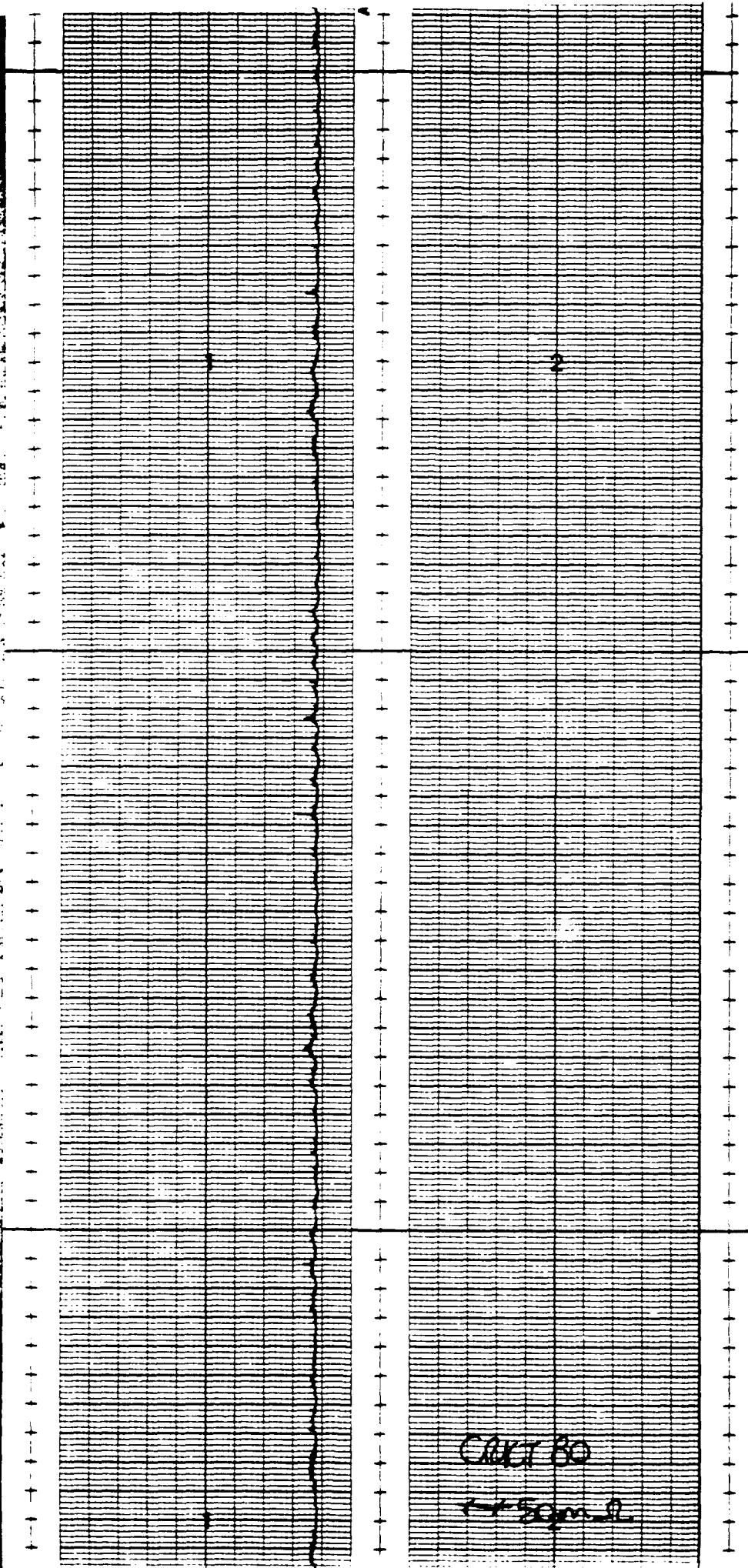
accus

C.R. 13
some

ACCUCHART® Gould Inc. Cleveland, Ohio Printed in U.S.A.

CRCT 79

Exam 2



CHIT 61

— 2000



Ind. Ohio

Printed in USA.

CETI 62

+ 50m.s

Printed in

Cleveland, Ohio

Gould Inc.

ACCUCHART®

Chart 83

1/1 form

OCT 64

+ 50m n

ACCUCHAR[®]

CCG 85

75 mm

Printed in U.S.A.

Cleveland, Ohio

CRICK 36

TY 50mm

CHART 67

- X 50m/s

ACCUCHART® Gould Inc. Printed in U.S.A.

Cleveland, Ohio

Oct 88

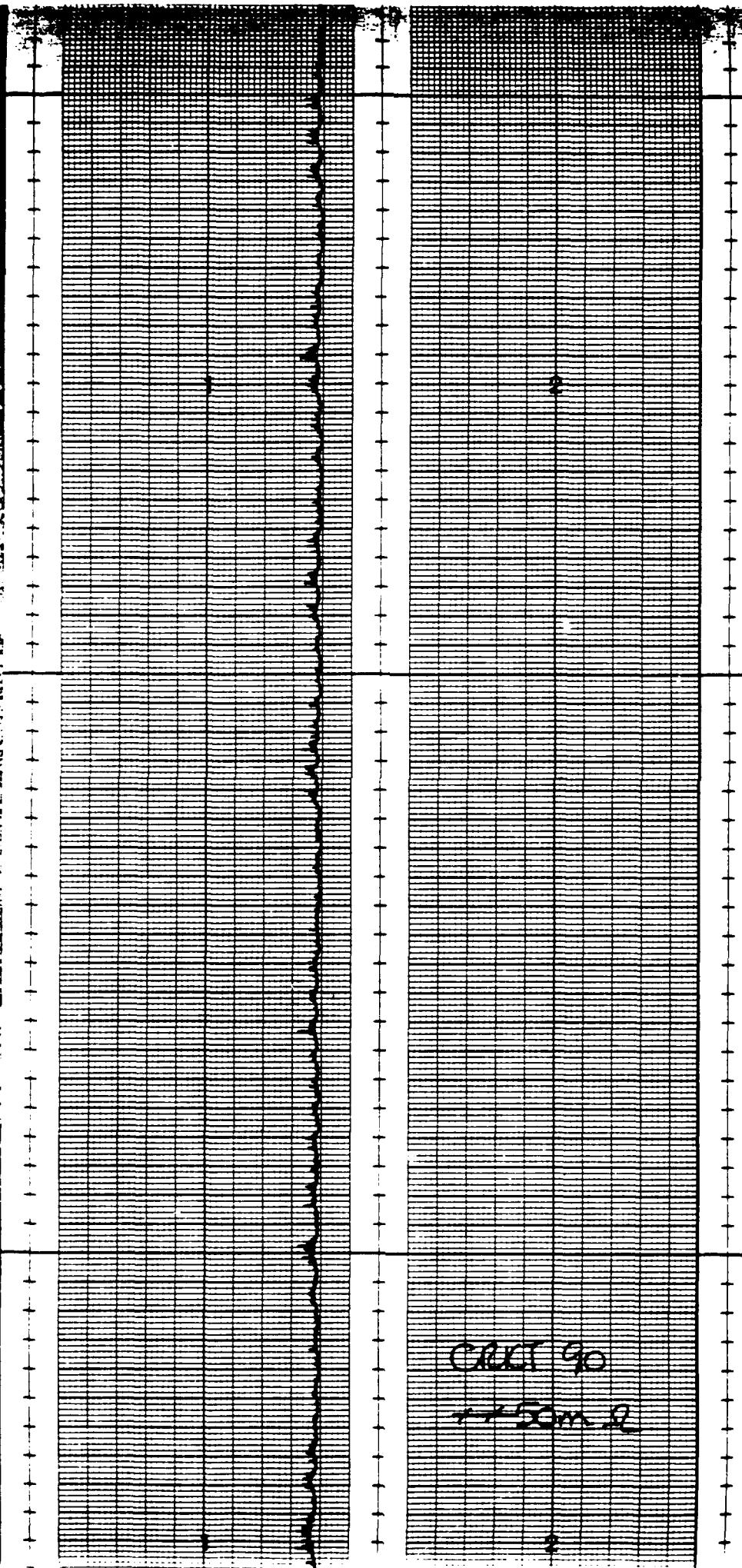
+ 5 min

ACCUCHART®

Gould Inc. Cleveland, Ohio

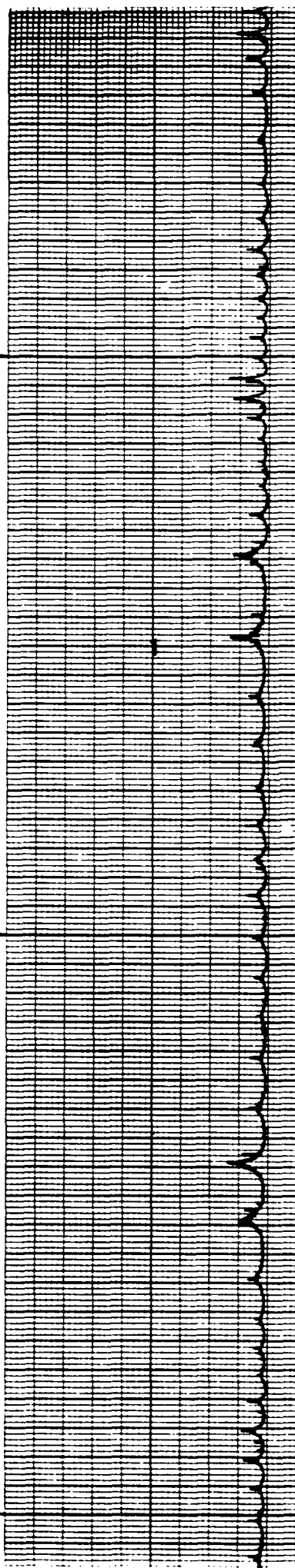
Printed in U.S.

Chart 8
- 50m a



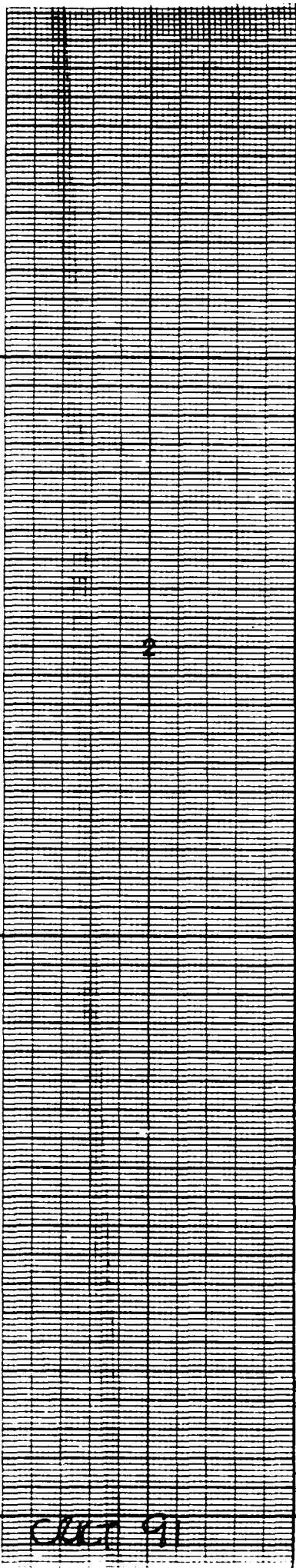
CART 90

+ 5cm 2

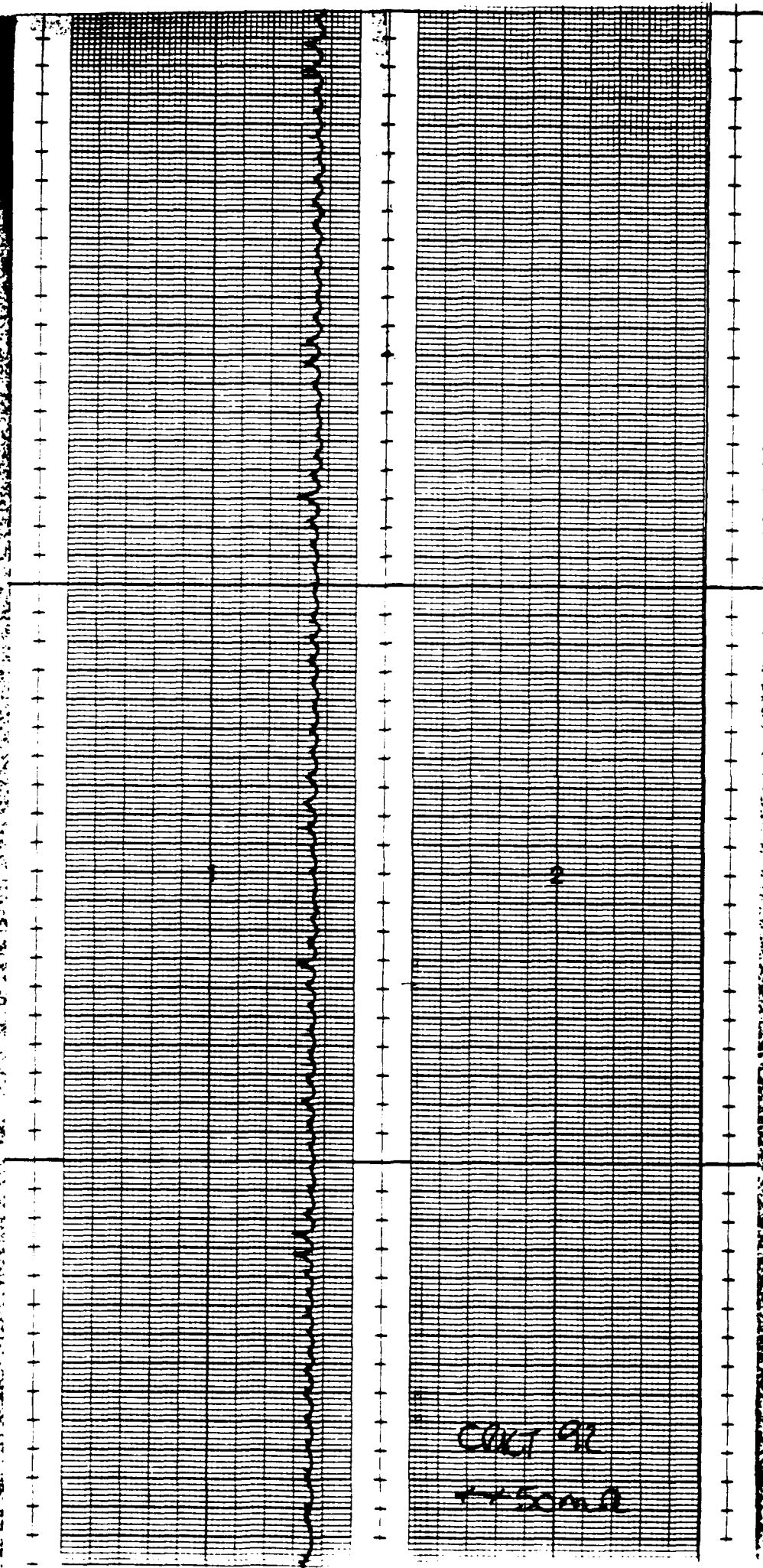


Gould Inc.

ACCUCHART®



08/07/91

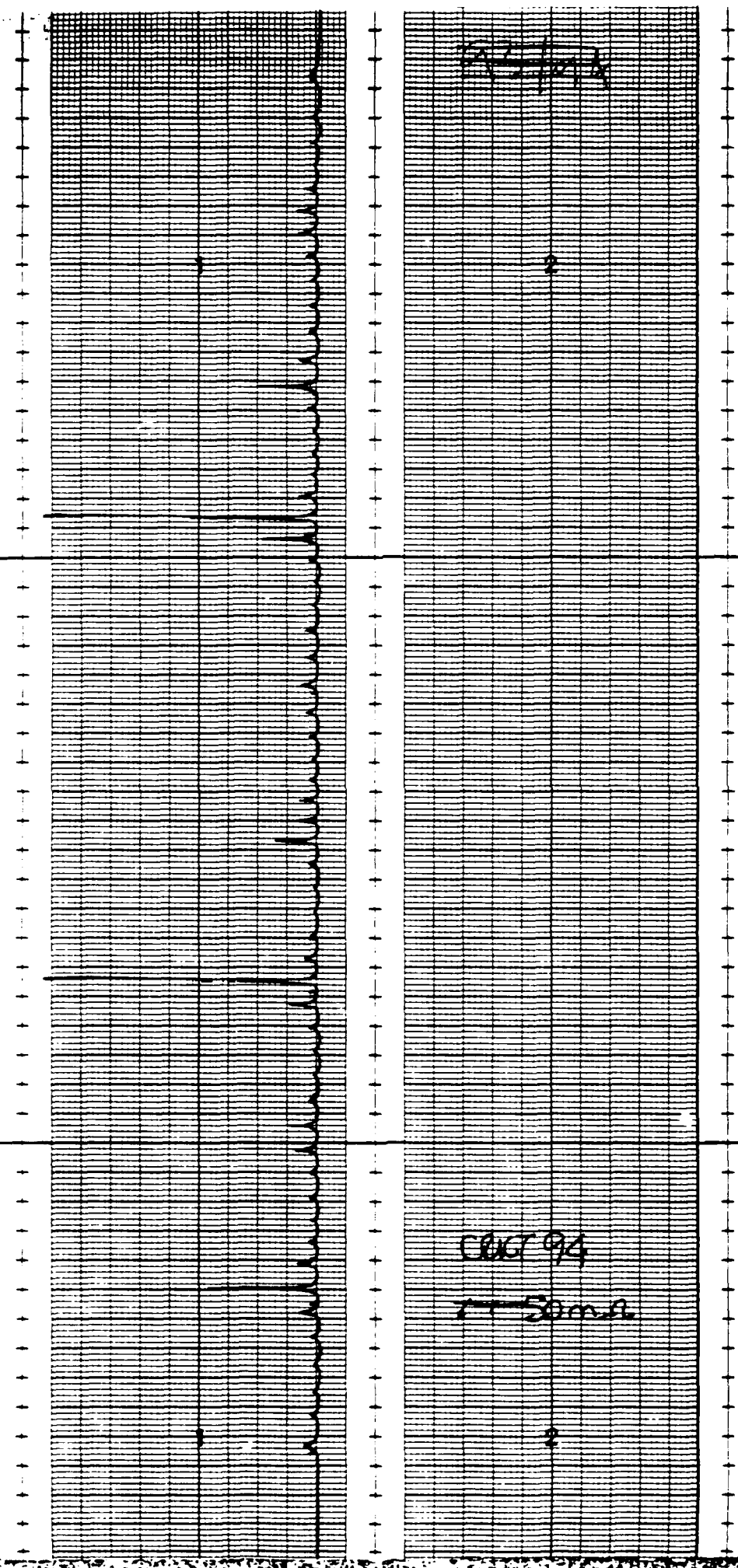


ACCUCHART®

CACT 93

✓ 50mV

0.5



1
2
3
4
5
6
7
8
9
10
11
12
13
14
15
16
17
18
19
20
21
22
23
24
25
26
27
28
29
30
31
32
33
34
35
36
37
38
39
40
41
42
43
44
45
46
47
48
49
50
51
52
53
54
55
56
57
58
59
60
61
62
63
64
65
66
67
68
69
70
71
72
73
74
75
76
77
78
79
80
81
82
83
84
85
86
87
88
89
90
91
92
93
94
95
96
97
98
99
100

CAL 95

ACCUCHART®

Gould Inc. Cleveland, Ohio Printed in U.S.A.

COOT 96
11-2000

ACCUCHART® Printed in U.S.A.

Gould Inc. Cleveland, Ohio

OCT 97
2000

COAST 98

75m.s

CERT 99

250m

ACCUCHART™

Gould Inc.

Printed in U.S.A.

Cleveland, Ohio

CRIT 100

← 50ma

Printed in U.S.A.

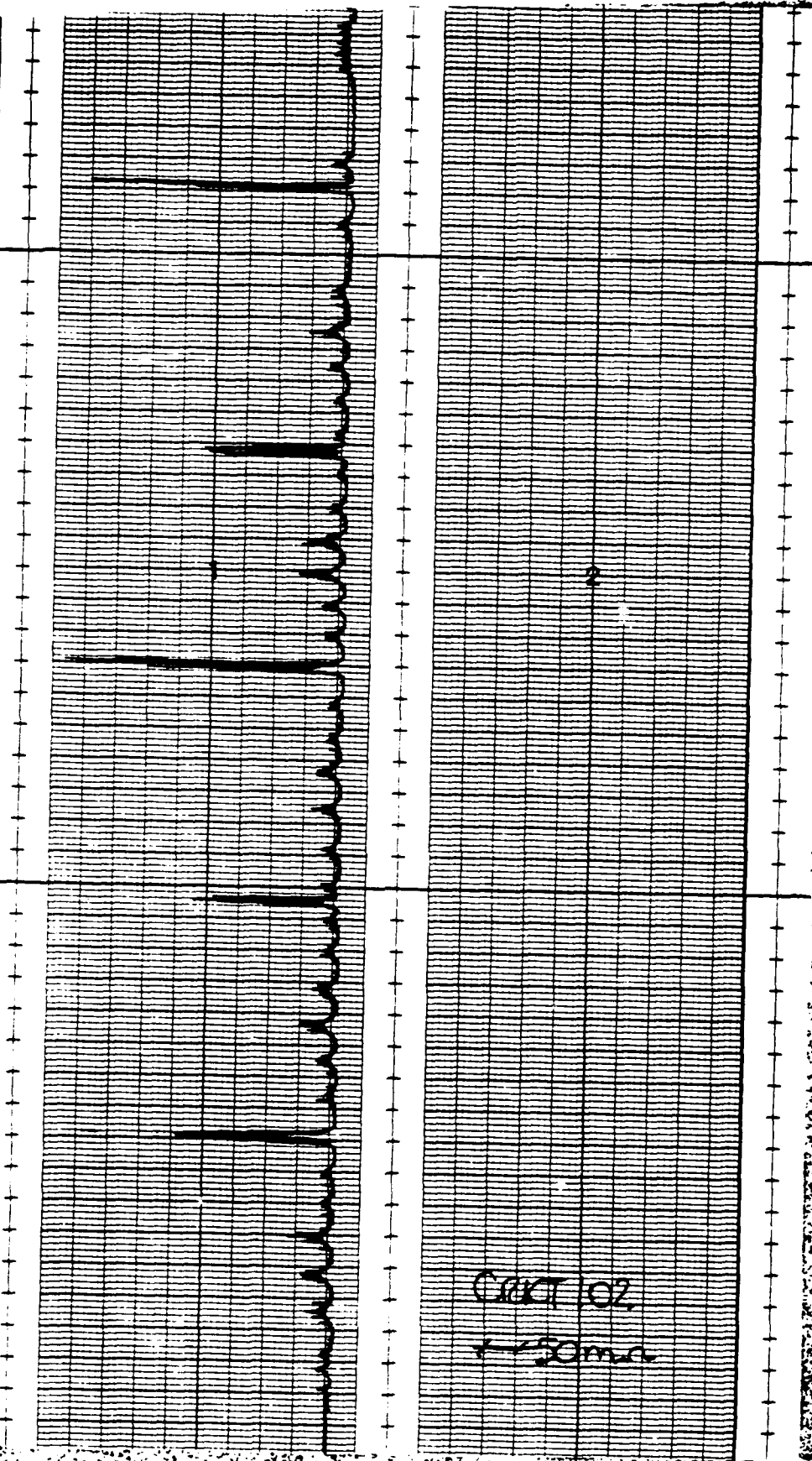
Cleveland, Ohio

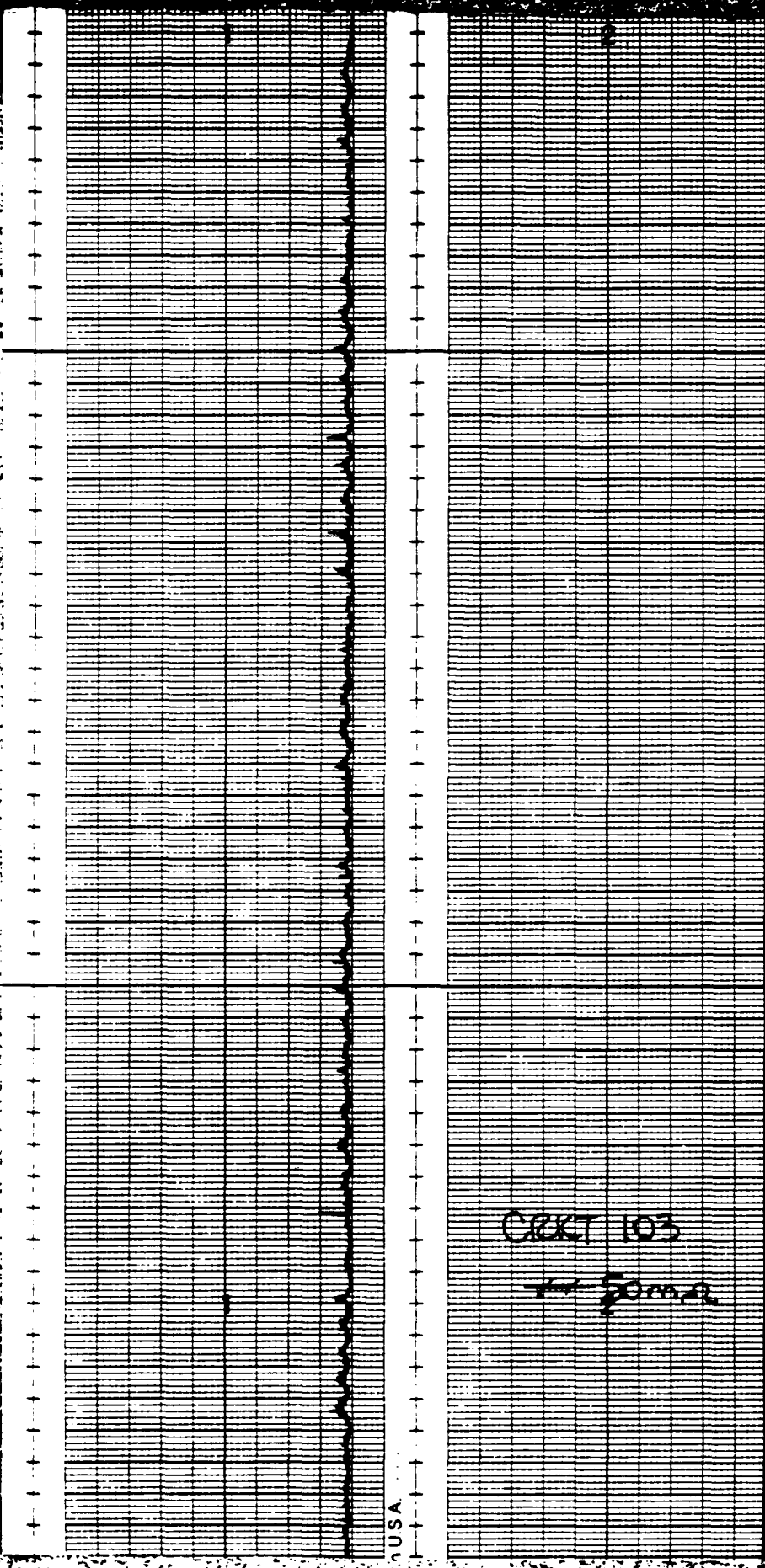
Gould Inc.

ACCUCHART®

Chart 10

* 150 m.s.





CRKT 103

→ 50 m/s

Cleveland, Oh

Gould Inc.

ACCUCHART®

COKE 104

2 - 5cm 2

Printed in USA

Cleveland, Ohio

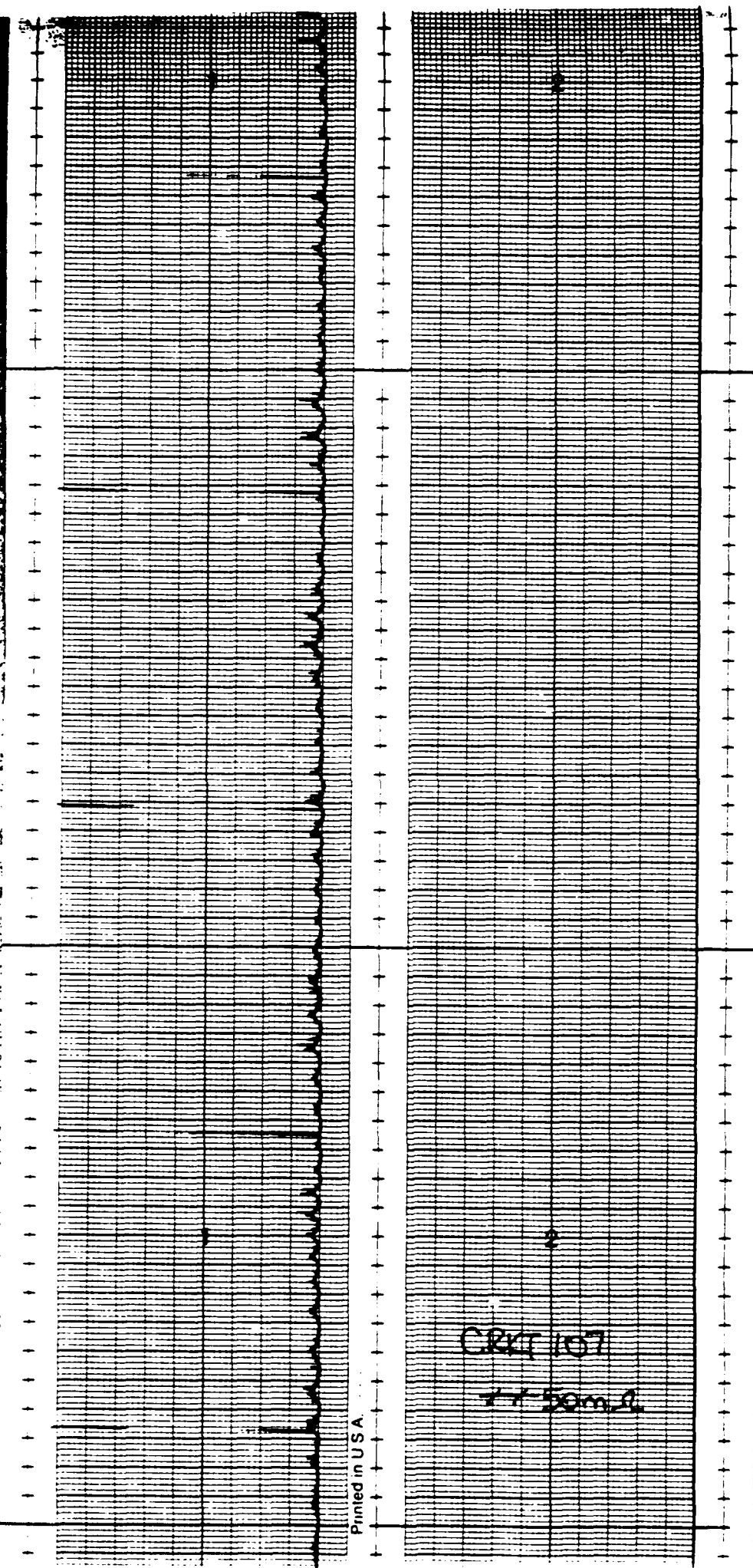
CRISTI KIDS

1-50000

ACCUCHART® Gould Inc. Cleveland, O

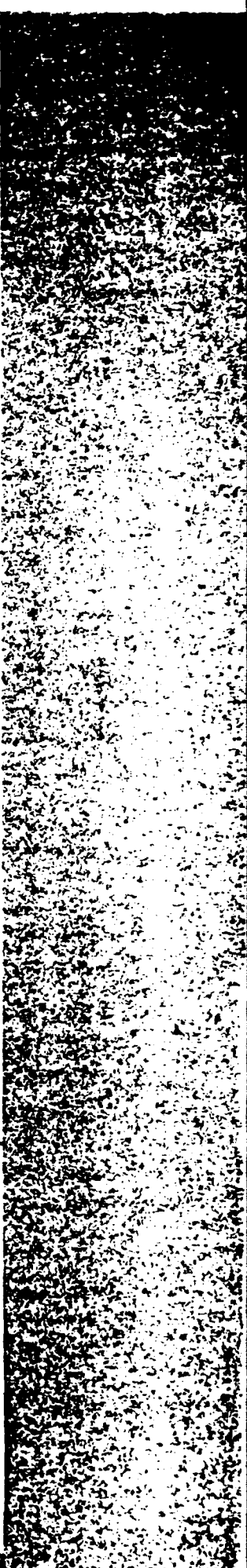
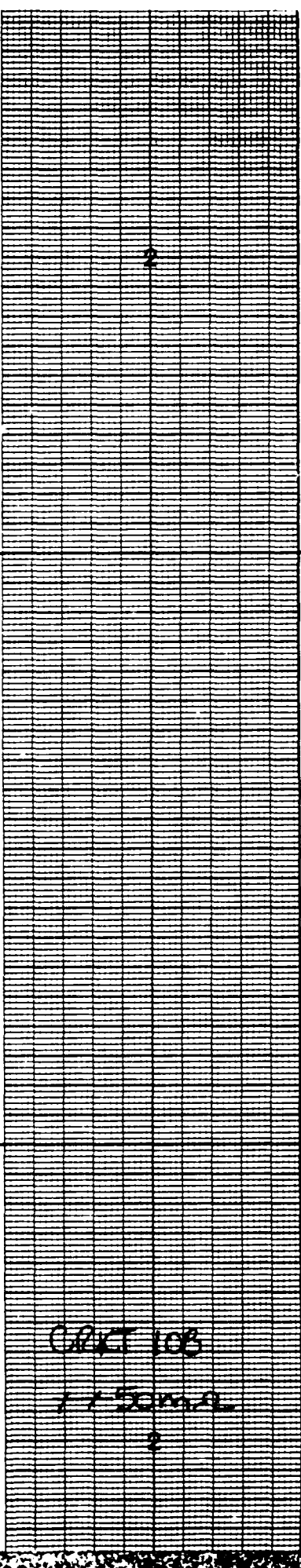
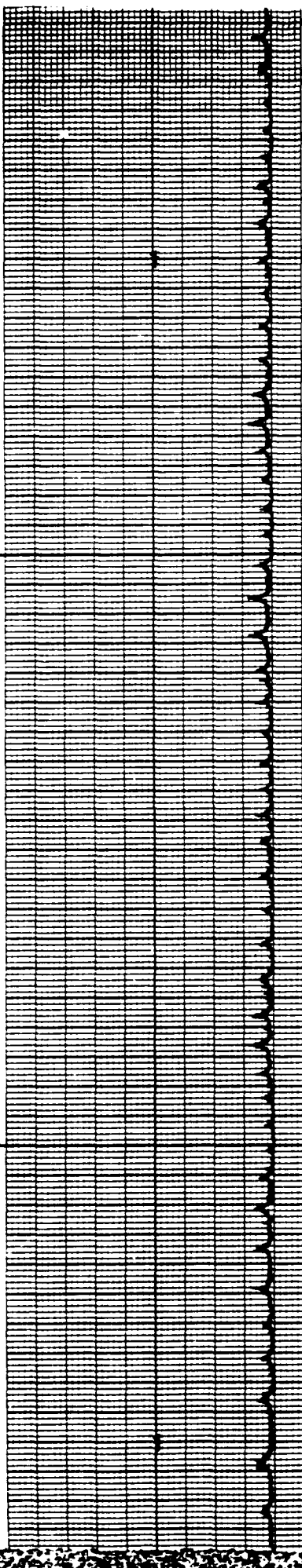
Chart 10

#15mm



CBET 107

++ Exam 2



CRCT 103

7/12/2012

~~CKT 109~~

~~50mR~~

Printed in U.S.A.

Cleveland, Ohio

Gould Inc.

ACCUCHART®

Chart 10

1/25 mm

CRG III

77.5 mm Q

ACCUCHART®

Gould Inc.

Cleveland, Ohio

Printed in U.S.A.

Chart 112

for 50mV

Ind. Ohio

Printed in U.S.A.

CACIS 113

200m 2

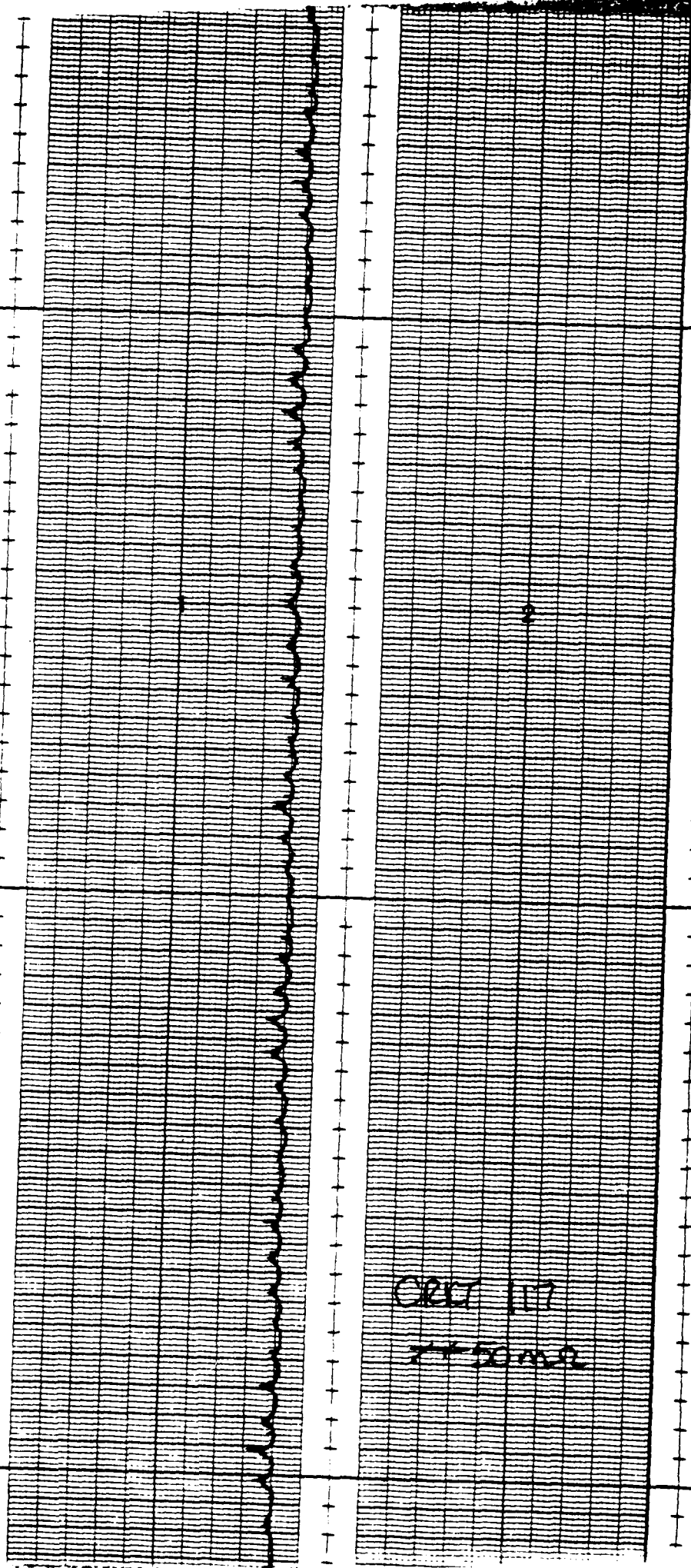
ACCUCHART® Gould Inc. Cleveland, Ohio Printed in U.S.A.

CACI 1A
→ Some

CRC 115
x - Sonar
Jan 2 1981

ACCUCHART®

CREST LINE
→ Sample



Printed in U.S.A.

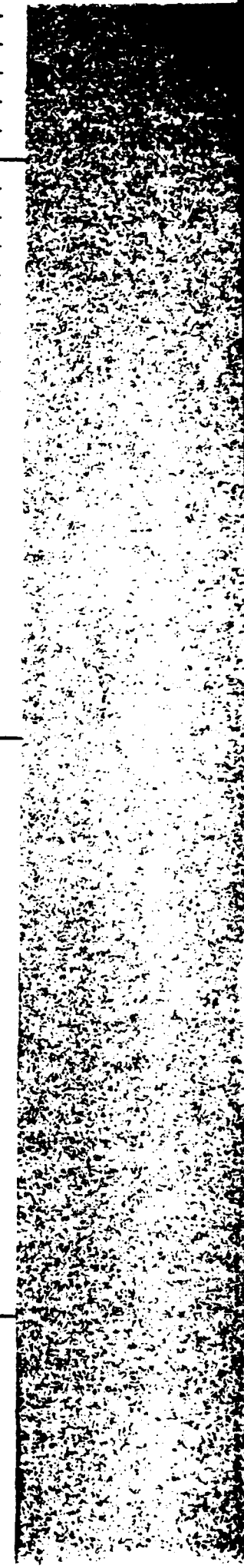
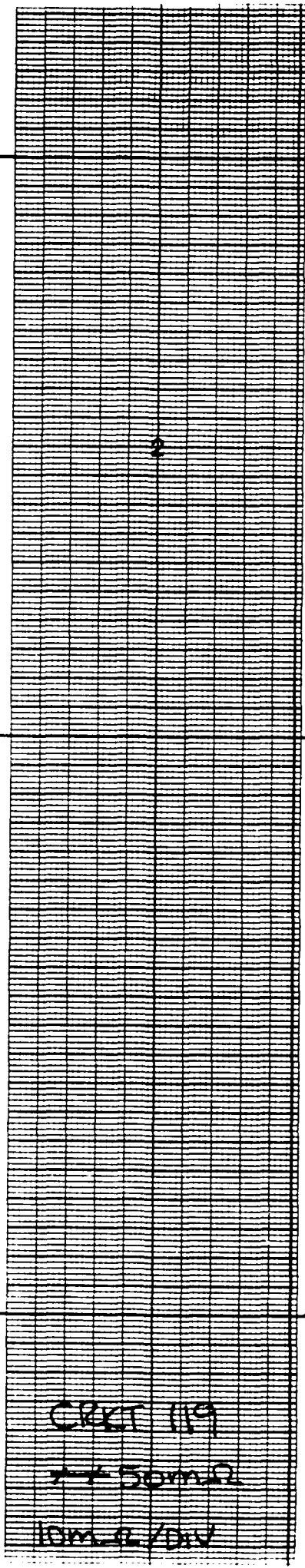
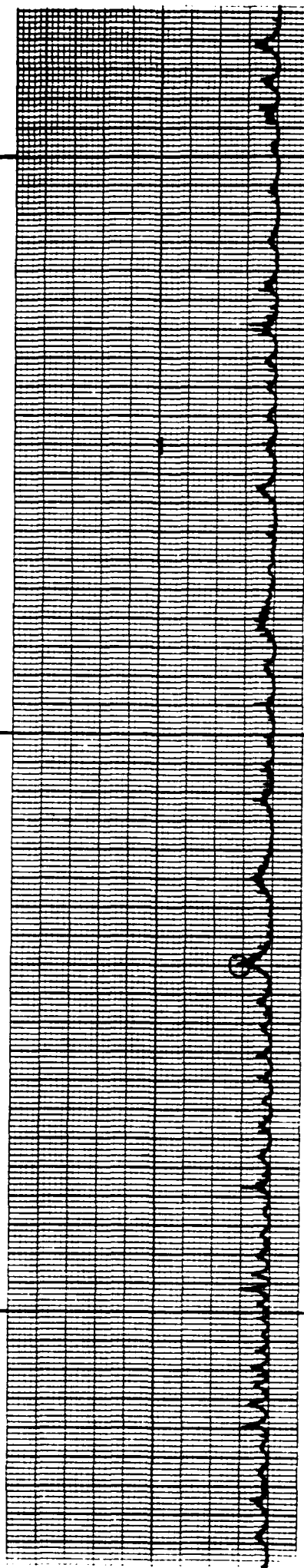
Gould Inc.

Cleveland, Ohio

ACCUCHART™

Chart 118

← 50mm



CRT 119

→ 50m/s

1mm = 1 /div

ACCUCHART® Gould Inc. Cleveland, Ohio Printed in U.S.A.

GCT 110
Form 2
10m a 10μV

Gould Inc. Cleveland, Ohio Printed in U.S.A.

CARDS 1-2

* 50m-1

ACCUCHART® Gould Inc. Cleveland, Ohio Printed in U.S.A.

CRPTS 3-4
2000-9

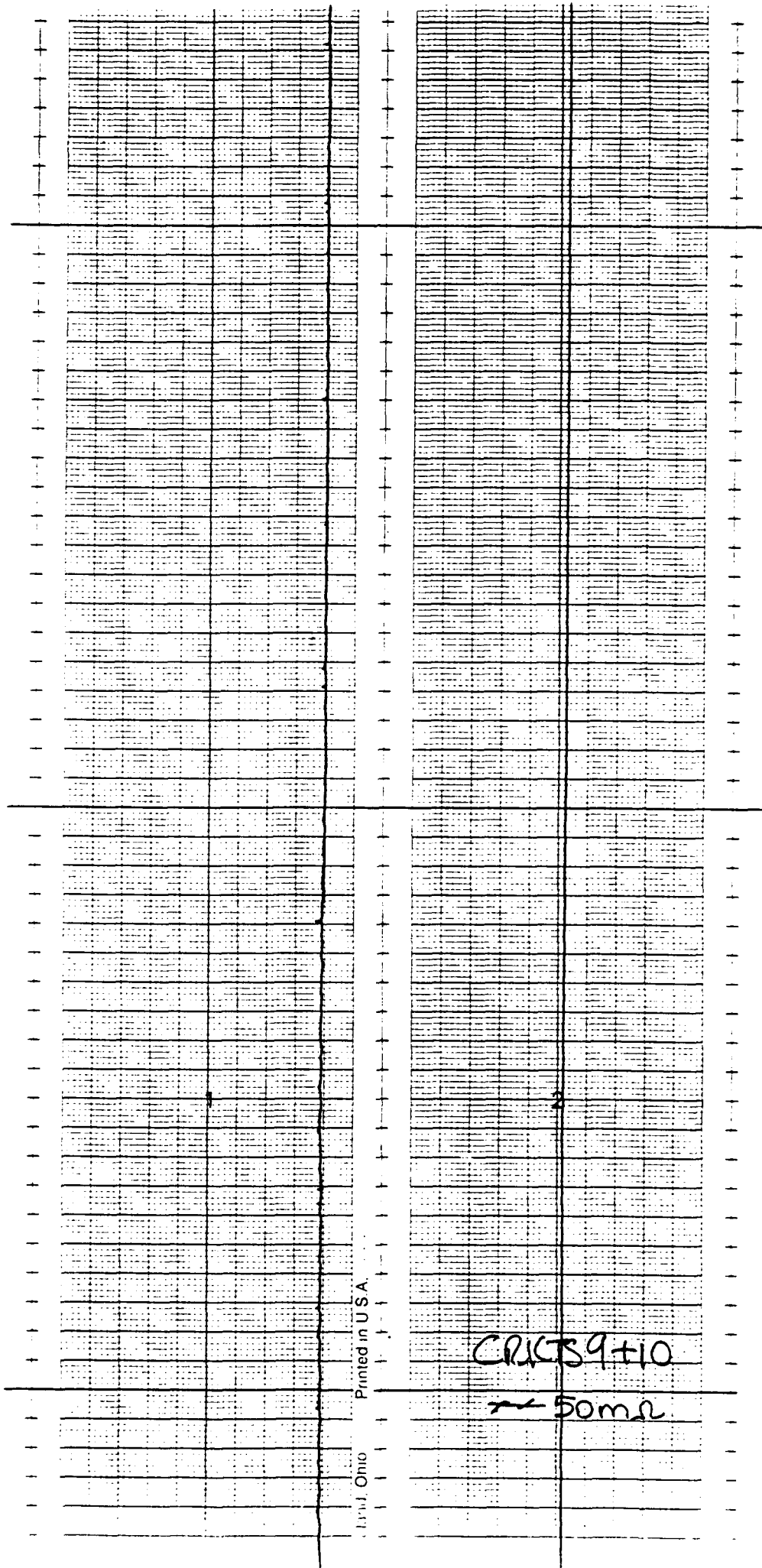
ACCUCH/

2

CRCTS 5th
+ 50ml

CRUTS 7+8

— 50m



Printed in U.S.A.

Cleveland, Ohio

ACCUCHART™

Gould Inc.

CRXTS 11+2

— 50 mV

Printed in U.S.A.

CARDS B+C
— 50m

ACCUCHART®
Gould Inc.
Cleveland, Ohio
Printed in U.S.A.

Chart 15-816

5 min

CMEC 17-2-1

- - - - -

COPY 12/20

CHET 21-27

50 m.s.

ACC

Gould Inc.

Printed in USA

CRACTS 23 + 24

~~+ + 50 mΩ~~

Cleveland, Ohio

Gould Inc.

ACCUCHART®

000075-42

-150msec

CRCS 27-78
+ 50m

CRIS 29+30

7-50m-2

CLCS 31 132

← 5 min

2

CCIT 33 B4
17-59m²

ACCUCHA

Cards 35 & 36
— Some

DATA

Gould Inc.

Cleveland, Ohio

Printed in U.S.A.

OMTS 37438
X-50m.s

C00T 39+40

+ 2 mm n

ACCUCHART®

Gould Inc.

Cleveland, Ohio

Printed in U.S.A.

CRCT54147

20 m.s.

ACCU

GRCIS 43744

— — 50m n

CHTS 45-46

50m

ACCUCHART®

Gould Inc.

Printed in U.S.A.

Cleveland, Ohio

CRUTS 47-48

50m/s

Gould Inc.

ACCUCHART®

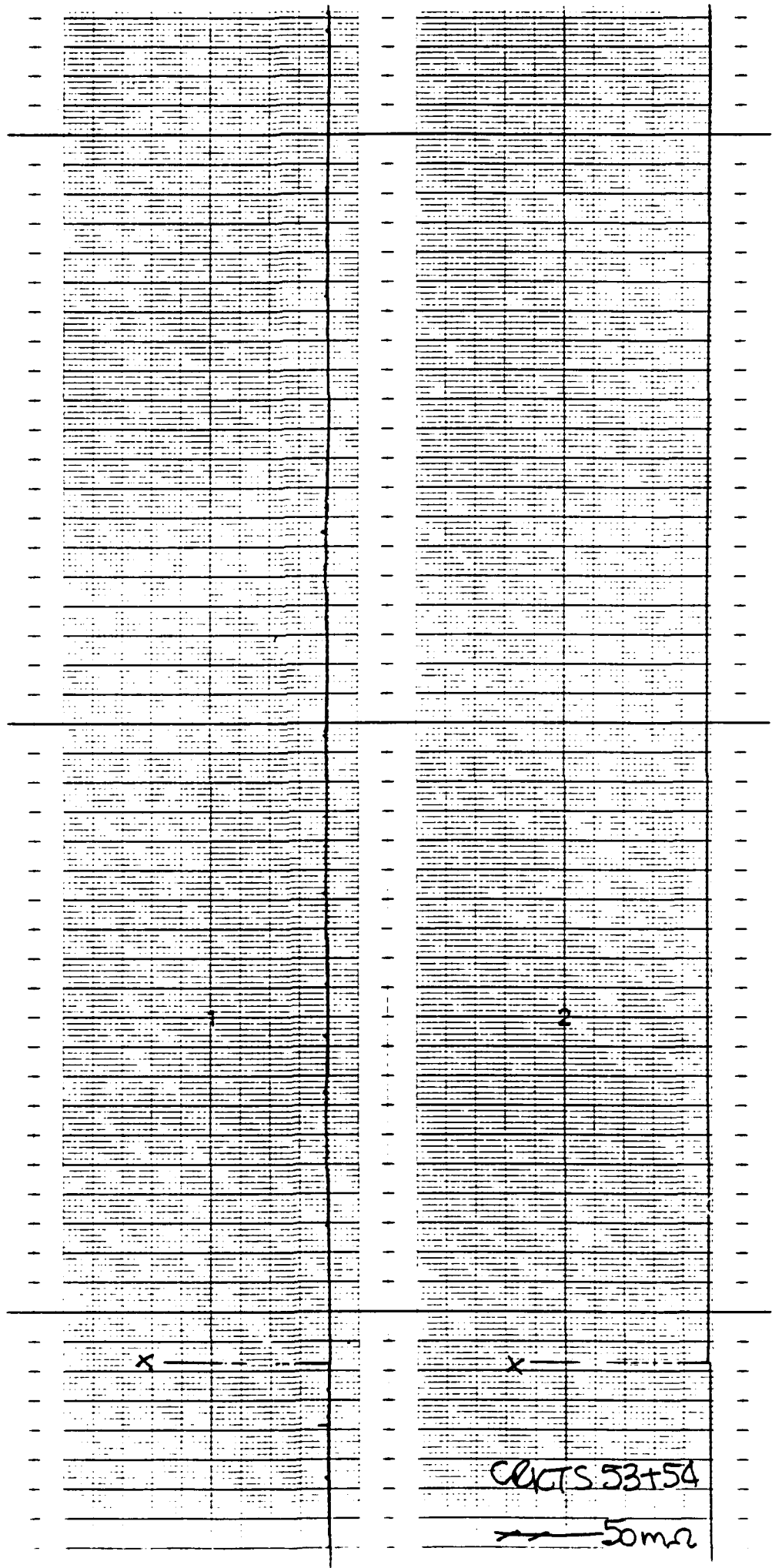
CHARTS 49-450

~~50mV~~

ACCUCHEAR

50

CANTS 51-52
Sample



CRCTB 55-55
— 50m²

CALTS 5150

— 20ms

ACCUCHART®

Gould Inc.

Cleveland, Ohio

Printed in U.S.A.

C26TS 50160

50mm

ACCUCHART

CER/SH-162

— 50mm

Printed in U.S.A.

Gould Inc. Cleveland, Ohio

ACCUCHART®

CRS 63864
T-5000

Gould Inc.

Printed in U.S.A.

Cleveland, Ohio

CRUT 65166

50ms

Cleveland, Ohio

Printed in U.S.A.

0000561768

1-50022

ACCUCHART®

CUTS 69+70

Cards 71-72
- 50m.a

Printed in U.S.A.

Cleveland, Ohio

Gould Inc.

ACCUCHART®

COLTS 73-74

— 50m2

CACST5
1720m.s

ACCUCHART®

Crane
Gould Inc.

01/05/77-78
→ 30mR

Cleveland, Ohio

Printed in U.S.A.

CCS 79+60
-50m2

ACCUCHART®
Gould Inc.
Cleveland, Ohio
Printed in U.S.A.

Cards 61+62
7-50m 2

ACCUCHART® Gould Inc. Printed in U.S.A.

Car 303+34
1150m.s

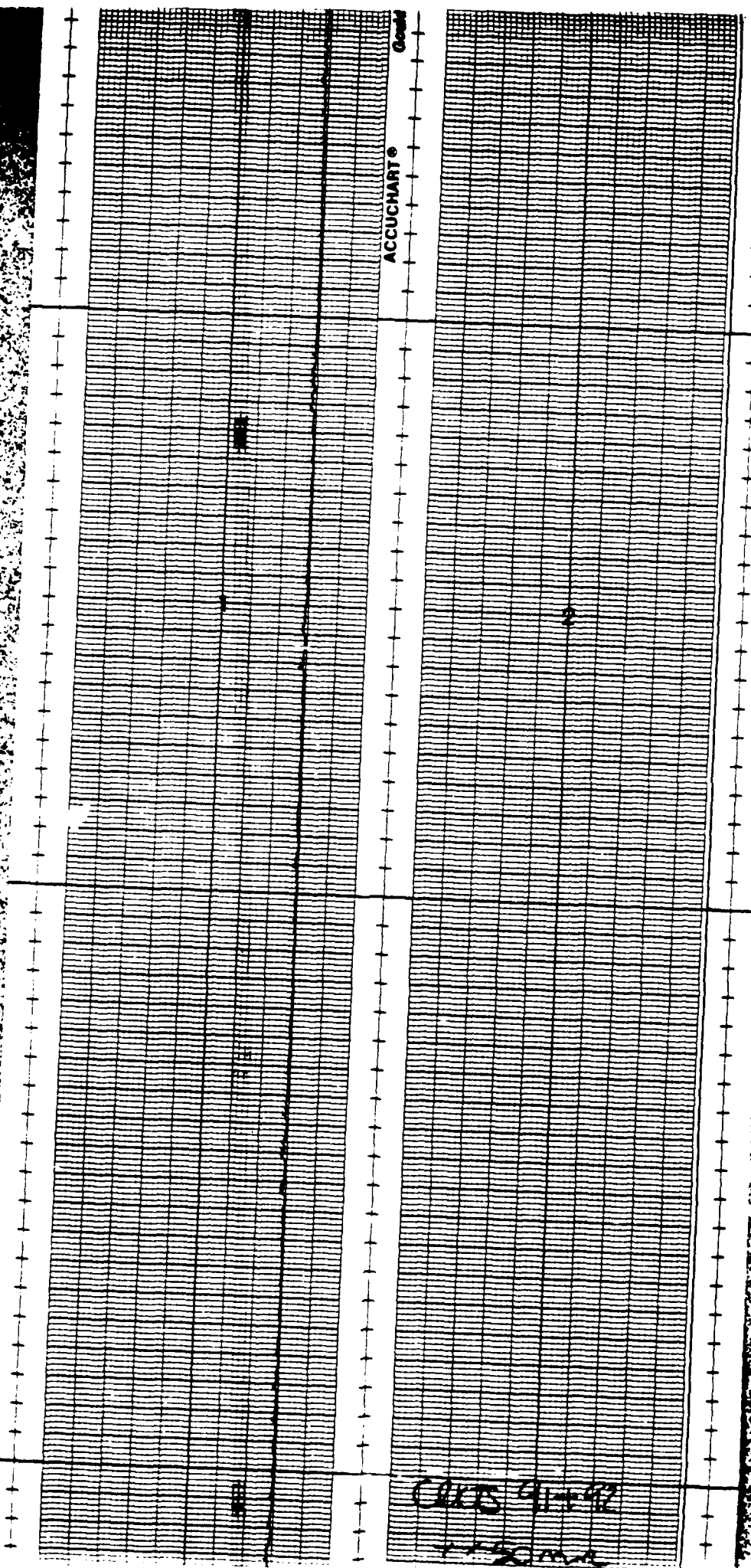
CELT 05 + 0
7-50m.s

Class 67 + 68

1150ma

CRIT 89-190

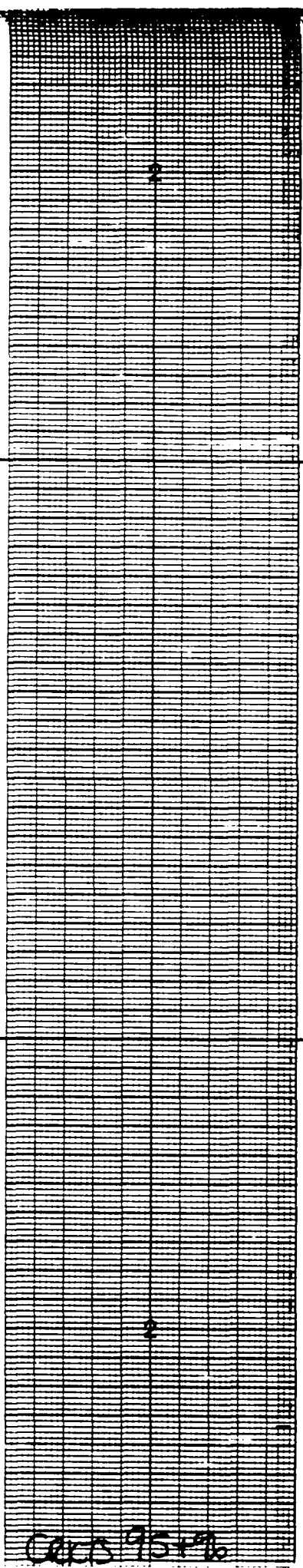
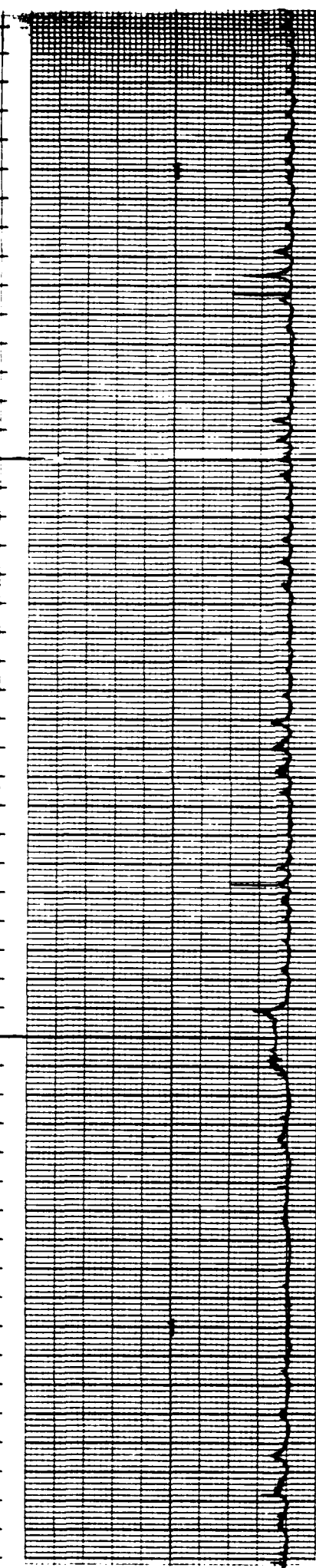
~~- 50m~~



ACCUCHART® Gold Inc.

CCGS 93-94

-50m.s



GCRS 95+%

Printed in U.S.A.

Cleveland, Ohio

02/15/97-98
-20000

HART®

Gould Inc.

Cleveland, Ohio

Printed in U.S.A.

COLTS 99-100

175mm

ACCUCHART® Gould Inc. Printed in U.S.

Cleveland, Ohio

CHTS 10-102

12m.s.

Ground

ACCUCHART®

CPMS 103-104

— 50 mm 2

0005105106

- 25cm 2

O2KTS 107 + 108

7750 m.s.n.m.

ACCUCHART®

Printed in USA

Gould Inc.

Cleveland, Ohio

CHART 104110
- 50ms

ACCUCHART®

Gould Inc.

Cleveland, Ohio Printed in U.S.A.

CAETS 111112

— 50m.Q

TON

CACKS 113 + 14

→ 50 m²

Cleveland, Ohio

Printed in USA

GETS 15+16
** Some

COTS II 7+18
+150m.s

Print
ACCUCHART® Gould Inc. Cleveland, Ohio

CACB 19-120

-50mV

10mA / 5mV